Neotropical Ichthyology

Original article

https://doi.org/10.1590/1982-0224-2025-0183

urn:lsid:zoobank.org:pub:7188A335-1876-4CE5-82C1-FDEED7A09B77

Revealing hidden diversity through iterative approaches: eight new species of *Cambeva* (Siluriformes: Trichomycteridae) from the highly endemic rio Iguaçu basin

Correspondence:
Renan B. dos Reis
reis.renanb@gmail.com

Renan B. dos Reis[1], Bruno H. M. Stabile[1], Alessandra V. Oliveira[1,2], Juliano Ferrer[3] and Weferson J. da Graça[1,2,4,5]

The rio Iguaçu basin can be considered a "hotspot" for *Cambeva* due to its high endemism and the increasing anthropogenic impacts it has been experiencing. Despite this, significant sampling gaps remain, particularly in the lower regions of the basin. Based on recently collected material deposited in ichthyological collections, we describe eight new species of *Cambeva* from the lower rio Iguaçu basin. Species delimitation was carried out through an iterative approach combining external morphological, osteological, and molecular data, with the application of delimitation methods such as GMYC and ASAP. In addition to the taxonomic descriptions, we discuss the potential occurrence of *Cambeva zonata* in the Iguaçu basin, as well as the low genetic distance observed between *C. papillifera* and *C. ventropapillata*, which raises important questions for future taxonomic revisions. Finally, we provide an updated identification key for the *Cambeva* species confirmed in the rio Iguaçu basin.

Keywords: Biodiversity conservation, Cytochrome *c* oxidase subunit I, DNA-barcoding, Fish taxonomy, Trichomycterinae.

Submitted October 22, 2025
Accepted June 6, 2026
Epub September 7, 2026

Associate Editor Carlos DoNascimiento
Section Editor Bruno Melo
Editor-in-chief José Birindelli

1 Universidade Estadual de Maringá, Centro de Ciências Biológicas, Departamento de Biologia, Programa de Pós-Graduação em Ecologia de Ambientes Aquáticos Continentais, Av. Colombo, 5790, 87020-900, Maringá, PR, Brazil. (RBR) reis.renanb@gmail.com (corresponding author), (BHMS) bhmstabile@gmail.com, (AVO) alessoli@hotmail.com, (WJG) weferson@nupelia.uem.br.

2 Universidade Estadual de Maringá, Centro de Ciências Biológicas, Departamento de Biotecnologia, Genética e Biologia Celular e Núcleo de Pesquisas em Limnologia, Ictiologia e Aquicultura, Maringá, PR, Brazil.

3 Universidade Federal do Rio Grande do Sul, Programa de Pós-Graduação em Biologia Animal, Departamento de Zoologia, Av. Bento Gonçalves, 9500, 91501-970, Porto Alegre, RS, Brazil. (JF) juliano.ferrer@gmail.com.

4 Universidade Estadual de Maringá, Centro de Ciências Biológicas, Programa de Pós-Graduação em Biologia Comparada, Maringá, PR, Brazil.

5 Universidade Estadual de Maringá, Centro de Ciências Biológicas, Instituto de Pesquisas em Limnologia, Ictiologia e Aquicultura (Nupélia), Maringá, PR, Brazil.

Online version ISSN 1982-0224
Print version ISSN 1679-6225

Neotrop. Ichthyol.
vol. 24, no. 3, 2026

A bacia do rio Iguaçu pode ser considerada um "hotspot" para *Cambeva* devido ao seu alto endemismo e aos crescentes impactos antrópicos que vem sofrendo. Apesar disso, ainda existem lacunas significativas de amostragem, especialmente nas regiões mais baixas da bacia. Com base em material recentemente coletado e depositado em coleções ictiológicas, descrevemos oito novas espécies de *Cambeva* provenientes da bacia do baixo rio Iguaçu. A delimitação das espécies foi realizada por meio de uma abordagem iterativa que combinou dados morfológicos externos, osteológicos e moleculares, aplicando métodos de delimitação como GMYC e ASAP. Além das descrições taxonômicas, discutimos a possível ocorrência de *Cambeva zonata* na bacia do Iguaçu, bem como a baixa distância genética observada entre *C. papillifera* e *C. ventropapillata*, o que levanta questões importantes para revisões taxonômicas futuras. Por fim, fornecemos uma chave de identificação atualizada para as espécies de *Cambeva* confirmadas na bacia do rio Iguaçu.

Palavras-chave: Conservação da biodiversidade, DNA barcoding, Subunidade I do citocromo c oxidase, Taxonomia de peixes, Trichomycterinae.

INTRODUCTION

The rio Iguaçu is one of the major tributaries on the left bank of the rio Paraná (La Plata Basin), flowing into the rio Paraná at Foz do Iguaçu. A key feature of its course is the Iguaçu Falls, a geological barrier that plays a crucial role in isolating the lower rio Iguaçu from the rio Paraná (Baumgartner *et al*., 2012; Casciotta *et al*., 2018; Piálek *et al*., 2019; Mezzaroba *et al*., 2021). The river's extension is approximately 1,320 km (Maack, 2012), and exhibits a high degree of endemism in fish species, attributed to its isolation and the compartmentalization of its sub-basins, including its tributaries and geological formations that separate the Paraná plateaus (Ingenito *et al*., 2004; Garavello, Sampaio, 2010; Baumgartner *et al*., 2012; Mezzaroba *et al*., 2021). Ingenito *et al.* (2004) categorizes the basin into upper and middle section, divided by the Salto Caiacanga, and the middle and lower section by the Salto Grande (Ingenito *et al*., 2004), important relief that divided the rio Iguaçu basin, now submerged by hydroelectric power plants.

Cambeva Katz, Barbosa, Mattos & Costa, 2018, was described by Katz *et al*. (2018), to reallocate *Trichomycterus* Valenciennes, 1832 species, initially with 25 species, and since then, 34 species have been described, bringing the current total to 61 valid species (Fricke *et al*., 2026). This diversity can be attributed to the species of the genus with high degree of endemism and restricted geographic distribution (Costa *et al*., 2022, 2024a,b; Ferrer, Malabarba, 2013; Reis *et al*., 2023). Moreover, morphological variations observed in some species, such as *Cambeva perobana* Martins, Reis, Stabile & da Graça, 2024 (Martins *et al*., 2024), and *Cambeva* cf. *perkos* (Datovo, Carvalho & Ferrer, 2012) [see dos Reis *et al.* (2025)] suggest the integration of multiple lines of evidence (iterative approaches) to accurately determine their distribution, conservation status, diagnostic characters and ecological aspects that may influence their biology (Ribeiro *et al*., 2021; Costa *et al*., 2023a; Martins *et al*., 2024).

In the rio Iguaçu basin, descriptions of *Cambeva* species began with the American zoologist John Diederich Haseman in the first decade of the 20th century that described *Pygidium davisi* Haseman, 1911, now *Cambeva davisi* (Haseman, 1911), the type species of the genus (Katz *et al*., 2018), from the middle section of the basin. It took 57 years before a second species was described for the basin by Miranda-Ribeiro (1968), *Cambeva stawiarski* (Miranda-Ribeiro, 1968), from lower section of the basin. Subsequently, de Pinna (1992) described *Cambeva castroi* (de Pinna, 1992), from upper section, followed by Wosiacki, Garavello (2004), who described *C. mboycy* (Wosiacki & Garavello, 2004), *C. taroba* (Wosiacki & Garavello, 2004), *C. plumbea* (Wosiacki & Garavello, 2004), and *C. papillifera* (Wosiacki & Garavello, 2004), as well as *C. igobi* (Wosiacki & de Pinna, 2008) and *C. crassicaudata* (Wosiacki & de Pinna, 2008) (Wosiacki, de Pinna, 2008a,b), from lower section of the basin, in the rio Jordão sub-basin, and *C. naipi* (Wosiacki & Garavello, 2004) from upper and middle section of the basin. More recently, *C. cauim* Reis, Ferrer & da Graça, 2022 was described in lower section of the basin (dos Reis *et al*., 2022) as part of the *C. stawiarski* group (*sensu* Wosiacki, de Pinna, 2008a), along with *C. piraquara* dos Reis, Wosiacki, Ferrer, Donin & da Graça, 2023 from the upper section of the basin (dos Reis *et al*., 2023), and five new species described , such as *C. melanoptera* Costa, Abilhoa, Dalcin & Katz, 2022 (Costa *et al*., 2022), from lower section of the basin, and *C. atrobrunnea* Costa, Feltrin & Katz, 2024, *C. galactica* Costa, Feltrin & Katz, 2024, *C. luteoreticulata* Costa, Feltrin & Katz, 2024, and *C. rotundipinna* Costa, Feltrin & Katz, 2024 (Costa *et al*., 2024a), from middle section of the basin.

Despite the increasing number of species descriptions in recent years and to the rio Iguaçu being considered a "hotspot" for the genus (dos Reis *et al*., 2022), harboring 17 species of which 16 are endemic (dos Reis *et al*., 2020a; Costa *et al*., 2022, 2024a), taxonomic efforts have remained concentrated in the upper and middle sections of the rio Iguaçu, and in the rio Jordão and some adjacent basins in the lower section of the basin (see distribution of species in Wosiacki, Garavello, 2004; dos Reis *et al*., 2022). In contrast, the lower rio Iguaçu tributaries have received comparatively less attention and have not yet been systematically explored with regard to alpha taxonomy of the genus. Thus, based on material deposited in ichthyological collections and specimens from recent field trips, this study aimed to describe eight new species of *Cambeva*, infer their phylogenetic position, assess their molecular delimitation and evaluate their conservation status from the lower section of rio Iguaçu using multiple lines of evidence (iterative approaches), ranging from the Iguaçu National Park (Parque Nacional do Iguaçu) in downstream of the Iguaçu Falls, to the rio Butiá region in the upper portion of the lower rio Iguaçu. Additionally, we provide a key for the identification of all *Cambeva* species from the basin.

MATERIAL AND METHODS

Sampling. Specimens utilized as type material and comparative material were deposited in scientific collections, such as Field Museum of Natural History, Chicago (FMNH); Museu de Ciência e Tecnologia da Pontifícia Universidade Católica do Rio Grande do Sul, Porto Alegre (MCP); Museu de História Natural Capão da Imbuia, Curitiba (MHNCI); Museu Paraense Emílio Goeldi, Belém (MPEG); Museu de Zoologia da

Universidade Estadual de São Paulo, São Paulo (MZUSP); and Coleção Ictiológica do Nupélia, Maringá (NUP). Institutional abbreviations follow Sabaj (2022).

Morphological data. Morphometric data were taken point to point with digital calipers (precision 0.1 mm) on the left side of specimens. Measurements followed by Tchernavin (1944), Costa (1992), Nascimento *et al.* (2017), and Donin *et al.* (2022), adapted and described in Martins *et al.* (2024). Clearing and staining (c&s) of specimens followed Taylor, Van Dyke (1985). Vertebral counts exclude those in the Weberian complex, and the compound caudal centrum (PU1+U1) was counted as a single element (Ferrer, Malabarba, 2013). The nomenclature of bones and cartilages followed Bockmann *et al*. (2004), except for using parurohyal instead of urohyal following Arratia, Schultze (1990), lateral sensory canals and associated pores following Rizzato, Bichuette (2017), opercular and interopercular odontodophores, which followed de Pinna, Dagosta (2022), sesamoid supraorbital following Adriaens *et al.* (2010), and ribs following Britz, Bartsch (2003), the last two are based on the justification provided by Costa (2021).

The counts of unsegmented rays (represented by a lowercase Roman numeral) in c&s specimens are given before the number of unbranched (represented by an uppercase Roman numeral) and branched rays (represented by an Arabic numeral). Interopercular, opercular odontodes, premaxilla, and dentary teeth were counted only in c&s specimens. Specimens poorly ossified or with dubious counts were not included in the range of variation. In descriptions, an asterisk denotes the counts of holotype and each meristic character is followed by the number of specimens examined in parentheses. Osteological illustrations were prepared in digital software, based on photographs and direct observation of c&s specimens under a stereomicroscope. The data obtained were compared directly with specimens (see comparative material) and specific literature. *Cambeva paolence* (Eigenmann, 1917) was not included in diagnosis due to evidence suggesting it does not belong to *Cambeva* (dos Reis *et al*., 2025a).

Conservation status. We calculated the Area of Occupancy (AOO) using the polygon area of sub-basins of the data made by HydroBASINS (available at: https://www.hydrosheds.org/products/hydrobasins). The sub-basin scale used in this study was defined according to the distribution range of each species, following the IUCN SSC Red List Technical Working Group (2019) standard criteria: level 10 for restricted-range species and level eight for widespread species. The final conservation status of the new species proposed was suggested using the categories and criteria of the IUCN Standards and Petition Subcommittee (2024).

Molecular data. The DNA of the specimens was extracted from muscular tissue using the Wizard Genomic DNA Purification kit (Promega), following the manufacturer's protocol and quantified using NanoDrop™ Lite Spectrophotometer. The analyses included a set of partial sequences of two mitochondrial genes: cytochrome *c* oxidase subunit I (COX1) and cytochrome *b* (CYTB). For amplification of the COX1 gene, primers FishF1 (Ward *et al*., 2005) and FR1d (Ivanova *et al*., 2007) were used with the following amplification conditions: initial denaturation at 95 °C for 5 min, followed by 35 cycles at 94 °C for 30 s, 52 °C for 40 s, and 72 °C for 1 min, with a final extension at

72 °C for 10 min (Ivanova *et al*., 2007); for the CYTB gene, primers Siluri F and Siluri R (Villa-Verde *et al*., 2012) were used with the following amplification conditions: initial denaturation at 94 °C for 4 min, followed by 35 cycles at 94 °C for 1 min, 62 °C for 1 min, and 72 °C for 1 min, with a final extension at 72 °C for 5 min (Villa-Verde *et al*., 2012). All samples were purified with polyethylene glycol 8000, following the protocol of Rosenthal *et al.* (1993), and later sequenced using an ABI 3500 Applied Biosystems automated sequencer, sequenced in forward direction. Additional sequences of *Cambeva* were obtained from GenBank, using species with morphological and molecular concordance and confirmation in previous studies (see Tab. **S1**). *Trichomycterus nigricans* Valenciennes, 1832 (GenBank access code: MN385796), and *Scleronema* cf. *guapa* Ferrer & Malabarba, 2020 (GenBank access code: PP319012) were used as outgroup for the COX1 tree, and *Scleronema operculatum* Eigenmann, 1917 (GenBank access code: MK123708) was used as outgroup for the CYTB tree. All the sequences of *Cambeva* obtained in this study are deposited in GenBank (Tab. **S1**).

The generated sequences were edited in BioEdit (Hall, 1999) and aligned by the ClustalW algorithm (Thompson *et al*., 1994) in MEGA7 (Kumar *et al*., 2016). MEGA7 was also used to calculate genetic distances using the Kimura-2-Parameter (K2P) model, between and within species groups. The best-fitting model of molecular evolution was calculated based on the Bayesian Information Criterion (BIC) implemented in the web server of IQ-TREE (available at: http://iqtree.cibiv.univie.ac.at/, Kalyaanamoorthy *et al*., 2017; Trifinopoulos *et al*., 2016).

We constructed a Bayesian phylogenetic tree for COX1 and CYTB gene, including unique haplotypes identified by DnaSP v. 6 (Rozas *et al*., 2017), this adjustment was made to address known problems in GMYC caused by identical sequences, where zero-length terminal branches result in the calculation of an infinite coalescent λ (Monaghan *et al*., 2009; Fujisawa, Barraclough, 2013). We built trees using an uncorrelated relaxed clock and a speciation birth-death model on an arbitrary timescale, implemented in BEAST v. 1.8.4 (Drummond *et al*., 2012). A random tree was used as the starting topology for Markov Chain Monte Carlo (MCMC) searches, which were conducted in two independent runs of 40,000,000 generations to assess convergence for COX1, and 10,000,000 generations for CYTB. Trees and log parameters were sampled every 4,000 generations for COX1, and 1,000 generations for CYTB. Chain convergence was identified in the Tracer v. 1.7.2 to determine the stationary phase and an effective sample size > 200 (Rambaut *et al*., 2018). Ten percent of the chain was discarded as a burn-in procedure in Tree Annotator v. 1.8.4 to find the Maximum Clade Credibility Tree (MCC) (Drummond *et al*., 2012). The final tree was edited using Interactive Tree of Life (iTOL) (Letunic, Bork, 2021). Additionally, we constructed a Maximum Likelihood (ML) tree, with the PHYML 3.0 (Guindon *et al*., 2010) webserver (available at: http://www.atgc-montpellier.fr/phyml/), with branch support tested using standard bootstrap with 1,000 replicates, for both alignments (COX1 and CYTB).

Species delimitation test. To test the delimitation of most *Cambeva* species, we applied species delimitation methods. We conducted five different tests: 1) Assemble Species by Automatic Partitioning (ASAP; Puillandre *et al*., 2021); 2) The General Mixed Yule Coalescent Model (GMYC; Fujisawa, Barraclough, 2013), using single and multiple thresholds; and 3) the Poisson tree process (PTP) and its Bayesian implementation

(bPTP) (Zhang *et al*., 2013). 1) The first test (ASAP) was designed to propose partitions of species hypotheses using genetic distances calculated between the sequences. The input file was the aligned sequences, and the analysis was performed in the web server (available at: https://bioinfo.mnhn.fr/abi/public/asap/), with Kimura (K80, ts/tv 2.0) distance model. 2) For the second method (GMYC), the MCC ultrametric tree was used (see section Molecular data). The MCC was checked in FigTree v. 1.4.4 and a newick tree was used as an input file for the GMYC analyses performed in the web server (available at: https://species.h-its.org/gmyc/) using a single threshold (sGMYC) and multiple threshold (mGMYC) methods. 3) For the PTP method we used the ML tree as input in the web server (available at: https://species.h-its.org/), and its Bayesian implementation utilized 500,000 MCMC generations with 0.2 burn-in, along with all other default parameters.

RESULTS

Cambeva kaingang, new species

urn:lsid:zoobank.org:act:8E6D183A-3A9B-45CC-A059-3C6BD8CC4C40

(Figs. 1, 2A–4A, 5–6; Tab. 1)

Trichomycterus sp. 2. —Baumgartner *et al*., 2012:112 (checklist from lower rio Iguaçu).
Cambeva sp. 2. —dos Reis *et al*., 2020:471 (checklist of freshwater fishes from Paraná State).

Holotype. NUP 19052, 50.6 mm SL, Brazil, Paraná State, municipality of Santa Tereza do Oeste, córrego Jumelo, tributary of rio Gonçalves Dias, lower rio Iguaçu basin, rio Paraná system, 25°04'47"S 53°37'26"W, 20 May 2015, R. Delariva.

Paratypes. All from Brazil, Paraná State, lower rio Iguaçu basin, rio Paraná system. UFRGS 30090, 5, 43.7–53.8 mm SL, same data as holotype. MZUSP 130924, 6, 27.0–36.9 mm SL, municipality of Cascavel, rio São João, tributary of rio Salto, rio Andrada basin, 25°00'43"S 53°19'51"W, 14 Mar 2017, R. Delariva. NUP 12661, 5, 25.8–44.2 mm SL, municipality of Santa Tereza do Oeste, rio Gonçalves Dias, 25°03'48"S 53°36'16"W, 20 Sep 2011, R. Delariva. NUP 19056, 1 c&s, 36.0 mm SL, municipality of Céu Azul, rio Manoel Gomes, 25°09'43"S 53°49'46"W, 16 Sep 2014, R. Delariva. NUP 19057, 1 c&s, 42.0 mm SL, municipality of Céu Azul, rio Manoel Gomes, 25°09'43"S 53°49'46"W, 18 Feb 2016, R. Delariva. NUP 24847, 1, 34.5 mm SL, municipality of Santa Tereza do Oeste, rio Gonçalves Dias, 25°04'51.10"S 53°37'18.6"W, 11 Sep 2023, R. B. Reis, B. H. M. Stabile, M. Z. Roloff, C. E. V. Grou, L. D. Lima & S. K. Utiyama.

Diagnosis. *Cambeva kaingang* is distinguished from all congeners except *C. balios* (Ferrer & Malabarba, 2013), *C. botuvera* Costa, Feltrin & Katz, 2021, *C. cubataonis* (Bizerril, 1994), and *C. urubici* Costa, Feltrin & Katz, 2021 by the lateral surface of body composed of large, with same size as opercular odontodophore, dark-brown rounded blotches coalescing and forming irregularly bordered and interrupted longitudinal stripe, from

FIGURE 1 | *Cambeva kaingang*, **A.** Holotype, NUP 19052, 50.6 mm SL, Brazil, Paraná State, córrego Jumelo, tributary of rio Gonçalves Dias, lower rio Iguaçu, rio Paraná system. **B.** Paratype, MZUSP 130924, 36.9 mm SL.

opercular region to base of caudal-fin ray (Fig. 1A), or in smaller specimens (< 40.0 mm SL), with midlateral row of dark-brown rounded blotches, with same size as opercular odontodophore, sometimes coalescing, always forming small interrupted stripes (Fig. 1B) (*vs*. absence of longitudinal stripe in the mid-lateral surface of body or, when present, formed by a narrow, continuous, and well-defined dark-brown longitudinal mid-lateral stripe in *C. naipi* (Wosiacki & Garavello, 2004), *C. pascuali* (Ochoa, Silva, Costa e Silva, Oliveira & Datovo, 2017); longitudinal mid-lateral stripe composed of rounded blotches, two or three times the size of the eyes, in *C. biseriata* Costa, Feltrin, Mattos, Dalcin, Abilhoa & Katz, 2023; wide, with size of opercular odontodophore, and well-defined dark-brown longitudinal mid-lateral stripe extending from the opercular odontodophore to the caudal-fin base in small specimens of *C. davisi*, *C. perkos*, *C. piraquara*, and *C. zonata* (Eigenmann, 1918); longitudinal mid-lateral stripe continuous and never interrupted or with gaps in *C. perkos*, *C. poikilos* (Ferrer & Malabarba, 2013),

and *C. longistriata*; narrow longitudinal stripe formed by closely spaced dark-brown spots, with size of eye diameter, from opercle to vertical through anal-fin origin, and continuing posteriorly to caudal peduncle in *C. tupinamba* (Wosiacki & Oyakawa, 2005). *Cambeva kaingang* is distinguished from *C. balios*, *C. biseriata*, and *C. botuvera* by the general color pattern of the body composed of dark-brown large rounded blotches (of the size of the opercular odontodophore) on the inner skin layer, in three rows on the lateral surface of body (dorso-lateral, mid-lateral, and ventro-lateral) (*vs.* dark-brown rounded blotches variables in size (from the size of the diameter of the eyes to the opercular odontodophore) in the mid-lateral surface of body). *Cambeva kaingang* is distinguished from *C. cubataonis* by the number of opercular odontodes (13 *vs.* 7–10), dorsal procurrent caudal-fin rays (16 *vs.* 18–22), and number of ribs (13–14 *vs.* 11–12). *Cambeva kaingang* is distinguished from C. *urubici* by the number of opercular odontodes (13 *vs.* 15–16), interopercular odontodes (21–22 *vs.* 18–20), dorsal procurrent caudal-fin rays (16 *vs.* 13–15), ventral procurrent caudal-fin rays (12–13 *vs.* 10–11), number of ribs (13–14 *vs.* 15–16), and number of vertebrae (36–37 *vs.* 38–40). Additionally, *C. kaingang* is distinguished from *C. balios* by the number of vertebrae (36–37 *vs.* 38–41); from *C. biseriata* by the number of opercular odontodes (13 *vs.* 15), interopercular odontodes (21–22 *vs.* 23), and the number of dorsal procurrent caudal-fin rays (16 *vs.* 17–19); and from *C. botuvera* by the number of opercular odontodes (13 *vs.* 15–18), number of interopercular odontodes (21–22 *vs.* 25–30), and number of vertebrae (36–37 *vs.* 39–40).

Description. Morphometric data in Tab. 1. Body elongate, trunk roughly cylindrical close to head and gradually becoming laterally compressed towards caudal fin. Dorsal profile of trunk slightly convex along anterior half of body to insertion of dorsal fin. Ventral profile of trunk slightly concave. Dorsal and ventral profiles of caudal peduncle straight.

Head depressed, trapezoidal in dorsal view, wider posteriorly. Dorsal and ventral profiles of head straight to slightly convex in lateral view. Snout straight to slightly convex in dorsal view. Eyes located dorsolaterally on anterior half region of head, at same longitudinal line of nasal barbel, anteroposteriorly elliptical, covered by thin and translucent skin. Orbital rim not free. Each eye located over posterior termination of shallow and small longitudinal crest beginning at posterior nostril and making eyes visible from lateral view.

Anterior nostril slightly smaller than size of eye, surrounded by flap of integument posterolaterally continuous with base of nasal barbel. Posterior nostril surrounded anterolaterally by thin flap of integument. Gill openings not constricted united with isthmus anteriorly, forming free fold reaching pectoral-fin insertion. Mouth subterminal and slightly curved with corners posteriorly oriented. Upper lip thicker laterally. Lower lip with conspicuous fleshy lobes in lateral limits, continuous with base of rictal barbels. Lips with small and numerous rounded papillae of approximately same size.

Barbels with broad base, tapering gradually towards tips. Nasal barbel emerging from lateral region of anterior nostril with posterior tip reaching infraorbital pores i10 and i11 when adpressed to head. Maxillary barbel emerging from lateral limit of mouth with tip reaching to anterior region of interopercular odontodophore when adpressed to head. Rictal barbel emerging from lateral limit of mouth, slightly shorter than maxillary barbel.

TABLE 1 | Morphometric data for *Cambeva kaingang*. N = number of specimens, Min = minimum, Max = maximum, SD = Standard deviation.

	Holotype	N	Min	Max	Mean	SD
Standard length (mm)	50.7	13	26.9	53.6	40.8	–
Percents of standard length						
Head length	19.5	13	18.6	20.0	19.3	0.5
Predorsal length	62.0	13	61.3	63.8	62.8	0.7
Prepelvic length	53.6	13	53.6	59.0	55.9	2.1
Preanal length	65.3	13	65.3	71.1	68.5	2.3
Pectoral girdle width	15.9	13	15.1	16.7	16.0	0.5
Trunk length	38.8	13	33.1	40.2	38.6	0.9
Anal-fin Length	17.2	13	14.6	17.7	16.2	1.4
Dorsal-fin length	19.8	13	17.8	20.4	19.0	1.1
Pectoral-fin length	14.9	13	12.4	16.0	14.4	1.7
Pelvic-fin length	10.2	13	8.6	10.2	9.5	0.5
Distance between pelvic-fin base and anus	11.0	13	7.6	11.0	9.6	0.8
Caudal peduncule length	23.1	13	15.5	24.2	22.8	0.9
Caudal peduncule depth	11.4	13	10.4	12.3	11.5	0.8
Body depth	15.3	13	12.5	15.3	14.3	1.1
Length of dorsal-fin base	11.9	13	10.5	13.4	12.3	1.0
Length of anal-fin base	9.1	13	8.1	9.6	8.9	0.6
Pelvic anal distance	14.9	13	11.8	14.9	13.5	1.2
Percents of head length						
Head width	92.9	13	73.4	92.9	90.0	1.8
Rictal barbel length	55.4	13	55.4	72.4	62.0	6.7
Maxillary barbel length	62.2	13	58.9	82.5	70.2	9.6
Nasal barbel length	57.4	13	57.4	71.7	64.8	6.5
Snout lenght	40.3	13	40.3	44.9	42.3	1.7
Interorbital distance	29.7	13	24.6	29.7	27.1	2.0
Mouth width	33.6	13	33.6	48.1	42.9	5.8
Eye diameter	9.5	13	7.0	11.3	8.8	1.6
Supra-orbital pore distance	15.2	13	13.4	17.1	15.1	1.3

Pectoral fin with distal margin rounded, I,6*(15) rays, and first ray unbranched, not prolonged as filament. Pelvic fin with distal margin rounded, not covering anterior margin of urogenital papilla; I,4*(15) rays. Pelvic-fin insertion anterior to origin of dorsal-fin origin. Inner margins of pelvic fins very close basally. Dorsal fin with distal margin straight to slightly convex, II,7*(15) rays. Origin of dorsal fin located at vertical line through last third of pelvic fin. Anal fin elongated with distal margin convex and with same size or slightly bigger than dorsal fin, II,5*(12), or II,6(3) rays. Origin of anal fin located vertical line in first third of dorsal-fin base. Caudal fin with distal margin truncated to slightly rounded; upper plate with I,5*(14), rays, lower plate with I,6*(11) or i,5(3) rays, one anomalous specimen with only i,4 rays on upper caudal plate.

Osteology. Mesethmoid with anterior margin straight to slightly concave and cornua short, with tapering distal ends. Anterior cranial fontanel restricted to small, rounded opening situated between frontals and epiphyseal bar. Posterior cranial fontanel long and

wide extending from posterior portion of frontals to parieto-supraoccipital. Epiphyseal bar, wider than long. Antorbital slightly elongate, extending over at least one-third of autopalatine. Sesamoid supraorbital elongate, slightly expanded anteriorly, with small medial process on anterior third. Anterior portion of sphenotic anterolaterally directed in dorsal view. Sphenotic, prootic and pterosphenoid fused. Vomer arrow-shaped with long posterior process extending to parasphenoid. Parasphenoid with long and pointed posterior process extending to basioccipital. Weberian capsule with lateral openings and anterior margin fused to basioccipital (Fig. 2A).

Premaxilla rectangular with 44(1) spatulate teeth similar in size and roughly distributed in four irregular transverse rows. Dentary with 41(1) teeth similar in size and roughly distributed in four irregular transverse rows, ranging from base of coronoid process to near dentary symphysis (Fig. 3A). Maxilla boomerang-shaped, shorter than premaxilla. Autopalatine with lateral margin concave; anterior margin slightly convex; medial margin slightly concave and long posterior process extending over posterior portion of metapterygoid. Metapterygoid large and laminar, connected to quadrate through cartilage. Quadrate L-shaped with deep concavity in anterior portion. Hyomandibula well-developed slightly concave in dorsal margin; and anterior margin with notch (Fig. 4A). Opercle longer than interopercle. Opercular odontodophores ovoid to rounded with 8(1) or 14(1) conical odontodes, gradually curving medially and increasing in size posteriorly, arranged in five irregular transverse rows. Interopercular odontodophore elongate with 21(1) or 22(1) conical odontodes, arranged in two transverse regular rows.

Ventral hypohyal trapezoid-shaped. Anterior ceratohyal elongate and wider at anterior and posterior ends. Posterior ceratohyal round with a pointed posterior process. Eight (2) branchiostegal rays: five in contact with anterior ceratohyal, two with interceratohyal cartilage, and one with posterior ceratohyal. Four posteriormost branchiostegal rays, wider distally. Parurohyal with expanded anterior head, two elongate lateral processes with wide bases and decreasing in width distally with rounded tips, and sharp and elongate posterior process. Posterior process of parurohyal shorter than lateral processes.

Basibranchials 2 and 3 elongated, connected to each other by cartilage; basibranchial 2 slightly wider than basibranchial 3. Basibranchial 4 hexagonal and entirely cartilaginous. Hypobranchial 1 elongated, with cartilaginous tips, approximately same size than basibranchial 2. Hypobranchials 2 and 3 with narrow anterolateral ossified processes with large area of cartilage distally; Hypobranchial 2 thinner and longer than Hypobranchial 3. Five elongate ceratobranchials with cartilaginous tips. Ceratobranchials 1 and 4 with straight margins. Ceratobranchials 2 and 3 with concavity on posterior margin, very prominent in ceratobranchial 3. Ceratobranchial 5 with 14(1) or 15(1) conical, elongated and pointed teeth arranged in three irregular rows. Four epibranchials; anteriormost three elongated and narrow with cartilage at tips. Epibranchials 1 and 2 with elongated and pointed process along anterior margins; epibranchial 3 with curved process on posterior margin. Epibranchial 4 rectangular, wider posteriorly and with cartilaginous tips. Pharyngobranchial 3 elongated, shorter than hypobranchial 1, with cartilage at tips. Pharyngobranchial 4 ossified and connected to curved plate with 31(1) or 32(1) conical, elongated and pointed teeth, arranged in up to three irregular rows; teeth increasing in size posteriorly.

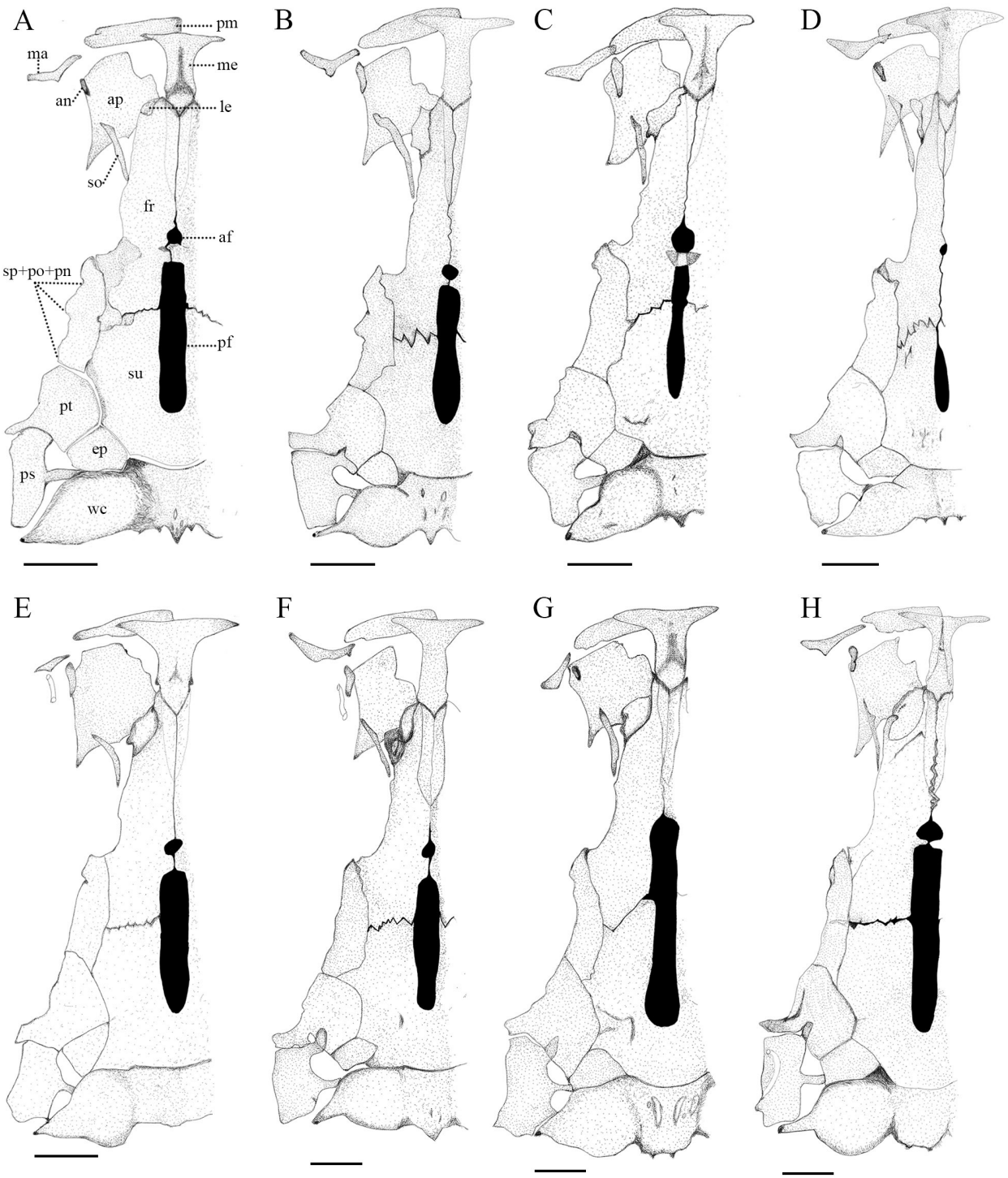

FIGURE 2 | Dorsal view of neurocranium of *Cambeva* species. **A.** *C. kaingang*, NUP 19057, 42.0 mm SL; **B.** *C. tessellata*, NUP 25868, 66.1 mm SL; **C.** *C. eriveltoi*, NUP 25870, 55.0 mm SL; **D.** *C. tupan*, NUP 25874, 60.0 mm SL; **E.** *C. meandrica*, NUP 25600, 46.5 mm SL; **F.** *C. wosiackii*, NUP 25602, 51.9 mm SL; **G.** *C. longistriata*, NUP 25603, 52.8 mm SL; **H.** *C. ytepopo*, NUP 25876, 43.1 mm SL. Abbreviations: Abbreviations: af, anterior fontanel; an, antorbital; ap, autopalatine; ep, epioccipital; fr, frontal; le, lateral ethmoid; i1 and i3, infraorbital sensory pores of the laterosensory system; me, mesethmoid; mx, maxilla; os, orbitosphenoid; pf, posterior fontanel; pm, premaxilla; ps, posttemporo-supracleithrum; pt, pterotic; so, sesamoid supraorbital; sp+po+pn, sphenotic-prootic-pterosphenoid complex bone; su, parieto-supraoccipital; and wc, Weberian capsule. Osteological features on the right side not shown. Cephalic pores are not shown, except for infraorbitals segments with pores i1, and i3, when present. Scale bars = 1 mm.

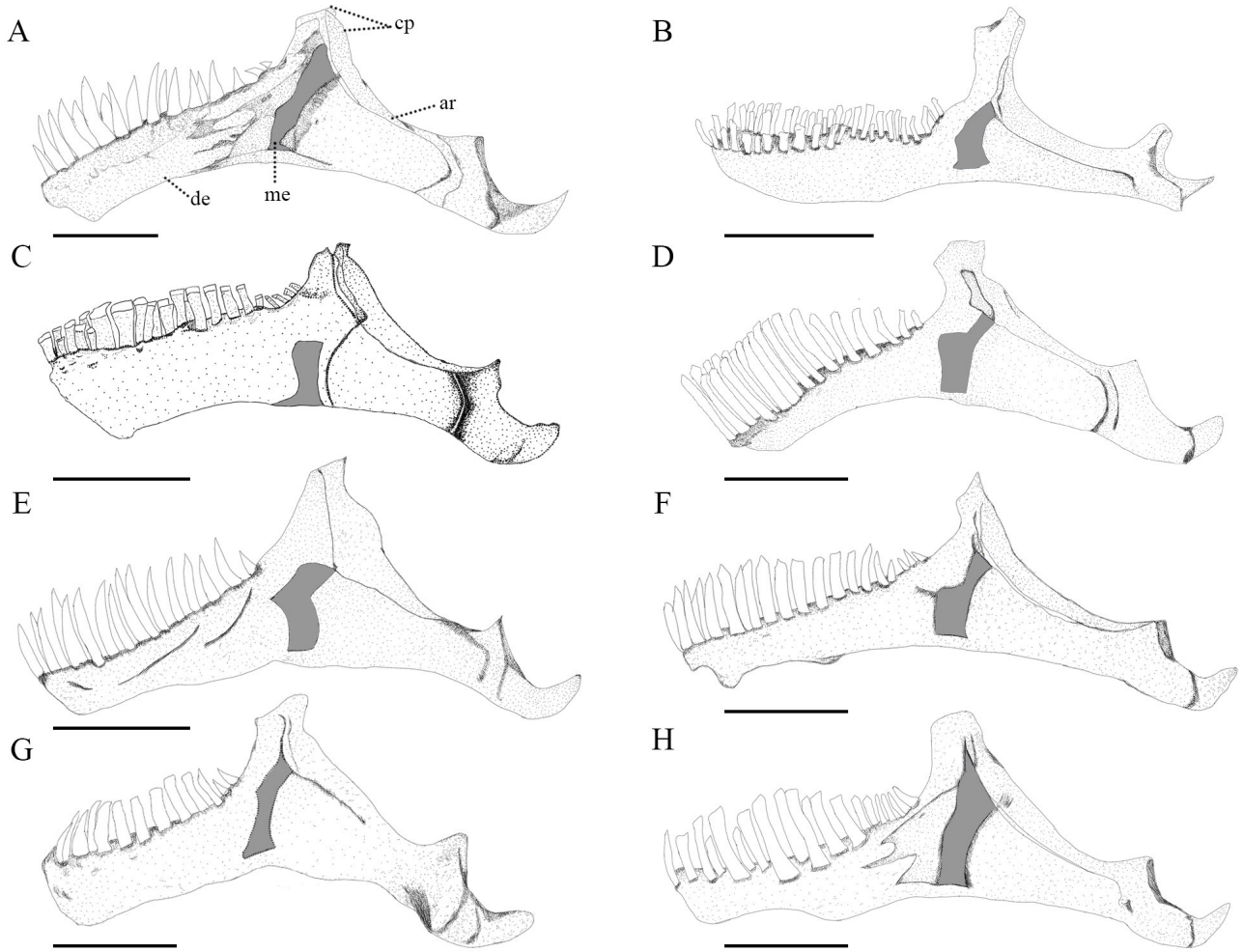

FIGURE 3 | Left lower jaw in lateral view of *Cambeva* species. **A.** *C. kaingang*, NUP 19057, 42.0 mm SL; **B.** *C. tessellata*, NUP 25868, 66.1 mm SL; **C.** *C. eriveltoi*, NUP 25870, 55.0 mm SL; **D.** *C. tupan*, NUP 25874, 60.0 mm SL; **E.** *C. meandrica*, NUP 25600, 46.5 mm SL; **F.** *C. wosiackii*, NUP 25602, 51.9 mm SL; **G.** *C. longistriata*, NUP 25603, 52.8 mm SL; **H.** *C. ytepopo*, NUP 25876, 43.1 mm SL. Abbreviations: ar, arguloarticular; cp, coronoid process; de, dentary; mc, Meckel's cartilage. Scale bars = 1 mm.

Dorsal fin with eight pterygiophores, first inserted anterior to neural spine of 18th or 19th vertebrae. Anal fin with six pterygiophores, first inserted anterior to haemal spine of 22nd (2) vertebrae. Procurrent caudal-fin rays 16(2) dorsally and 12(1) or 13(1) ventrally. Hypural 3 free and hypurals 4 and 5 fused to each other. Parhypural and hypurals 1 and 2 co-ossified and fused to compound caudal centrum. Free vertebrae 36(1) or 37(1), and 13(1) or 14(1) pairs of ribs.

Laterosensory system. Laterosensory canals with simple (non-dendritic) branches ending in single pores. Nasal and frontal canals of supraorbital branch continuous, with three (15) paired pores s1, s3 and s6. Supraorbital pore s1 located at posterior portion of anterior nostrils, pore s3 at same longitudinal line of pore s1 posteriorly to posterior nostrils and pore s6 aligned with posterior margin of eyes. Antorbital segment of infraorbital canal absent. Sphenotic canal present with two (15) pores, i10, located

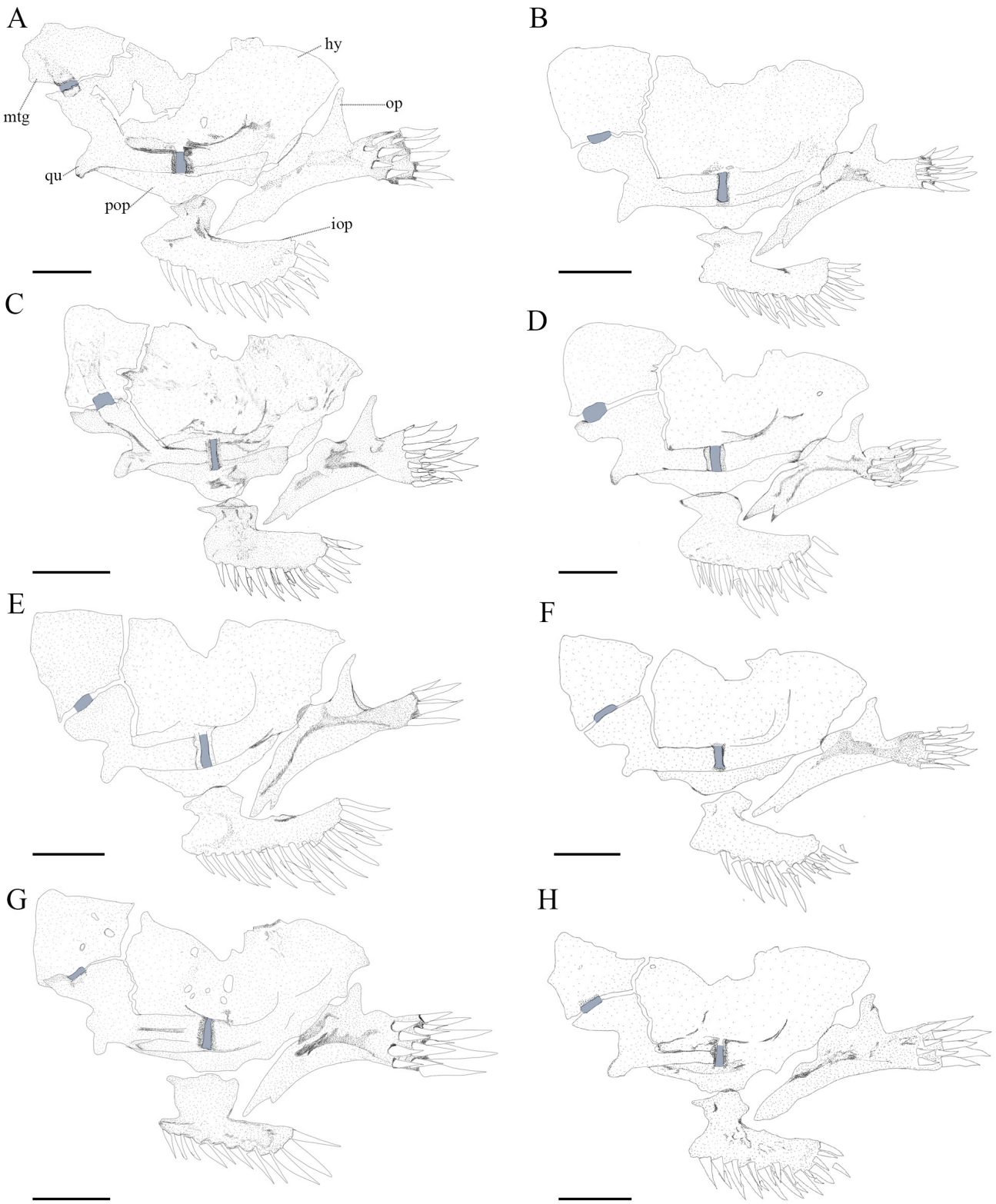

FIGURE 4 | Lateral view of left suspensory of *Cambeva* species. **A.** *C. kaingang*, NUP 19057, 42.0 mm SL; **B.** *C. tessellata*, NUP 25868, 66.1 mm SL; **C.** *C. eriveltoi*, NUP 25870, 55.0 mm SL; **D.** *C. tupan*, NUP 25874, 60.0 mm SL; **E.** *C. meandrica*, NUP 25600, 46.5 mm SL; **F.** *C. wosiackii*, NUP 25602, 51.9 mm SL; **G**. *C. longistriata*, NUP 25603, 52.8 mm SL; **H.** *C. ytepopo*, NUP 25876, 43.1 mm SL. Abbreviations: hy, hyomandibula; iop, interopercle; mtg, metapterygoid; op, opercle; pop, preopercle; qu, quadrate. Scale bars = 1 mm.

behind eyes, and pore i11 located laterally to posterior margin of eye. Otic and postotic canals present with two (15) pores associated: po1 located anterolaterally to opercular odontodophore and po2 located laterally to half-length of opercular odontodophore. Lateral line canal short with two (15) pores located above pectoral-fin insertion and posterior to gill opening.

Coloration in alcohol. Dorsal region of body and head with irregular dark-brown rounded blotches, with same size as opercular odontodophore, from snout to caudal peduncle. Lateral surface of body composed of large, with same size as opercular odontodophore, dark-brown rounded blotches coalescing and forming irregularly bordered and sometimes interrupted longitudinal band, from opercular region to base of caudal-fin rays. Rounded smaller dark-brown blotches randomly distributed between sagittal line of body and lateral line of body, and in ventral portion of lateral surface of body. Background of body yellowish, readily visible in ventral surface of body and head. Pectoral, dorsal, anal, and caudal fins with few inconspicuous dark-brown blotches equivalent or slightly larger in size to eye diameter, over yellowish background. Pelvic fin yellowish. Barbels with dark-brown melanophores on dorsal surface. Smallers specimens (< 40.0 mm SL) with midlateral row of dark-brown rounded blotches, with same size as opercular odontodophore, sometimes coalescing, always forming small interrupted stripes (Fig. 1B).

Geographical distribution. *Cambeva kaingang*, is known from the córrego Jumelo (type locality), a tributary of rio Gonçalves Dias, rio Manoel Gomes, rio São João, a tributary of rio Salto, rio Andrada basin, all from the lower section of rio Iguaçu *sensu* Ingenito *et al*. (2004), Paraná State, Brazil (Fig. 5).

Ecological notes. The type locality of *Cambeva kaingang* is located at an elevation of 600 m above sea level, near the boundary of Iguaçu National Park, one of the most important environmental preservation areas in Brazil. The water depth is approximately 30 to 60 cm, and the habitat consists of fast-flowing waters, with a substrate composed of rocks ranging from 5 to 30 cm in diameter (Fig. 6). The species occurs in sympatry in the type locality with *Ancistrus mullerae* Bifi, Pavanelli & Zawadzki, 2009, *Bryconamericus pyahu* Azpelicueta, Casciotta & Almirón, 2003, *Cambeva wosiackii*, *Phalloceros circummontanus* Souto-Santos, Mejia, Arcila & Buckup, 2025, *Psalidodon bifasciatus* (Garavello & Sampaio, 2010), *Psalidodon dissimilis* (Garavello & Sampaio, 2010), and *Rhamdia branneri* Haseman, 1911.

Conservation status. *Cambeva kaingang* can be found in three localities, in the córrego Jumelo, a tributary of rio Gonçalves Dias (type locality), rio Manoel Gomes, and rio São João, a tributary of rio Salto, rio Andrada basin. The new species has an EOO of 454.7 km² (< 5,000 km² in criteria B1 for EN), and can be found in river basins inside the Iguaçu National Park. Therefore, *C. kaingang* does not meet any other condition of this criteria, and according to the International Union for Conservation of Nature (IUCN) categories and criteria (IUCN Standards and Petitions Subcommittee, 2024), thus our recommendations is that this species can be classified as Least Concern (LC).

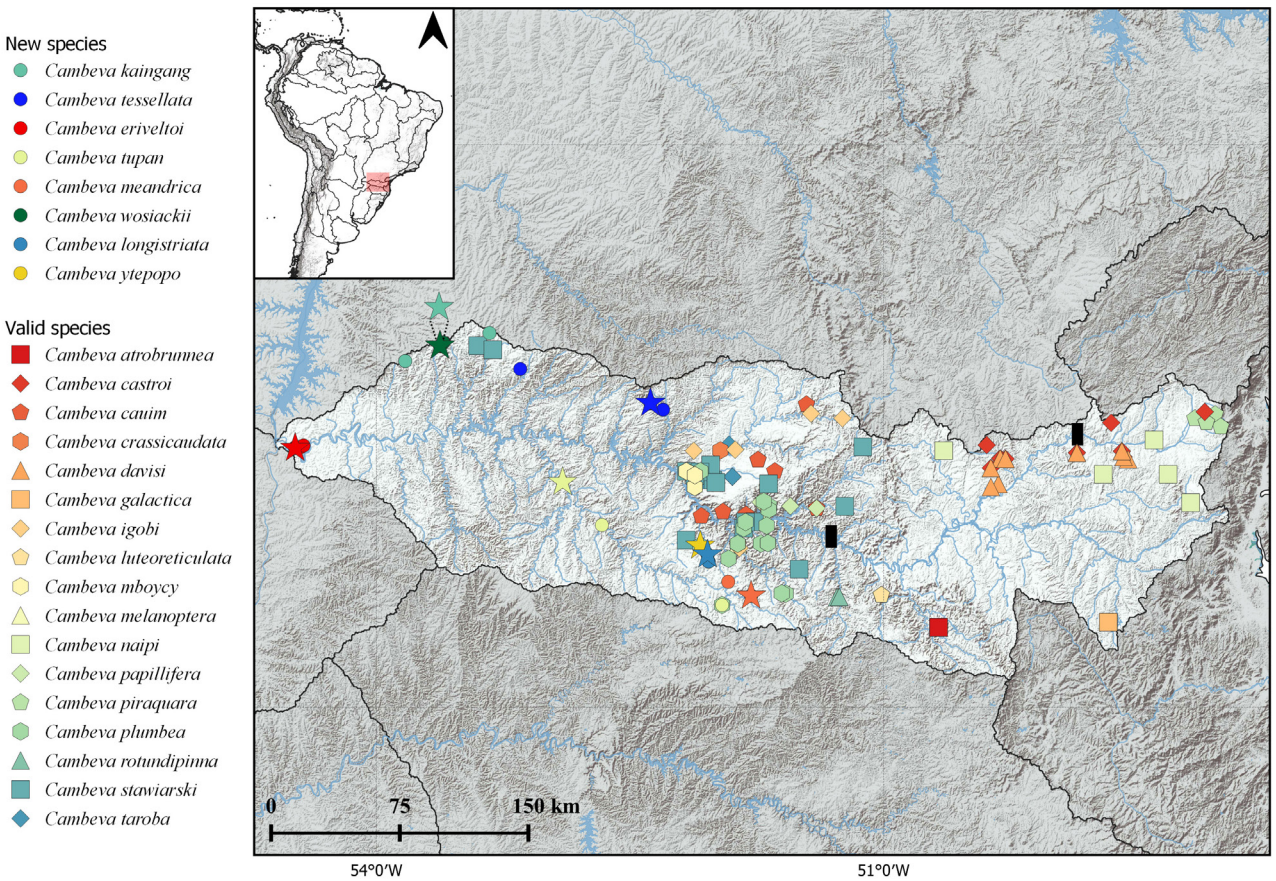

FIGURE 5 | Partial map of South America, highlighting rio Iguaçu basin, and geographical distribution map of *Cambeva* species from rio Iguaçu and new species described here. Symbols color represented in figure legend. Stars represent type localities, and black rectangles represent the limits of the upper, middle and lower section of rio Iguaçu.

Etymology. The specific name "*kaingang*" is an allusion to the ethnic group of people who lived in southern Brazil, encompassing the neighboring areas of the rio Iguaçu. Additionally, in the Tupi-Guarani legend about the origin of the Iguaçu waterfalls, the characters "Naipi" and "Taroba", are "Kaingangs" or "Caingangues" (Baumgartner *et al*., 2012), and specific names of *Cambeva* species. A noun in apposition.

FIGURE 6 | Collection point of *Cambeva kaingang*, NUP 24844, and *C. wosiackii*, NUP 24848, close to both type localities.

Cambeva tessellata, new species

urn:lsid:zoobank.org:act:574EC441-C2C6-4461-B603-1F9AB0CF2BD4

(Figs. 2B–4B, 5, 7–8; Tab. 2)

Holotype. NUP 16002, 64.8 mm SL, Brazil, Paraná State, municipality of Laranjeiras do Sul, unknown name stream, tributary of rio Tapera, 25°23'10"S 52°22'44"W, 25 Jan 2014, W. J. Graça, W. M. Domingues, F. A. Teixeira & R. J. Graça.

Paratype. All from Brazil, Paraná State, lower rio Iguaçu basin, rio Paraná system. NUP 15631, 7, 25.4–65.3 mm SL, NUP 25869, 15, 28.9–79.8 mm SL, UFRGS 30091, 4, 42.8–64.4 mm SL, same data as holotype. MZUSP 130925, 5, 46.4–59.8 mm SL, NUP 15686, 4, 52.7–57.4 mm SL, NUP 16097, 20, 28.9–79.8 mm SL, NUP 25868, 4 c&s, 55.3–66.1 mm SL, municipality of Laranjeiras do Sul, unknown name stream, tributary of rio Tapera, 25°25'19.00"S 52°18'15.01"W, 25 Jan 2014, W. J. Graça, W. M. Domingues, F. A. Teixeira & R. J. Graça.

Diagnosis. *Cambeva tessellata* is distinguished from all congeners, except *C. alphabelardense* Costa, Feltrin & Katz, 2022, *C. concolor* (Costa, 1992), *C. damnata* (Costa, Azevedo-Santos, Ottoni, Vilardo & Katz, 2024), *C. flavopicta* Costa, Feltrin & Katz, 2020, *C. eriveltoi*, *C. panthera* Costa, Feltrin & Katz, 2021, *C. piraquara*, *C. taroba*, and

FIGURE 7 | *Cambeva tessellata*, holotype, NUP 16002, 64.8 mm SL, Brazil, Paraná State, unknown stream, tributary of rio Tapera, lower rio Iguaçu, rio Paraná system.

C. variegata (Costa, 1992) by having in the first pectoral-fin ray extending as a short or long filament (*vs*. absence of filament, or when present, in the form of a rudimentary filament in *C. gamabelardense* Costa, Feltrin & Katz, 2022, *C. imaruhy* Costa, Feltrin & Katz, 2021, and *C. pascuali*). *Cambeva tessellata* is distinguished from *C. alphabelardense* by the number of pelvic-fin rays (I,4 *vs*. I,3), number of dorsal procurrent caudal-fin rays (23–25 *vs*. 21), and number of branchiostegal rays (8 or 9 *vs*. 7); from *C. concolor*, *C. damnata*, and *C. variegata* by the absence of a prominent skin crest on the dorsal margin of the caudal peduncle (*vs*. presence of a prominent skin crest on the dorsal margin of the caudal peduncle); from *C. flavopicta* by the presence of pelvic fin and pelvic girdle (*vs*. absence of pelvic fin and pelvic girdle); from *C. eriveltoi*, *C. panthera*, and *C. piraquara* by the color pattern of the body composed of rounded dark-brown spots or blotches, variable in size, sometimes coalescing and being densely mottled on the lateral surface of the body (*vs*. color pattern of the body on dorsal and lateral surface of body densely composed of coalescent dark-brown blotches, equally in size of opercular odontodophore, forming a vermicular pattern in *C. eriveltoi*; color pattern of the body composed of round brown spots with dark-brown to black margin in *C. panthera*; and the presence of conspicuous and well-defined dark-brown longitudinal mid-lateral stripe, extending from the opercular odontodophore to the first third of caudal-fin rays in *C. piraquara*); and from *C. taroba* by the number of pectoral fin-rays (I,6 *vs*. I,5). Additionally, *Cambeva tessellata* is distinguished from *C. panthera* by the number of ribs (12–13 *vs*. 14), and the presence of smaller maxillary barbel, with its tip reaching the middle of interopercular odontodophore (*vs*. longer maxillary barbel, with its tip reaching the middle of pectoral-fin base); and from *C. piraquara* by the number of vertebrae (36–38 *vs*. 40).

Description. Morphometric data in Tab. 2. Body elongate, trunk roughly cylindrical close to head and gradually becoming laterally compressed towards caudal fin. Dorsal profile of trunk slightly convex along anterior half of body to insertion of dorsal fin. Ventral profile of trunk convex. Dorsal and ventral profiles of caudal peduncle slightly concave.

Head depressed, trapezoidal in dorsal view, wider posteriorly. Dorsal profile of head straight to slightly convex, and ventral convex, in lateral view. Snout straight convex in dorsal view. Eyes located dorsolaterally on anterior half region of head, at same longitudinal line of nasal barbel, anteroposteriorly elliptical, covered by thin and translucent skin. Orbital rim not free. Each eye located over posterior termination of shallow and small longitudinal crest beginning at posterior nostril and making eyes visible from lateral view.

Anterior nostril slightly smaller than size of eye, surrounded by flap of integument posterolaterally continuous with base of nasal barbel. Posterior nostril surrounded anterolaterally by thin flap of integument. Gill openings not constricted united with isthmus anteriorly, forming free fold reaching pectoral-fin insertion. Mouth subterminal and slightly curved with corners posteriorly oriented. Upper lip thicker laterally. Lower lip with conspicuous fleshy lobes in lateral limits, continuous with base of rictal barbels. Lips with small and numerous rounded papillae of approximately same size.

TABLE 2 | Morphometric data for *Cambeva tessellata*. N = Number of specimens, Min = Minimum, Max = Maximum, SD = Standard deviation.

	Holotype	N	Min	Max	Mean	SD
Standard length (mm)	76.8	20	45.7	78.3	66.5	–
Percents of standard length						
Head length	18.6	20	18.6	20.4	19.2	0.7
Predorsal length	65.2	20	63.3	68.9	66.3	2.1
Prepelvic length	57.2	20	56.7	60.7	59.2	1.4
Preanal length	72.8	20	71.9	74.8	73.6	1.2
Pectoral girdle width	15.4	20	14.5	15.4	15.0	0.3
Trunk length	40.6	20	39.2	43.2	41.6	0.9
Anal-fin Length	17.2	20	14.5	17.2	15.6	1.0
Dorsal-fin length	18.7	20	17.0	18.7	17.9	0.6
Pectoral-fin length	13.4	20	11.2	14.7	13.9	0.6
Pelvic-fin length	9.0	20	7.8	9.9	9.0	0.7
Distance between pelvic-fin base and anus	12.8	20	9.0	12.8	10.5	1.3
Caudal peduncule length	20.6	20	17.9	21.2	19.9	1.4
Caudal peduncule depth	11.5	20	11.5	12.9	12.2	0.5
Body depth	11.4	20	10.5	14.0	12.5	1.5
Length of dorsal-fin base	11.1	20	9.8	11.1	10.6	0.5
Length of anal-fin base	8.2	20	7.3	8.3	7.9	0.4
Pelvic anal distance	14.8	20	13.5	14.8	14.2	0.5
Percents of head length						
Head width	93.1	20	84.3	93.1	89.7	2.3
Rictal barbel length	65.1	20	61.3	81.7	67.7	8.2
Maxillary barbel length	79.7	20	70.3	88.5	80.5	6.6
Nasal barbel length	71.1	20	63.4	77.1	72.9	5.8
Snout lenght	45.4	20	43.2	47.1	44.8	1.5
Interorbital distance	23.3	20	23.3	28.0	26.0	1.9
Mouth width	53.1	20	39.2	55.8	47.5	7.8
Eye diameter	7.4	20	5.7	9.0	7.6	1.2
Supra-orbital pore distance	12.1	20	11.6	15.1	12.9	1.4

Barbels with broad base, tapering gradually towards tips. Nasal barbel emerging from lateral region of anterior nostril with posterior tip reaching postotic pore po1 when adpressed to head. Maxillary barbel emerging from lateral limit of mouth with tip reaching half region of interopercular odontodophore when adpressed to head. Rictal barbel emerging from lateral limit of mouth, slightly shorter than maxillary barbel.

Pectoral fin with distal margin rounded, I,6*(20) rays, and first ray unbranched, prolonged as small filament, about one-seventh pectoral-fin length. Pelvic fin with distal margin rounded, not covering anterior margin of anus; I,4*(20) rays. Pelvic-fin insertion anterior to origin of dorsal-fin origin. Inner margins of pelvic fins very close basally. Dorsal fin with distal margin convex, II,7*(20) rays. Origin of dorsal fin located at vertical line through half portion of pelvic fin. Anal fin elongated with distal margin convex and slightly smaller than dorsal fin, II,5*(20) rays. Origin of anal fin located vertical line in last third of dorsal-fin base. Caudal fin with distal margin truncated; upper plate with I,5*(20), rays, lower plate with I,6*(20) rays.

Osteology. Mesethmoid with anterior margin straight to slightly concave and cornua short, with tapering distal ends. Anterior cranial fontanel restricted to small, rounded opening situated between frontals and epiphyseal bar. Posterior cranial fontanel long and wide extending from posterior portion of frontals to parieto-supraoccipital. Epiphyseal bar, longer than wide. Antorbital slightly elongate, extending over at least one-third of autopalatine. Sesamoid supraorbital elongate, rod-like shape, slightly expanded anteriorly, with small medial process on anterior third. Anterior portion of sphenotic anterolaterally directed in dorsal view. Sphenotic, prootic and pterosphenoid fused. Vomer arrow-shaped with long posterior process extending to parasphenoid. Vomer arrow-shaped with long posterior process extending to parasphenoid. Parasphenoid with long and pointed posterior process extending to basioccipital. Weberian capsule with lateral openings and anterior margin fused to basioccipital (Fig. 2B).

Premaxilla rectangular with 40(1) or 51(1) spatulate teeth similar in size and roughly distributed in four irregular transverse rows. Dentary with 40(1) or 44(1) teeth similar in size and roughly distributed in three irregular transverse rows, ranging from base of coronoid process to near dentary symphysis (Fig. 3B). Maxilla boomerang-shaped, shorter than premaxilla. Autopalatine with lateral margin concave; anterior margin slightly convex; medial margin slightly concave and long posterior process extending over posterior portion of metapterygoid. Metapterygoid large and laminar, connected to quadrate through cartilage, notch on posterior margin present in only one specimen c&s. Quadrate L-shaped with concavity in anterior portion. Hyomandibula well-developed slightly concave in dorsal margin (Fig. 4B). Opercular odontodophore ovoid to rounded with 10–13(4) conical odontodes, gradually curving medially and increasing in size posteriorly, arranged in five irregular transverse rows. Interopercular odontodophore elongate with 30–32(4) conical odontodes, arranged in two regular transverse rows.

Ventral hypohyal trapezoid-shaped. Anterior ceratohyal elongate and wider at anterior and posterior ends. Posterior ceratohyal round with a pointed posterior process. Eight (2) or nine (2) branchiostegal rays: five in contact with anterior ceratohyal, two with interceratohyal cartilage, one or two with posterior ceratohyal. Four posteriormost branchiostegal rays, wider distally. Parurohyal with expanded anterior head, two elongate lateral processes with wide bases and decreasing in width distally with rounded tips, and sharp and elongate posterior process. Posterior process of parurohyal shorter than lateral processes.

Basibranchials 2 and 3 elongated, connected to each other by cartilage; basibranchial 2 slightly wider than basibranchial 3. Basibranchial 4 hexagonal and entirely cartilaginous. Hypobranchial 1 elongated, with cartilaginous tips, approximately same size than basibranchial 2. Hypobranchials 2 and 3 with narrow anterolateral ossified processes with large area of cartilage distally; Hypobranchial 2 thinner and longer than Hypobranchial 3. Five elongate ceratobranchials with cartilaginous tips. Ceratobranchials 1 and 4 with straight margins. Ceratobranchials 2 and 3 with concavity on posterior margin, very prominent in ceratobranchial 3. Ceratobranchial 5 with 26(2) conical, elongated and pointed teeth arranged in three irregular transverse rows. Four epibranchials; anteriormost three elongated and narrow with cartilage at tips. Epibranchials 1 and 2 with elongated and pointed process along anterior margins; epibranchial 3 with curved

process on posterior margin. Epibranchial 4 rectangular, wider posteriorly and with cartilaginous tips. Pharyngobranchial 3 elongated, shorter than hypobranchial 1, with cartilage at tips. Pharyngobranchial 4 ossified and connected to curved plate with 32(1) or 35(1) conical, elongated and pointed teeth, arranged in three irregular transverse rows; teeth increasing in size posteriorly.

Dorsal fin with eight pterygiophores (4), first inserted anterior to neural spine of 18th (2) or 19th (2) vertebrae. Anal fin with six pterygiophores (4), first inserted anterior to haemal spine of 21st (3) and 23nd (1) vertebrae. Procurrent caudal-fin rays 18–25(4) dorsally and 11–15(4) ventrally. Hypural 3 free and hypurals 4 and 5 fused to each other. Parhypural and hypurals 1 and 2 co-ossified and fused to compound caudal centrum. Free vertebrae 36(1), 37(2), or 38(1), and 12(1) or 13(3) pairs of ribs.

Laterosensory system. Laterosensory canals with simple (non-dendritic) branches ending in single pores. Nasal and frontal canals of supraorbital branch continuous, with three (20) paired pores s1, s3 and s6. Supraorbital pore s1 located at posterior portion of anterior nostrils, pore s3 at same longitudinal line of pore s1 posteriorly to posterior nostrils and pore s6 aligned with posterior margin of eyes. One specimen with presence of additional pore between s1 and s3, only in left side. Antorbital segment of infraorbital canal absent. Sphenotic canal present with two pores (20), i10, located behind eyes, and pore i11 located laterally to posterior margin of eye. Otic and postotic canals present with two (20) pores associated: po1 located anterolaterally to opercular odontodophore and po2 located laterally to half-length of opercular odontodophore. Lateral line canal short with two (20) pores located above pectoral-fin insertion and posterior to gill opening.

Coloration in alcohol. Dorsal and lateral surface of body composed of rounded dark-brown spots or blotches, variable in size, sometimes coalescing and being densely mottled on the lateral surface of the body. Background of body yellowish, visible on ventral region of body and head, and between blotches. Head densely pigmented by rounded blotches, being scattered on lateral region of head. Pectoral, dorsal, anal, and caudal fins with few inconspicuous dark-brown spots equivalent or slightly larger in size to eye diameter, over yellowish background. Pelvic fin yellowish. Barbels with dark-brown spots of melanophores on dorsal surface, and yellowish ventrally.

Geographical distribution. *Cambeva tessellata*, is known from two unknown name streams, tributaries of rio Tapera, from the lower section of rio Iguaçu (*sensu* Ingenito *et al*., 2004), Paraná State, Brazil (Fig. 5).

Ecological notes. The type locality of *Cambeva tessellata* is located at an elevation of 700 m to 850 m above sea level. The water depth is approximately 30 to 60 cm, and the habitat consists of fast-flowing waters, with a substrate composed of rocks ranging from 5 to 60 cm in diameter (Fig. 8). The species occurs in sympatry with *Hypostomus derbyi* (Haseman, 1911), *Phalloceros circummontanus*, *Psalidodon bifasciatus*, and *Rineloricaria maacki* Ingenito, Ghazi, Duboc & Abilhoa, 2008.

Conservation status. *Cambeva tessellata* can be found in two localities, in the rio Tapera basin, in the lower section of the rio Iguaçu basin. The new species has an EOO of 188 km² (< 5,000 km² in criteria B1 for EN), although no threat has been found in the localities of occurrence of the new species. Therefore, *C. tessellata* does not meet any condition of this criteria, and according to the International Union for Conservation of Nature (IUCN) categories and criteria (IUCN Standards and Petitions Subcommittee, 2024), thus our recommendations is that this species can be classified as Least Concern (LC).

FIGURE 8 | Type locality of *Cambeva tessellata*, unknown name stream, tributary of rio Tapera, tributary of the lower rio Iguaçu basin, Paraná State, Brazil. Upper downstream, lower upstream.

Etymology. The specific name "*tessellata*" is derived from the Latin *tesselatus*, meaning "mosaic" or "checkered", referring to the body pattern formed by small, interconnected spots or blotches. An adjective in the feminine form.

Cambeva eriveltoi, new species

urn:lsid:zoobank.org:act:F83E6B39-8EFE-449B-A6FE-0A739E1D23EA

(Figs. 2C–4C, 5, 9–10; Tab. 3)

Holotype. NUP 25050, 54.9 mm SL, municipality of Foz do Iguaçu, rio São João, tributary of rio Iguaçu, rio Paraná system, 25°37'33.17"S 54°28'49.85"W, 12 Sep 2023, R. B. Reis, B. H. M. Stabile, M. Z. Roloff, C. E. V. Grou, L. D. Lima, S. K. Utiyama & N. Paula.

Paratypes. All from Brazil, Paraná State, municipality of Foz do Iguaçu, rio São João, tributary of lower rio Iguaçu, rio Paraná system: NUP 25037, 2, 34.6–43.2 mm SL, NUP 25871, 5, 48.8–68.5 mm SL, same data as holotype. MZUSP 130926, 1, 48.2 mm SL, 25°37'13.37"S 54°28'34.77"W, 10 Feb 2022, J. O. Santos, L. D. Lima & S. K. Utiyama. NUP 24850, 3, 39.1–46.6 mm SL, UFRGS 30092, 7, 42.9–50.1 mm SL, 25°36'47.34"S 54°25'52.20"W, 16 Sep 2023, R. B. Reis, B. H. M. Stabile, M. Z. Roloff, C. E. V. Grou, L. D. Lima, S. K. Utiyama & N. Paula. NUP 25034, 1, 39.5 mm SL, 25°37'14.95"S 54°28'13.09"W, 14 Sep 2023, R. B. Reis, B. H. M. Stabile, M. Z. Roloff, C. E. V. Grou, L. D. Lima, S. K. Utiyama & N. Paula. NUP 25035, 6, 35.8–53.2 mm SL, NUP 25047, 11, 33.6–68.5 mm SL, 25°37'18.42"S 54°28'45.43"W, 13 Sep 2023, R. B. Reis, B. H. M. Stabile, M. Z. Roloff, C. E. V. Grou, L. D. Lima, S. K. Utiyama & N. Paula. NUP 25036, 3, 29.9–57.7 mm SL, NUP 25870, 2 c&s, 55.0–56.0 mm SL, 25°37'20.98"S 54°26'54.43"W, 16 Sep 2023, R. B. Reis, B. H. M. Stabile, M. Z. Roloff, C. E. V. Grou, L. D. Lima, S. K. Utiyama & N. Paula.

Diagnosis. *Cambeva eriveltoi* is distinguished from all congeners, except *C. alphabelardense*, *C. concolor*, *C. damnata*, *C. flavopicta*, *C. panthera*, *C. piraquara*, *C. taroba*, *Cambeva tessellata*, and *C. variegata* by having the first pectoral-fin ray extending as a short filament (*vs.* absence of filament, or when present, in the form of a rudimentary filament in *C. gamabelardense*, *C. imaruhy*, *C. pascuali*). *Cambeva eriveltoi* is distinguished from *C. alphabelardense* by the number of pelvic-fin rays (I,4 *vs.* I,3), number of dorsal procurrent caudal-fin rays (18–20 *vs.* 21), and number of branchiostegal rays (8 *vs.* 7); from *C. concolor*, *C. damnata*, and *C. variegata* by the absence of a prominent skin crest on the dorsal margin of the caudal peduncle (*vs.* presence of a prominent skin crest on the dorsal margin of the caudal peduncle); from *C. flavopicta* by the presence of pelvic fin and pelvic girdle (*vs.* absence of pelvic fin and pelvic girdle); from *C. panthera*, *C. piraquara*, and *Cambeva tessellata* by the color pattern on dorsal and lateral surface of body densely composed of coalescent dark-brown blotches, equally in size of opercular odontodophore, forming a vermicular pattern (*vs.* color pattern of the body composed of round brown spots with dark-brown to black margin in *C. panthera*; the presence of conspicuous and well-defined dark-brown longitudinal mid-lateral stripe, extending

from the opercular odontodophore to the first third of caudal-fin rays in *C. piraquara*; the color pattern of the body composed of rounded dark-brown spots or blotches, variable in size, coalescing and being densely mottled on the lateral surface of the body in *Cambeva tessellata*); and from *C. taroba* by the number of pectoral fin-rays (I,6 *vs*. I,5). Additionally, *Cambeva eriveltoi* is distinguished from *C. stawiarski* by the smaller body depth (10.5–15.2 *vs*. 15.4–21.6% of SL), number of dorsal procurrent caudal-fin rays (18–20 *vs*. 21–27), number of teeth on ceratobranchial 5 (13–19 *vs*. 23–27), and number of teeth on tooth plate connected to pharyngobranchial 4 (24–25 *vs*. 31–39).

Description. Morphometric data in Tab. 3. Body elongate, trunk roughly cylindrical close to head and gradually becoming laterally compressed towards caudal fin. Dorsal profile of trunk convex along anterior half of body to insertion of dorsal fin. Ventral profile of trunk concave along anterior half and convex along posterior half to the insertion of pelvic fin. Dorsal and ventral profiles of caudal peduncle slightly concave to straight.

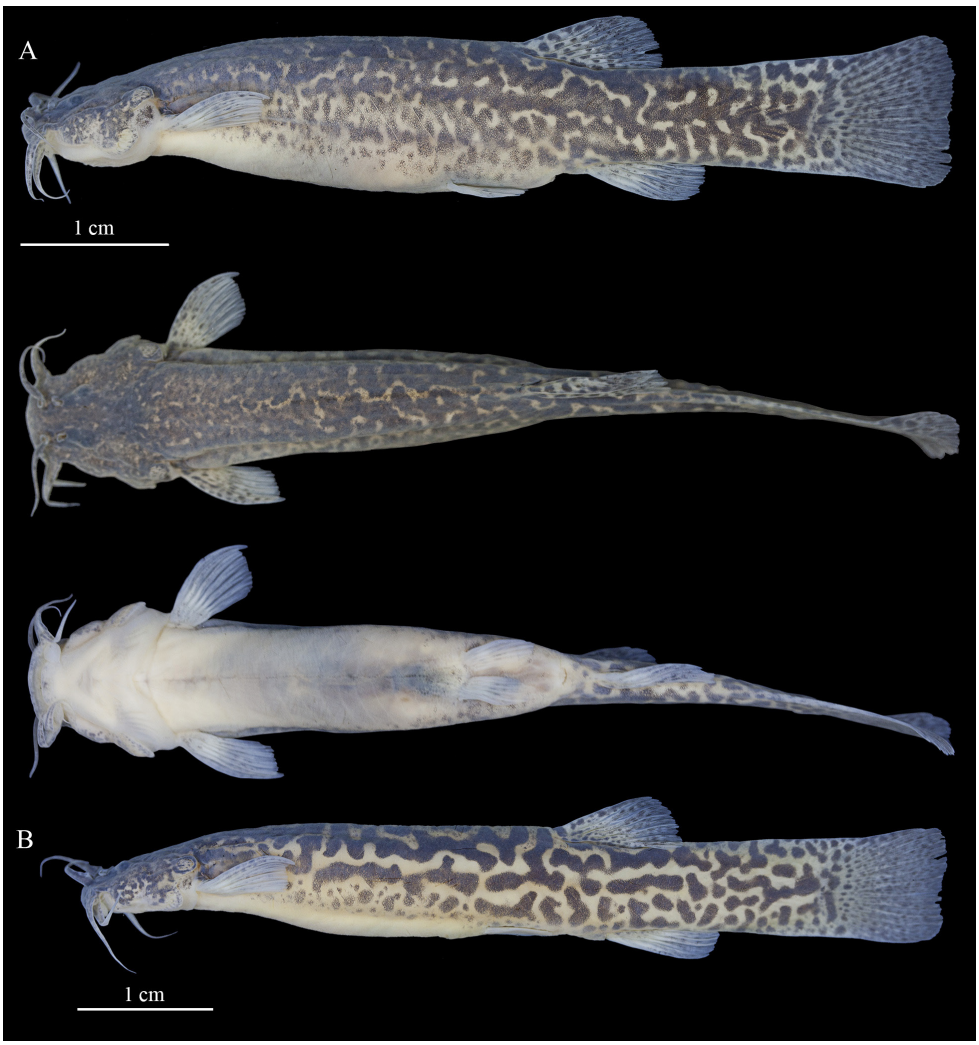

FIGURE 9 | *Cambeva eriveltoi* **A.** Holotype, NUP 25050, 54.9 mm SL, Brazil, Paraná State, rio São João, tributary of lower rio Iguaçu, rio Paraná system; **B.** Paratype, NUP 25871, 48.8 mm SL.

Head depressed, trapezoidal in dorsal view, wider posteriorly. Dorsal profile of head straight and ventral profile of head convex in lateral view. Snout straight to slightly convex in dorsal view. Eyes located dorsolaterally on anterior half region of head, at same longitudinal line of nasal barbel, rounded to anteroposteriorly elliptical, covered by thin and translucent skin. Orbital rim not free. Each eye located over posterior termination of shallow and small longitudinal crest beginning at posterior nostril and making eyes visible from lateral view.

Anterior nostril slightly smaller than size of eye, surrounded by flap of integument posterolaterally continuous with base of nasal barbel. Posterior nostril surrounded anterolaterally by thin flap of integument. Gill openings not constricted united with isthmus anteriorly, forming free fold reaching pectoral-fin insertion. Mouth subterminal and slightly curved with corners posteriorly oriented. Upper lip thicker laterally. Lower lip with conspicuous fleshy lobes in lateral limits, continuous with base of rictal barbels. Lips with small and numerous rounded papillae of approximately same size.

TABLE 3 | Morphometric data for *Cambeva eriveltoi*. N = Number of specimens, Min = Minimum, Max = Maximum, SD = Standard deviation.

	Holotype	N	Min	Max	Mean	SD
Standard length (mm)	53.5	16	39.2	67.6	52.7	–
Percents of standard length						
Head length	17.9	16	17.4	19.9	18.4	0.9
Predorsal length	64.7	16	61.8	65.3	64.0	1.4
Prepelvic length	56.4	16	54.0	56.4	55.3	0.9
Preanal length	71.7	16	69.2	71.7	70.1	1.0
Pectoral girdle width	15.7	16	13.6	15.7	14.9	0.8
Trunk length	38.1	16	36.9	39.6	38.4	1.0
Anal-fin Length	16.5	16	14.7	17.2	16.3	0.7
Dorsal-fin length	19.2	16	14.9	19.2	17.0	1.6
Pectoral-fin length	14.6	16	12.7	15.1	14.6	0.3
Pelvic-fin length	10.1	16	8.7	10.1	9.3	0.5
Distance between pelvic-fin base and anus	10.3	16	9.2	12.8	10.4	1.3
Caudal peduncule length	21.6	16	20.2	22.4	22.0	0.3
Caudal peduncule depth	12.3	16	10.7	12.9	12.3	0.8
Body depth	13.7	16	10.5	15.2	13.5	1.8
Length of dorsal-fin base	11.2	16	9.7	11.5	10.6	0.7
Length of anal-fin base	8.7	16	7.7	9.4	8.3	0.7
Pelvic anal distance	16.8	16	12.7	16.8	15.3	1.4
Percents of head length						
Head width	96.9	16	80.6	98.9	91.3	6.9
Rictal barbel length	58.4	16	54.8	62.5	58.9	2.7
Maxillary barbel length	64.5	16	61.7	73.0	66.0	4.4
Nasal barbel length	68.0	16	60.3	68.0	64.1	2.9
Snout lenght	46.8	16	40.7	46.8	42.9	2.5
Interorbital distance	22.5	16	22.5	26.6	24.8	1.7
Mouth width	47.2	16	43.8	47.8	46.1	1.6
Eye diameter	10.1	16	7.9	10.1	9.1	0.9
Supra-orbital pore distance	13.9	16	12.6	16.3	14.1	1.3

Barbels with broad base, tapering gradually towards tips. Nasal barbel emerging from lateral region of anterior nostril with posterior tip surpassing in one eye diameter infraorbital pore i11 when adpressed to head. Maxillary barbel emerging from lateral limit of mouth with tip reaching to posterior region of interopercular odontodophore when adpressed to head. Rictal barbel emerging from lateral limit of mouth, slightly shorter than maxillary barbel.

Pectoral fin with distal margin slightly rounded on last posterior ray, I,6*(14) or i,7(2) rays, and first ray unbranched, prolonged as short filament, about one tenth pectoral-fin length. Pelvic fin with distal margin rounded, not covering anterior margin of anus; I,4*(16) rays. Pelvic-fin insertion anterior to origin of dorsal-fin origin. Inner margins of pelvic fins close to each other basally by one eye diameter. Dorsal fin with distal margin convex, II,7* (16) rays. Origin of dorsal fin located at vertical line through tip of pelvic fin. Anal fin elongated with distal margin convex and smaller than dorsal fin, II,5*(16) rays. Origin of anal fin located vertical line in last third of dorsal-fin base. Caudal fin with distal margin truncated; upper plate with I,5*(16), rays, lower plate with I,6*(16) rays.

Osteology. Mesethmoid with anterior margin straight to slightly concave and cornua short, with tapering distal ends. Anterior cranial fontanel restricted to small, rounded opening situated between frontals and epiphyseal bar. Posterior cranial fontanel long and wide extending from posterior portion of frontals to parieto-supraoccipital. Epiphyseal bar, longer than wide. Antorbital slightly elongate, extending over at least one-third of autopalatine. Sesamoid supraorbital elongate, rod-like shape, slightly expanded anteriorly, with small medial process on anterior third. Anterior portion of sphenotic anterolaterally directed in dorsal view. Sphenotic, prootic and pterosphenoid fused. Vomer arrow-shaped with long posterior process extending to parasphenoid. Vomer arrow-shaped with long posterior process extending to parasphenoid. Parasphenoid with long and pointed posterior process extending to basioccipital. Weberian capsule with lateral openings and anterior margin fused to basioccipital (Fig. 2C).

Premaxilla rectangular with 40(1) or 42(1) spatulate teeth similar in size and distributed in three regular transverse rows. Dentary with 40(1) or 43(1) spatulate teeth, similar in size, distributed in three irregular transverse rows, and ranging from base of coronoid process to near dentary symphysis (Fig. 3C). Maxilla boomerang-shaped, shorter than premaxilla. Autopalatine with lateral margin concave; anterior margin slightly convex; medial margin slightly concave and long posterior process extending over posterior portion of metapterygoid. Metapterygoid large and laminar, connected to quadrate through cartilage. Quadrate L-shaped with concavity in anterior portion. Hyomandibula well-developed slightly concave in dorsal margin (Fig. 4C). Opercular odontodophore ovoid to rounded with 15(2) conical odontodes, gradually curving medially and increasing in size posteriorly, arranged in four irregular rows. Interopercular odontodophore elongate with 23(2) conical odontodes, arranged in two regular rows.

Ventral hypohyal trapezoid-shaped. Anterior ceratohyal elongate and wider at anterior and posterior ends. Posterior ceratohyal round with a pointed posterior process. Eight branchiostegal rays: five in contact with anterior ceratohyal, two with interceratohyal cartilage, one with posterior ceratohyal. Four posteriormost branchiostegal rays, wider

distally. Parurohyal with expanded anterior head, two elongate lateral processes with wide bases and decreasing in width distally with rounded tips, and sharp and elongate posterior process. Posterior process of parurohyal shorter than lateral processes.

Basibranchials 2 and 3 elongated, connected to each other by cartilage; basibranchial 2 slightly wider than basibranchial 3. Basibranchial 4 hexagonal and entirely cartilaginous. Hypobranchial 1 elongated, with cartilaginous tips, approximately same size than basibranchial 2. Hypobranchials 2 and 3 with narrow anterolateral ossified processes with large area of cartilage distally; Hypobranchial 2 thinner and longer than Hypobranchial 3. Five elongate ceratobranchials with cartilaginous tips. Ceratobranchials 1 and 4 with straight margins. Ceratobranchials 2 and 3 with concavity on posterior margin, very prominent in ceratobranchial 3. Ceratobranchial 5 with 13(1) or 19(1) conical, elongated and pointed teeth arranged in three irregular rows. Four epibranchials; anteriormost three elongated and narrow with cartilage at tips. Epibranchials 1 and 2 with elongated and pointed process along anterior margins; epibranchial 3 with curved process on posterior margin. Epibranchial 4 rectangular, wider posteriorly and with cartilaginous tips. Pharyngobranchial 3 elongated, shorter than hypobranchial 1, with cartilage at tips. Pharyngobranchial 4 ossified and connected to curved plate with 24(1) or 25(1) conical, elongated and pointed teeth, arranged in up to three irregular rows; teeth increasing in size posteriorly.

Dorsal fin with eight or nine pterygiophores, first inserted anterior to neural spine of 18th or 19th vertebrae. Anal fin with six pterygiophores, first inserted anterior to haemal spine of 22nd (2) vertebrae. Procurrent caudal-fin rays 20(1) or 18(1) dorsally and 11(1) or 13(1) ventrally (Fig. 4). Hypural 3 free and hypurals 4 and 5 fused to each other. Parhypural and hypurals 1 and 2 co-ossified and fused to compound caudal centrum. Free vertebrae 36(1) or 37(1), and 11(1) or 13(1) pairs of ribs.

Laterosensory system. Laterosensory canals with simple (non-dendritic) branches ending in single pores. Nasal and frontal canals of supraorbital branch continuous, with three (16) paired pores s1, s3 and s6. Supraorbital pore s1 located at posterior portion of anterior nostrils, pore s3 at same longitudinal line of pore s1 posteriorly to posterior nostrils and pore s6 aligned with posterior margin of eyes. Antorbital segment of infraorbital canal absent. Sphenotic canal present with two (16) pores, i10, located behind eyes, and pore i11 located laterally to posterior margin of eye. Otic and postotic canals present with two (16) pores associated: po1 located anterolaterally to opercular odontodophore and po2 located laterally to half-length of opercular odontodophore. Lateral line canal short with two (16) pores located above pectoral-fin insertion and posterior to gill opening.

Coloration in alcohol. Dorsal and lateral surface of body densely composed of coalescent dark-brown blotches, equally in size of opercular odontodophore, forming vermicular pattern, with few yellowish gaps between blotches, more visible in specimens smaller than 45.0 mm SL (Fig. 11B). Background of body yellowish, readily visible in ventral surface of body and head. Pectoral, dorsal, anal, and caudal fins with few inconspicuous dark-brown blotches equivalent or slightly larger in size to eye diameter, over yellowish background. Pelvic fin yellowish. Barbels with dark-brown melanophores on dorsal surface.

Geographical distribution. *Cambeva eriveltoi*, is only known from the rio São João (type locality), downstream of the Iguaçu waterfalls, in the lower section of rio Iguaçu (*sensu* Ingenito *et al*., 2004) (Fig. 5).

Ecological notes. The type locality of *Cambeva eriveltoi* is located at an elevation of 150 m above sea level, inside the Iguaçu National Park, one of the most important environmental preservation areas in Brazil. The substrate of type locality is composed of fast flowing waters in sandy bottom, and areas with pebbles of 5 to 40 cm (Fig. 10). The species occurs in sympatry with *Ancistrus mullerae*, *Bryconamericus ikaa* Casciotta, Almirón & Azpelicueta, 2004, *Characidium* aff. *zebra* Eigenmann, 1909, *Hoplisoma* aff. *carlae* (Nijssen & Isbrücker, 1983), *Phalloceros circummontanus*, *Psalidodon bifasciatus*, *Hypostomus albopunctatus* (Regan, 1908), and *Rhamdia branneri*.

Conservation status. *Cambeva eriveltoi* can be found in only one locality, in the rio São João, inside the Iguaçu National Park. The new species has an EOO of 243 km² (< 5,000 km² in criteria B1 for EN). The presence of the species in a federal well-conserved protected area suggests the absence of risks related to the species, however the lack of population data and distribution data in surrounding areas (not found to date) suggests the increase of specific studies involving the distribution of the species.

FIGURE 10 | Type locality of *Cambeva eriveltoi*, rio São João, tributary of lower rio Iguaçu, Paraná State, Brazil. Left upstream, right downstream.

Therefore, according to the International Union for Conservation of Nature (IUCN) categories and criteria (IUCN Standards and Petitions Subcommittee, 2024), thus our recommendations is that this species can be classified as Data Deficient (DD).

Etymology. The specific name "*eriveltoi*" is named in honor of prof. Dr. Erivelto Goulart, retired Zoology professor from UEM, one of the mentors and founders of the Núcleo de Pesquisas em Limnologia, Ictiologia e Aquicultura (Nupélia-UEM). He has made significant contributions, and continues to do so, in the field of fish evolution, morphology and ecology, particularly regarding the fishes of the upper rio Paraná. A genitive.

Cambeva tupan, new species

urn:lsid:zoobank.org:act:23CB99AB-37F7-4442-AA5F-685E1A22E70D

(Figs. 2D–4D, 5, 11–12; Tab. 4)

Holotype. NUP 25872, 98.3 mm SL, Brazil, Paraná State, municipality of São João, rio Chopim, tributary of rio Iguaçu, rio Paraná system, 25°48'28.13"S 52°53'55.23"W, 2 Jul 2020, INEO staff.

FIGURE 11 | *Cambeva tupan*, holotype, NUP 25872, 98.3 mm SL, Brazil, Paraná State, rio Chopim, tributary of lower rio Iguaçu, rio Paraná system.

Paratypes. All from Brazil, Paraná State, rio Chopim, tributary of lower rio Iguaçu basin, rio Paraná system. NUP 25873, 5, 60.8–96.9 mm SL, NUP 25874, 2 c&s, 76.7–86.7 mm SL, same data as holotype. NUP 24857, 1, 60.9 mm SL, municipality of Palmas, unknown name stream, 26°27'36.46"S 51°57'18.97"W, 11 Oct 2023, W. J. da Graça, A. Frota, W. M. Domingues & V. A. Teixeira. UFRGS 30093, 2, 60.0–66.0 mm SL, municipality of Pato Branco, rio Ligeiro, 26°2'9.94"S 52°39'57.56"W, 12 Dec 2022, Gerpel staff.

Diagnosis. *Cambeva tupan* is distinguished from all congeners, except *C. castroi*, *C. diabola* (Bockmann, Casatti & de Pinna, 2004), *C. difficilis* (Costa, Feltrin & Katz, 2024), and *C. melanoptera* by the color pattern of the caudal fin presenting a pale-yellow to unpigmented stripe in the proximal region (*vs.* proximal and distal margin of the caudal fin with dark-brown spots or blotches, but never forming a pale-yellow or white stripe in the proximal region). *Cambeva tupan* is distinguished from *C. castroi* by the color pattern of the body composed of irregular large dark-brown blotches, sometimes coalescing and forming vermiculations (*vs.* by the color pattern of the body composed of well-defined round blotches large as interopercular odontodophores to small size as eye diameter); sub-terminal mouth (*vs.* inferior mouth), nasal barbel length (47.1–54.8% *vs.* 32.0–46.0% of head length). *Cambeva tupan* is distinguished from *C. diabola* by the pale-yellow to unpigmented stripe in the proximal region being equivalent in size in the two lobes of the caudal fin (*vs.* by the pale-yellow to unpigmented stripe in the proximal region of the caudal fin being more evident in the dorsal lobe and forming a white ocellus). *Cambeva tupan* is distinguished from *C. melanoptera* by the color pattern of the distal region of all fins having blotches two or three times the diameter of the eyes (*vs.* the distal region of all fins having a broad black zone); the eye diameter (8.1–10.1% *vs.* 14.7–16.6% of HL); and the tip of the nasal barbel reaching the pore i11 (*vs.* tip of the nasal barbel reaching posterior margin of opercular odontodophores or slightly surpassing it). *Cambeva tupan* is distinguished from *C. difficilis* by the color pattern of the body composed of irregular large dark-brown blotches, sometimes coalescing and forming vermiculations (*vs.* by the color pattern of the body composed of black dots that are larger along the longitudinal midlateral line of body).

Description. Morphometric data in Tab. 4. Body elongate, trunk roughly cylindrical close to head and gradually becoming laterally compressed towards caudal fin. Dorsal profile of trunk slightly convex along anterior half of body to insertion of dorsal fin. Ventral profile of trunk concave along anterior half and convex along posterior half to the insertion of pelvic fin. Dorsal profile of caudal peduncle slightly convex to straight and ventral profile of caudal peduncle slightly concave to straight.

Head depressed, trapezoidal in dorsal view, wider posteriorly. Dorsal profile of head straight and ventral profile of head convex in lateral view. Snout convex in dorsal view. Eyes located dorsolaterally on anterior half region of head, at same longitudinal line of nasal barbel, rounded to anteroposteriorly elliptical, covered by thin and translucent skin. Orbital rim not free. Each eye located over posterior termination of shallow and small longitudinal crest beginning at posterior nostril and making eyes visible from lateral view.

TABLE 4 | Morphometric data for *Cambeva tupan*. N = Number of specimens, Min = Minimum, Max = Maximum, SD = Standard deviation.

	Holotype	N	Min	Max	Mean	SD
Standard length (mm)	97.0	8	62.6	96.9	80.4	–
Percents of standard length						
Head length	20.1	8	19.4	21.3	20.3	0.6
Predorsal length	63.7	8	61.9	65.0	63.7	1.1
Prepelvic length	56.4	8	55.0	58.8	56.4	1.4
Preanal length	70.9	8	69.2	74.3	71.6	1.6
Pectoral girdle width	16.1	8	15.1	17.7	16.9	0.6
Trunk length	38.0	8	36.8	39.1	38.7	0.4
Anal-fin Length	15.5	8	14.6	17.1	15.7	0.9
Dorsal-fin length	18.0	8	16.6	18.8	18.0	0.8
Pectoral-fin length	13.6	8	13.1	15.5	14.1	1.0
Pelvic-fin length	9.9	8	9.5	10.5	10.0	0.4
Distance between pelvic-fin base and anus	8.7	8	8.1	10.2	9.5	0.5
Caudal peduncule length	21.4	8	19.5	24.4	22.1	1.8
Caudal peduncule depth	15.2	8	12.7	15.7	14.5	0.8
Body depth	15.5	8	15.3	18.0	16.8	0.9
Length of dorsal-fin base	11.8	8	9.4	11.9	11.8	0.1
Length of anal-fin base	9.2	8	8.2	9.6	9.2	0.5
Pelvic anal distance	16.9	8	15.0	17.0	16.4	0.8
Percents of head length						
Head width	83.5	8	83.5	93.4	89.1	4.2
Rictal barbel length	37.8	8	37.8	44.9	41.9	2.7
Maxillary barbel length	36.0	8	36.0	45.6	41.2	3.9
Nasal barbel length	51.4	8	45.0	54.8	49.9	3.8
Snout lenght	43.3	8	43.3	49.3	46.5	2.3
Interorbital distance	21.4	8	21.4	26.7	23.9	2.2
Mouth width	40.0	8	37.4	40.4	39.1	1.4
Eye diameter	8.1	8	8.1	8.8	8.5	0.2
Supra-orbital pore distance	9.0	8	6.9	14.2	10.4	2.7

Anterior nostril slightly smaller than size of eye, surrounded by flap of integument posterolaterally continuous with base of nasal barbel. Posterior nostril surrounded anterolaterally by thin flap of integument. Gill openings not constricted united with isthmus anteriorly, forming free fold reaching pectoral-fin insertion. Mouth subterminal and slightly curved with corners posteriorly oriented. Upper lip thicker laterally. Lower lip with conspicuous fleshy lobes in lateral limits, continuous with base of rictal barbels. Lips with small and numerous rounded papillae of approximately same size.

Barbels with broad base, tapering gradually towards tips. Nasal barbel emerging from lateral region of anterior nostril with posterior tip surpassing in one eye diameter infraorbital pore i11 when adpressed to head. Maxillary barbel emerging from lateral limit of mouth with tip reaching to anterior region of interopercular odontodophore when adpressed to head. Rictal barbel emerging from lateral limit of mouth, slightly shorter than maxillary barbel.

Pectoral fin with distal margin slightly rounded on last posterior ray, I,7*(8) rays, and first ray unbranched, not prolonged as filament. Pelvic fin with distal margin rounded, covering anterior margin of urogenital papillae; I,4*(8) rays. Pelvic-fin insertion anterior to origin of dorsal-fin origin. Inner margins of pelvic fins very close to each other basally. Dorsal fin with distal margin convex, II,7*(8) rays. Origin of dorsal fin located at vertical line through last third of pelvic fin. Anal fin elongated with distal margin convex and smaller than dorsal fin, II,5*(8) rays. Origin of anal fin located vertical line through last third of dorsal-fin base. Caudal fin with distal margin truncated; upper plate with I,5*(8), rays, lower plate with I,6*(8) rays.

Osteology. Mesethmoid with anterior margin straight to slightly concave and cornua short, with tapering distal ends. Anterior cranial fontanel restricted to small, rounded opening. Epiphyseal bar totally ossified and difficult visualization. Posterior cranial fontanel short and narrow, restricted from anterior portion of parieto-supraoccipital to posterior margin. One specimen lacking epiphyseal bar, anterior and posterior cranial fontanel connected, forming long and narrow fontanel, from frontal to posterior margin of parieto-supraoccipital. Antorbital slightly elongate, extending over at least one-third of autopalatine. Sesamoid supraorbital elongate, rod-like shape, slightly expanded anteriorly, with small medial process on anterior third. Anterior portion of sphenotic anterolaterally directed in dorsal view. Sphenotic, prootic and pterosphenoid fused. Vomer arrow-shaped with long posterior process extending to parasphenoid. Vomer arrow-shaped with long posterior process extending to parasphenoid. Parasphenoid with long and pointed posterior process extending to basioccipital. Weberian capsule with lateral openings and anterior margin fused to basioccipital (Fig. 2D).

Premaxilla rectangular with 54 (2) spatulate to conical teeth similar in size and roughly distributed in three irregular transverse rows. Dentary with 49(1) or 58(1) spatulate teeth, similar in size, distributed in three irregular transverse rows, and ranging from base of coronoid process to near dentary symphysis (Fig. 3D). Maxilla boomerang-shaped, shorter than premaxilla. Autopalatine with lateral margin concave; anterior margin slightly convex; medial margin slightly concave with conspicuous process posteriorly extending slightly over lateral ethmoid; and long postero-lateral process pointed extending over posterior portion of metapterygoid. Metapterygoid large and laminar, connected to quadrate through cartilage. Quadrate L-shaped with concavity in anterior portion. Hyomandibula well-developed, concave in dorsal margin. Opercular odontodophore ovoid to rounded with 18(2) conical odontodes, gradually curving medially and increasing in size posteriorly, arranged in five irregular transverse rows. Interopercular odontodophore elongate with 31(1) or 36(1) conical odontodes, arranged in two regular transverse rows (Fig. 4D).

Ventral hypohyal trapezoid-shaped. Anterior ceratohyal elongate and wider at anterior and posterior ends. Posterior ceratohyal round with a pointed posterior process. Eight (1) or nine (1) branchiostegal rays: five in contact with anterior ceratohyal, two with interceratohyal cartilage, one or two with posterior ceratohyal. Four posteriormost branchiostegal rays, wider distally. Parurohyal with expanded anterior head, two elongate lateral processes with wide bases and decreasing in width distally with rounded tips, and sharp and elongate posterior process. Posterior process of parurohyal shorter than lateral processes.

Basibranchials 2 and 3 elongated, connected to each other by cartilage; basibranchial 2 slightly wider than basibranchial 3. Basibranchial 4 hexagonal and entirely cartilaginous. Hypobranchial 1 elongated, with cartilaginous tips, approximately same size than basibranchial 2. Hypobranchials 2 and 3 with narrow anterolateral ossified processes with large area of cartilage distally; Hypobranchial 2 thinner and longer than Hypobranchial 3. Five elongate ceratobranchials with cartilaginous tips. Ceratobranchials 1 and 4 with straight margins. Ceratobranchials 2 and 3 with concavity on posterior margin, very prominent in ceratobranchial 3. Ceratobranchial 5 with 22(1) or 28(1) conical, elongated and pointed teeth arranged in three irregular transverse rows. Four epibranchials; anteriormost three elongated and narrow with cartilage at tips. Epibranchials 1 and 2 with elongated and pointed process along anterior margins; epibranchial 3 with curved process on posterior margin. Epibranchial 4 rectangular, wider posteriorly and with cartilaginous tips. Pharyngobranchial 3 elongated, shorter than hypobranchial 1, with cartilage at tips. Pharyngobranchial 4 ossified and connected to curved plate with 34(1) or 43(1) conical, elongated and pointed teeth, arranged in up to three irregular transverse rows; teeth increasing in size posteriorly.

Dorsal fin with eight or nine pterygiophores, first inserted anterior to neural spine of 17th (1) or 18th (1) vertebrae. Anal fin with six pterygiophores, first inserted anterior to haemal spine of 21st (2) vertebrae. Procurrent caudal-fin rays 27(2) dorsally and 13(2) ventrally. Hypural 3 free and hypurals 4 and 5 fused to each other. Parhypural and hypurals 1 and 2 co-ossified and fused to compound caudal centrum. Free vertebrae 37(1) or 38(1), and 11(2) pairs of ribs.

Laterosensory system. Laterosensory canals with simple (non-dendritic) branches ending in single pores. Nasal and frontal canals of supraorbital branch continuous, with three (8) paired pores s1, s3 and s6. Supraorbital pore s1 located at posterior portion of anterior nostrils, pore s3 at same longitudinal line of pore s1 posteriorly to posterior nostrils and pore s6 aligned with posterior margin of eyes. Antorbital segment of infraorbital canal absent. Sphenotic canal present with two (8) pores, i10, located behind eyes, and pore i11 located laterally to posterior margin of eye. Otic and postotic canals present with two (8) pores associated: po1 located anterolaterally to opercular odontodophore and po2 located laterally to half-length of opercular odontodophore. Lateral line canal short with two (1), or three* (7) pores located above pectoral-fin insertion and posterior to gill opening.

Coloration in alcohol. Dorsal and lateral surface of body densely composed of coalescent dark-brown blotches, equally in size of opercular odontodophore, forming vermicular pattern, with few yellowish gaps between blotches, more visible in specimens smaller than 63.0 mm SL. Background of body yellowish, readily visible in ventral surface of body and head. Pectoral, pelvic, dorsal, anal, and caudal fins with conspicuous dark-brown blotches equivalent or slightly larger in size to eye diameter, more concentrated distally, over yellowish background. Caudal fin presenting pale-yellow to unpigmented stripe in proximal region. Barbels with dark-brown blotches on dorsal surface.

Geographical distribution. *Cambeva tupan*, is known from the rio Chopim (type locality) and unknown name stream, tributary of rio Chopim, all tributary of the left margin of the lower section of rio Iguaçu (*sensu* Ingenito *et al*., 2004), Paraná State, Brazil (Fig. 5).

Ecological notes. The type locality of *Cambeva tupan* is located at an elevation of 500 m to 1,000 m above sea level. The collection point of the new species in tributaries of rio Chopim has fast-flowing waters and the substrate is composed of bedrocks and peebles of 5 to 30 cm (Fig. 12). The species occurs in sympatry with *Cambeva plumbea*, *Heptapterus* sp., and *Psalidodon bifasciatus*.

Conservation status. *Cambeva tupan* can be found in two localities, in the rio Chopim basin. The new species has an EOO of 7,483 km² (< 20,000 km² in criteria B1 for VU), although no threat has been found in the localities of occurrence of the new species. Therefore, *C. tupan* does not meet any condition of this criteria, and according to the International Union for Conservation of Nature (IUCN) categories and criteria (IUCN Standards and Petitions Subcommittee, 2024), thus our recommendations is that this species can be classified as Least Concern (LC).

Etymology. The specific name "*tupan*" is an allusion to the kaigang god Tupã. In the Tupi-Guarani legend about the origin of the Iguaçu waterfalls Tupã is the father of the serpent god M'Boy (Baumgartner *et al*., 2012). A noun in apposition.

FIGURE 12 | Type locality of *Cambeva tupan*, unknown name stream, tributary of rio Chopim, lower rio Iguaçu. Left upstream, right downstream.

Cambeva meandrica, new species

urn:lsid:zoobank.org:act:FD796DCB-992C-4EA1-B4FA-2F1B73E65E0E

(Figs. 2E–4E, 5, 13–14; Tab. 5)

Holotype. NUP 24953, 51.6 mm SL, Brazil, Paraná State, municipality of Palmas, unknown name stream, tributary of rio Chopim, 26°24'37.91"S 51°46'59.99"W, 11 Oct 2023, W. J. da Graça, A. Frota, W. M. Domingues & V. A. Teixeira.

Paratypes. All from Brazil, Paraná State, rio Chopim, tributary of lower rio Iguaçu basin, rio Paraná system. NUP 24855, 3, 39.1–47.4 mm SL, UFRGS 30094, 1, 39.8 mm SL, same data as holotype. NUP 25424, 4, 30.5–54.1 mm SL, NUP 25600, 2 c&s, 36.2–46.5 mm SL, unknown name stream, municipality of Palmas, 26°24'37.91"S, 51°46'59.99"W, 24 Apr 2024, W. J. da Graça, A. Frota, W. M. Domingues & V. A. Teixeira. NUP 25469, 2, 30.0–51.5 mm SL, unknown name stream, municipality of Coronel Domingos Soares, 26°20'13"S 51°55'08"W, 23 Apr 2024, W. J. da Graça, A. Frota, W. M. Domingues & V. A. Teixeira.

FIGURE 13 | *Cambeva meandrica*, holotype, NUP 24953, 51.6 mm SL, Brazil, Paraná State, unknown name stream, tributary of rio Chopim, lower rio Iguaçu, rio Paraná system.

Diagnosis. *Cambeva meandrica* can be distinguished by all congeners except *C. brachykechenos* (Ferrer & Malabarba, 2013), *C. flavopicta*, *C. grisea* Costa, Feltrin & Katz, 2021, *C. mboycy*, *C. naipi*, *C. podostemophila* Costa, Feltrin & Katz, 2023, *C. poikilos*, *C. taroba*, *C. tourensis* Costa, Feltrin & Katz, 2023, *C. galactica* by the number of pectoral-fin rays (I,5 *vs*. I,4; I,6; or I,7). *Cambeva meandrica* can be distinguished by *C. flavopicta*, *C. podostemophila*, and *C. tourensis* by the presence of pelvic fin and girdle (*vs*. absent); from *C. taroba* by the absence of filament in the first unbranched pectoral-fin ray (*vs*. presence); and from remaining congeners by the color pattern of dorsal and lateral surface of body composed of four rows (dorso-sagittal, dorso-lateral, midlateral, and ventrolateral) of rounded light-brown blotches, sometimes coalescing, and with dark-brown to black marks delimiting blotches on margins (*vs*. densely mottled dark brown over a light yellow background and progressively lighter ventrally in *C. brachykechenos*; pale brownish grey, sometimes with dark grey pigment irregularly distributed in *C. grisea*; small dark-brown spots in *C. mboycy*; presence of three well-delimited paired stripes on dorso-sagittal, lateral midline and ventrolateral surface of body in *C. naipi* and some specimens *C. poikilos*, or remaining specimens of *C. poikilos* with mottled dark-brown blotches over a light yellow background; and background of flank and dorsum only visible by longitudinal rows of interconnected yellowish white vermiculate diffuse marks in *C. galactica*).

Description. Morphometric data in Tab. 5. Body elongate, trunk roughly cylindrical close to head and gradually becoming laterally compressed towards caudal fin. Dorsal profile of trunk convex along anterior half, then slightly concave to insertion of dorsal fin. Ventral profile of trunk convex. Dorsal and ventral profile of caudal peduncle slightly convex.

Head depressed, trapezoidal in dorsal view, wider posteriorly. Dorsal profile of head straight, and ventral profile of head convex in lateral view. Snout straight to slightly convex in dorsal view. Eyes located dorsolaterally on anterior half region of head, at same longitudinal line of nasal barbel, rounded to anteroposteriorly elliptical, covered by thin and translucent skin. Orbital rim not free. Each eye located over posterior termination of shallow and small longitudinal crest beginning at posterior nostril and making eyes visible from lateral view.

Anterior nostril slightly smaller than size of eye, surrounded by flap of integument posterolaterally continuous with base of nasal barbel. Posterior nostril surrounded anterolaterally by thin flap of integument. Gill openings not constricted united with isthmus anteriorly, forming free fold reaching pectoral-fin insertion. Mouth subterminal and slightly curved with corners posteriorly oriented. Upper lip thicker laterally. Lower lip with inconspicuous fleshy lobes in lateral limits, continuous with base of rictal barbels. Lips with small and numerous rounded papillae of approximately same size.

Barbels with broad base, tapering gradually towards tips. Nasal barbel emerging from lateral region of anterior nostril with posterior tip surpassing in one eye diameter infraorbital pore i11 when adpressed to head. Maxillary barbel emerging from lateral limit of mouth with tip reaching to posterior region of interopercular odontodophore when adpressed to head. Rictal barbel emerging from lateral limit of mouth, shorter than maxillary barbel.

TABLE 5 | Morphometric data for *Cambeva meandrica*. N = Number of specimens, Min = Minimum, Max = Maximum, SD = Standard deviation.

	Holotype	N	Min	Max	Mean	SD
Standard length (mm)	51.0	8	30.0	54.1	41.4	–
Percents of standard length						
Head length	20.0	8	19.0	21.9	20.3	1.0
Predorsal length	64.7	8	63.9	66.3	65.2	0.8
Prepelvic length	61.8	8	58.0	62.4	60.4	1.9
Preanal length	74.9	8	70.7	77.0	73.4	2.4
Pectoral girdle width	16.1	8	15.4	17.7	16.6	0.9
Trunk length	43.0	8	37.9	43.0	41.5	1.6
Anal-fin Length	16.5	8	16.2	18.4	17.4	1.0
Dorsal-fin length	17.7	8	17.7	20.4	19.3	1.1
Pectoral-fin length	12.1	8	11.5	14.1	12.7	1.1
Pelvic-fin length	8.1	8	8.1	9.8	9.2	0.6
Distance between pelvic-fin base and anus	8.8	8	7.4	9.5	8.5	0.7
Caudal peduncule length	22.1	8	17.3	22.1	20.6	0.8
Caudal peduncule depth	12.9	8	12.1	14.0	13.4	0.8
Body depth	14.4	8	14.0	16.9	15.8	0.9
Length of dorsal-fin base	11.3	8	10.6	13.2	11.7	0.9
Length of anal-fin base	8.1	8	8.1	10.6	9.6	0.9
Pelvic anal distance	13.2	8	11.3	13.9	12.9	0.7
Percents of head length						
Head width	88.5	8	84.1	96.6	90.7	5.2
Rictal barbel length	77.8	8	70.2	77.8	74.2	3.5
Maxillary barbel length	72.5	8	72.5	89.9	82.5	9.0
Nasal barbel length	76.2	8	70.5	80.6	76.4	3.9
Snout lenght	39.8	8	39.8	47.0	43.0	3.5
Interorbital distance	26.9	8	26.9	35.9	31.4	3.6
Mouth width	45.9	8	34.7	54.6	45.0	7.0
Eye diameter	7.4	8	7.0	9.7	8.4	1.1
Supra-orbital pore distance	7.4	8	3.6	11.6	8.1	3.3

Pectoral fin with distal margin very rounded, I,5*(11) rays, and first ray unbranched, not prolonged as filament. Pelvic fin with distal margin rounded, reaching anterior margin of anus; I,3*(1), or I,4*(10) rays. Pelvic-fin insertion anterior to origin of dorsal-fin origin. Inner margins of pelvic fins close to each other basally by half one eye diameter. Dorsal fin with distal margin convex, II,7*(11) rays. Origin of dorsal fin located at vertical line through half of pelvic fin. Anal fin elongated with distal margin convex and smaller than dorsal fin; I,6(1), or II,5*(10) rays. Origin of anal fin located vertical line in tip of dorsal-fin base. Caudal fin with distal margin rounded; upper plate with I,4(1), or I,5*(10), rays, lower plate with I,5(1), or I,6*(10) rays.

Osteology. Mesethmoid with anterior margin straight to slightly concave and cornua short, with tapering distal ends; lateral margins with robots process, notched in posterior portion, near lateral ethmoid. Anterior cranial fontanel restricted to small, rounded opening situated between frontals and epiphyseal bar. Posterior cranial fontanel long and

wide extending from posterior portion of frontals to parieto-supraoccipital. Epiphyseal bar, longer than wide. Antorbital slightly elongate, extending over at least one-third of autopalatine. Sesamoid supraorbital elongate, rod-like shape, slightly expanded anteriorly, with small medial process on anterior third. Anterior portion of sphenotic anterolaterally directed in dorsal view. Sphenotic, prootic and pterosphenoid fused. Vomer arrow-shaped with long posterior process extending to parasphenoid. Vomer arrow-shaped with long posterior process extending to parasphenoid. Parasphenoid with long and pointed posterior process extending to basioccipital. Weberian capsule with lateral openings and anterior margin fused to basioccipital (Fig. 2E).

Premaxilla rectangular with 36(1) or 40(1) conical teeth similar in size and roughly distributed in three irregular transverse rows. Dentary with 35(1) conical teeth, similar in size, distributed in three irregular transverse rows, and ranging from base of coronoid process to near dentary symphysis (Fig. 3E). Maxilla boomerang-shaped, shorter than premaxilla. Autopalatine with lateral margin concave; anterior margin slightly convex; medial margin slightly concave with conspicuous process posteriorly extending slightly over lateral ethmoid, and long postero-lateral process pointed extending over posterior portion of metapterygoid. Metapterygoid large and laminar, connected to quadrate through cartilage. Quadrate L-shaped with concavity in anterior portion. Hyomandibula well-developed, concave in dorsal margin (Fig. 4E). Opercular odontodophore ovoid to rounded with 11(1) or 12(1) conical odontodes, gradually curving medially and increasing in size posteriorly, arranged in four irregular transverse rows. Interopercular odontodophore elongate with 26(1) or 32(1) conical odontodes, arranged in two regular transverse rows.

Ventral hypohyal trapezoid-shaped. Anterior ceratohyal elongate and wider at anterior and posterior ends. Posterior ceratohyal round with a pointed posterior process. Nine (2) branchiostegal rays: six in contact with anterior ceratohyal, two with interceratohyal cartilage, and one with posterior ceratohyal (counted in one c&s specimen). Four posteriormost branchiostegal rays, wider distally. Parurohyal with expanded anterior head, two elongate lateral processes with wide bases and decreasing in width distally with rounded tips, and sharp and elongate posterior process. Posterior process of parurohyal shorter than lateral processes.

Basibranchials 2 and 3 elongated, connected to each other by cartilage; basibranchial 2 slightly wider than basibranchial 3. Basibranchial 4 hexagonal and entirely cartilaginous. Hypobranchial 1 elongated, with cartilaginous tips, approximately same size than basibranchial 2. Hypobranchials 2 and 3 with narrow anterolateral ossified processes with large area of cartilage distally; Hypobranchial 2 thinner and longer than Hypobranchial 3. Five elongate ceratobranchials with cartilaginous tips. Ceratobranchials 1 and 4 with straight margins. Ceratobranchials 2 and 3 with concavity on posterior margin, very prominent in ceratobranchial 3. Ceratobranchial 5 with 11(1) or 13(1) conical, elongated and pointed teeth arranged in three irregular transverse rows. Four epibranchials; anteriormost three elongated and narrow with cartilage at tips. Epibranchials 1 and 2 with elongated and pointed process along anterior margins; epibranchial 3 with curved process on posterior margin. Epibranchial 4 rectangular, wider posteriorly and with cartilaginous tips. Pharyngobranchial 3 elongated, shorter than hypobranchial 1, with cartilage at tips. Pharyngobranchial 4 ossified and connected to curved plate with 14(1) or 18(1) conical, elongated and pointed teeth, arranged in three irregular transverse rows; teeth increasing in size posteriorly.

Dorsal fin with eight (2) pterygiophores, first inserted anterior to neural spine of 20th (2) vertebrae. Anal fin with six (2) pterygiophores, first inserted anterior to haemal spine of 23rd (1) or 24th (1) vertebrae. Procurrent caudal-fin rays 18(1) or 21(1) dorsally and 14(1) or 16(1) ventrally. Hypural 3 free and hypurals 4 and 5 fused to each other. Parhypural and hypurals 1 and 2 co-ossified and fused to compound caudal centrum. Free vertebrae 37(1) or 38(1), and 14(1) or 16(1) pairs of ribs.

Laterosensory system. Laterosensory canals with simple (non-dendritic) branches ending in single pores. Nasal and frontal canals of supraorbital branch continuous, with three (11) paired pores s1, s3 and s6. Supraorbital pore s1 located at posterior portion of anterior nostrils, pore s3 at same longitudinal line of pore s1 posteriorly to posterior nostrils and pore s6 aligned with posterior margin of eyes. Antorbital segment of infraorbital canal present with two (11) pores, i1 laterally through posterior region of anterior nostril, and pore i3 laterally through anterior region of posterior nostril. Sphenotic canal present with two (11) pores, i10, located behind eyes, and pore i11 located laterally to posterior margin of eye. One specimen with two i11 pores in left side of head. Otic and postotic canals present with two (11) pores associated: po1 located anterolaterally to opercular odontodophore and po2 located laterally to half-length of opercular odontodophore. Lateral line canal short with two (10) or four (1) pores located above pectoral-fin insertion and posterior to gill opening.

Coloration in alcohol. Dorsal and lateral surface of body composed of four rows (dorso-sagittal, dorso-lateral, midlateral, and ventrolateral) rounded light-brown blotches, sometimes coalescing, with dark-brown to black marks delimiting blotches on margins. Background of body yellowish, visible on ventral region of body and head, and between rows of blotches. Head densely pigmented by smaller rounded blotches, being scattered on lateral region of head. Pectoral, dorsal, anal, and caudal fins with few inconspicuous dark-brown spots equivalent or slightly larger in size to eye diameter, over yellowish background. Pelvic fin yellowish. Barbels with dark-brown spots of melanophores on dorsal surface, and yellowish ventrally.

Geographical distribution. *Cambeva meandrica*, is known from two different unknown name streams, both tributaries of rio Chopim, tributary of the left margin of the lower section of rio Iguaçu (*sensu* Ingenito *et al*., 2004), Paraná State, Brazil (Fig. 5).

Ecological notes. The type locality of *Cambeva meandrica* is situated at an elevation of 1,100 m above sea level. The terrestrial forest is dominated by *Araucaria angustifolia* (Bertol.) Kuntze, with grasses interspersed among the trees. The water depth is approximately 30 cm, and the habitat consists of fast-flowing waters, with a substrate composed of rocks ranging from 5 to 30 cm in diameter (Fig. 14). The species occurs in sympatry with *Cnesterodon* sp. and *Psalidodon* sp.

FIGURE 14 | Type locality of *Cambeva meandrica*, unknown name stream, tributary of rio Chopim, lower rio Iguaçu basin, Paraná State, Brazil. Left downstream, right upstream.

Conservation status. *Cambeva meandrica* can be found in two localities, in the rio Chopim basin. The new species has an EOO of 226 km² (< 5,000 km2 in criteria B1 for EN), although no threat has been found in the localities of occurrence of the new species. Therefore, *C. meandrica* does not meet any condition of this criteria, and according to the International Union for Conservation of Nature (IUCN) categories and criteria (IUCN Standards and Petitions Subcommittee, 2024), thus our recommendations is that this species can be classified as Least Concern (LC).

Etymology. The specific name "*meandrica*" is derived from the Latinized Greek word *meandros* (Μαίανδρος), referring to a winding or sinuous pattern, in allusion to the intricate network of light-brown blotches bordered by dark margins on the body of the species. An adjective in feminine form.

Cambeva wosiackii, new species

urn:lsid:zoobank.org:act:14CBBF9B-D097-46D1-BC88-6E6451C6E697

(Figs. 2F–4F, 5–6, 15; Tab. 6)

Trichomycterus sp. 1. —Baumgartner *et al*., 2012:111 (checklist from lower rio Iguaçu).
Cambeva sp. 1. — dos Reis *et al*., 2020:471 (checklist of freshwater fishes from Paraná State).

Holotype. NUP 19053, 51.6 mm SL, Brazil, Paraná State, municipality of Santa Tereza do Oeste, córrego Jumelo, tributary of rio Gonçalves Dias, lower rio Iguaçu basin, rio Paraná system, 25°04'47"S 53°37'26"W, 20 May 2015, R. Delariva.

Paratypes. All from Brazil, Paraná State, rio Gonçalves dias, tributary of lower rio Iguaçu basin, rio Paraná system. NUP 25602, 2 c&s, 51.9–60.0 mm SL, UFRGS 30095, 3, 45.2–66.7 mm SL, same data as holotype. MZUSP 130927, 5, 41.6–63.2 mm SL, municipality of Santa Tereza do Oeste, 25°03'48"S 53°36'16"W, 20 Sep 2011, R. Delariva. NUP 16944, 2, 52.2–74.1 mm SL, municipality of Santa Tereza do Oeste, riacho Jumelo, 25°04'47"S 53°37'26"W, 30 Nov 2011, R. Delariva. NUP 24848, 1,

FIGURE 15 | *Cambeva wosiackii*. **A.** Holotype, NUP 19053, 51.6 mm SL, Brazil, Paraná State, córrego Jumelo, tributary of rio Gonçalves Dias, lower rio Iguaçu, lower rio Paraná system. **B.** Paratype, MZUSP 130927, 42.8 mm SL.

40.8 mm SL, municipality of Santa Tereza do Oeste, 25°04'51.10"S 53°37'18.62"W, 11 Sep 2023, R. B. Reis, B. H. M. Stabile, M. Z. Roloff, C. E. V. Grou, L. D. Lima & S. K. Utiyama.

Diagnosis. *Cambeva wosiackii* can be distinguished by all congeners except *C. chrysornata* Costa, Feltrin, Mattos, Dalcin, Abilhoa & Katz, 2023, *C. diatropoporos* (Ferrer & Malabarba, 2013), *C. difficilis*, *C. duplimaculata* Costa, Feltrin & Katz, 2021, *C. flavopicta*, *C. galactica*, *C. guaraquessaba* (Wosiacki, 2005), *C. guaratuba* Costa, Feltrin, Mattos, Dalcin, Abilhoa & Katz, 2023, *C. iheringi* (Eigenmann, 1917), *C. longipalata* Costa, Feltrin & Katz, 2021, some specimens of *C. mboycy*, *C. meandrica*, *C. notabilis* Costa, Feltrin & Katz, 2021, *C. taroba*, *C. tropeiro* (Ferrer & Malabarba, 2011), *C. tupinamba*, *C. urubici*, *C. papillifera* and *C. ventropapillata* Costa, Feltrin, Mattos, Dalcin, Abilhoa & Katz, 2023 by the modally presence of the infraorbital pores i1, and i3 (*vs*. absent). *Cambeva wosiackii* can be distinguished by *C. flavopicta*, and *C. tropeiro* by the presence of pelvic fin and girdle (*vs*. absent); by *C. papillifera*, and *C. ventropapillata* by the absence of hypertrophied papillae on ventral region of head (*vs*. present); by the number of pectoral-fin rays (I,6 *vs*. I,5 in *C. galactica*, *C. meandrica*, *C. mboycy*, *C. taroba*; I,7 in *C. difficilis*, *C. guaraquessaba*, *C. iheringi*, and *C. tupinamba*). *Cambeva wosiackii* can be distinguished by the color pattern of body and surface of body composed of dark-brown spots concentrated, and forming irregular dark-brown blotches, sometimes ring-like (clear on middle region) (*vs*. presence of irregularly shaped yellow reticulation, forming a golden longitudinal dorso-lateral stripe, from opercular odontodophores region to dorsal-fin origin in *C. chrysornata*; presence of dark-brown blotches, coalescing and forming irregular blotches, with few light yellow gaps in *C. diatropoporos* and *C. guaratuba*; presence of rounded well-defined blotches on inner skin layer in *C. duplimaculata*, *C. longipalata*, and *C. notabilis*; and blotches on mid-lateral line of body coalescing and forming irregular stripe in *C. urubici*).

Description. Morphometric data in Tab. 6. Body elongate, trunk roughly cylindrical close to head and gradually becoming laterally compressed towards caudal fin. Dorsal profile of trunk straight to slightly concave. Ventral profile of trunk convex. Dorsal profile of caudal peduncle slightly convex and ventral profile of caudal peduncle slightly concave.

Head depressed, trapezoidal in dorsal view, wider posteriorly. Dorsal profile of head straight, and ventral profile of head convex in lateral view. Snout straight to slightly convex in dorsal view. Eyes located dorsolaterally on anterior half region of head, at same longitudinal line of nasal barbel, rounded to anteroposteriorly elliptical, covered by thin and translucent skin. Orbital rim not free. Each eye located over posterior termination of shallow and small longitudinal crest beginning at posterior nostril and making eyes visible from lateral view.

Anterior nostril slightly smaller than size of eye, surrounded by flap of integument posterolaterally continuous with base of nasal barbel. Posterior nostril surrounded anterolaterally by thin flap of integument. Gill openings not constricted united with isthmus anteriorly, forming free fold reaching pectoral-fin insertion. Mouth subterminal and slightly curved with corners posteriorly oriented. Upper lip thicker laterally. Lower lip with inconspicuous fleshy lobes in lateral limits, continuous with base of rictal barbels. Lips with small and numerous rounded papillae of approximately same size.

Barbels with broad base, tapering gradually towards tips. Nasal barbel emerging from lateral region of anterior nostril with posterior tip reaching infraorbital pore i11 when adpressed to head. Maxillary barbel emerging from lateral limit of mouth with tip reaching to posterior region of interopercular odontodophore when adpressed to head. Rictal barbel emerging from lateral limit of mouth, shorter than maxillary barbel.

Pectoral fin with distal margin straight to slightly convex, I,5(3), I,6*(11) rays, and first ray unbranched, not prolonged as filament* (9), or prolonged as small filament (5) about one-fourteenth pectoral-fin length. Pelvic fin with distal margin rounded, not reaching anterior margin of anus; I,4*(14) rays. Pelvic-fin insertion anterior to origin of dorsal-fin origin. Inner margins of pelvic fins very close basally. Dorsal fin with distal margin convex, II,6,I(1) or II,7*(13) rays. Origin of dorsal fin located at vertical line through last third of pelvic fin. Anal fin elongated with distal margin convex and smaller than dorsal fin; II,5*(14) rays. Origin of anal fin located vertical line through last third dorsal-fin base. Caudal fin with distal margin rounded; upper plate with I,5*(14) rays, lower plate with I,5(2), or I,6*(12) rays.

TABLE 6 | Morphometric data for *Cambeva wosiackii*. N = Number of specimens, Min = Minimum, Max = Maximum, SD = Standard deviation.

	Holotype	N	Min	Max	Mean	SD
Standard length (mm)	73.5	14	40.6	75.4	55.3	–
Percents of standard length						
Head length	19.7	14	17.8	20.3	19.2	1.0
Predorsal length	66.3	14	63.4	66.3	65.3	0.7
Prepelvic length	60.9	14	56.4	60.9	59.2	2.0
Preanal length	75.4	14	69.9	75.4	73.0	1.7
Pectoral girdle width	14.9	14	13.5	16.3	15.2	1.0
Trunk length	42.5	14	38.9	42.5	40.8	1.4
Anal-fin Length	15.9	14	15.4	16.7	16.1	0.5
Dorsal-fin length	19.1	14	16.6	20.0	18.6	1.4
Pectoral-fin length	11.1	14	11.1	16.7	13.0	2.5
Pelvic-fin length	8.9	14	8.3	9.5	8.8	0.5
Distance between pelvic-fin base and anus	9.6	14	8.8	11.3	10.2	1.2
Caudal peduncule length	19.4	14	18.0	20.7	20.0	0.5
Caudal peduncule depth	12.4	14	11.2	12.9	12.7	0.2
Body depth	15.3	14	11.3	15.3	14.1	1.0
Length of dorsal-fin base	11.4	14	10.3	12.5	11.6	0.9
Length of anal-fin base	8.2	14	6.8	9.5	8.9	0.7
Pelvic Anal distance	14.8	14	13.2	14.8	14.3	0.7
Percents of head length						
Head width	81.5	14	81.5	89.2	85.8	3.2
Rictal barbel length	52.0	14	52.0	71.0	59.3	8.4
Maxillary barbel length	60.0	14	60.0	74.9	69.0	6.4
Nasal barbel length	56.9	14	56.9	72.0	67.0	6.8
Snout lenght	38.9	14	38.9	45.8	43.2	3.0
Interorbital distance	26.8	14	23.7	28.6	26.7	2.1
Mouth width	42.2	14	37.3	47.5	42.4	4.1
Eye diameter	6.5	14	5.9	9.4	7.6	1.6
Supra-orbital pore distance	12.0	14	12.0	15.9	14.4	1.8

Osteology. Mesethmoid with anterior margin straight to slightly concave and cornua short, with tapering distal ends. Anterior cranial fontanel restricted to small, rounded opening situated between frontals and epiphyseal bar. Posterior cranial fontanel long and wide extending from posterior portion of frontals to parieto-supraoccipital. Epiphyseal bar, longer than wide. Antorbital slightly elongate, extending over at least one-third of autopalatine. Sesamoid supraorbital elongate, rod-like shape, slightly expanded anteriorly, with small medial process on anterior third. Anterior portion of sphenotic anterolaterally directed in dorsal view. Sphenotic, prootic and pterosphenoid fused. Vomer arrow-shaped with long posterior process extending to parasphenoid. Vomer arrow-shaped with long posterior process extending to parasphenoid. Parasphenoid with long and pointed posterior process extending to basioccipital. Weberian capsule with lateral openings and anterior margin fused to basioccipital (Fig. 2F).

Premaxilla rectangular with 51(1) or 53(1) conical teeth similar in size and roughly distributed in four irregular rows. Dentary with 49 or 58(2) conical to spatulate teeth, similar in size, distributed in three irregular transverse rows, and ranging from base of coronoid process to near dentary symphysis (Fig. 3F). Maxilla boomerang-shaped, shorter than premaxilla. Autopalatine with lateral margin concave; anterior margin slightly convex; medial margin slightly concave and long posterior process extending over posterior portion of metapterygoid. Metapterygoid large and laminar, connected to quadrate through cartilage. Quadrate L-shaped with concavity in anterior portion. Hyomandibula well-developed slightly concave in dorsal margin (Fig. 4F). Opercular odontodophore ovoid to rounded with 13(1) or 15(1) conical odontodes, gradually curving medially and increasing in size posteriorly, arranged in six irregular rows. Interopercular odontodophore elongate with 24(1) or 25(1) conical odontodes, arranged in two regular transverse rows.

Ventral hypohyal trapezoid-shaped. Anterior ceratohyal elongate and wider at anterior and posterior ends. Posterior ceratohyal round with a pointed posterior process. Eight (2) branchiostegal rays: five in contact with anterior ceratohyal, two with interceratohyal cartilage, and one with posterior ceratohyal. Four posteriormost branchiostegal rays, wider distally. Parurohyal with expanded anterior head, two elongate lateral processes with wide bases and decreasing in width distally with rounded tips, and sharp and elongate posterior process. Posterior process of parurohyal shorter than lateral processes.

Basibranchials 2 and 3 elongated, connected to each other by cartilage; basibranchial 2 slightly wider than basibranchial 3. Basibranchial 4 hexagonal and entirely cartilaginous. Hypobranchial 1 elongated, with cartilaginous tips, approximately same size than basibranchial 2. Hypobranchials 2 and 3 with narrow anterolateral ossified processes with large area of cartilage distally; Hypobranchial 2 thinner and longer than Hypobranchial 3. Five elongate ceratobranchials with cartilaginous tips. Ceratobranchials 1 and 4 with straight margins. Ceratobranchials 2 and 3 with concavity on posterior margin, prominent in ceratobranchial 3. Ceratobranchial 5 with 22(1) conical, elongated and pointed teeth arranged in three irregular transverse rows. Four epibranchials; anteriormost three elongated and narrow with cartilage at tips. Epibranchials 1 and 2 with elongated and pointed process along anterior margins; epibranchial 3 with curved process on posterior margin. Epibranchial 4 rectangular, wider posteriorly and with cartilaginous tips. Pharyngobranchial 3 elongated, shorter than hypobranchial 1, with

cartilage at tips. Pharyngobranchial 4 ossified and connected to curved plate with 26(1) conical, elongated and pointed teeth, arranged in up to three irregular transverse rows; teeth increasing in size posteriorly.

Dorsal fin with eight pterygiophores, first inserted anterior to neural spine of 18th vertebrae. Anal fin with six pterygiophores, first inserted anterior to haemal spine of 22nd vertebrae. Procurrent caudal-fin rays 20(1) dorsally and 12(1) ventrally. Hypural 3 free and hypurals 4 and 5 fused to each other. Parhypural and hypurals 1 and 2 co-ossified and fused to compound caudal centrum. Free vertebrae 37(2), and 14(2) pairs of ribs.

Laterosensory system. Laterosensory canals with simple (non-dendritic) branches ending in single pores. Nasal and frontal canals of supraorbital branch continuous, with three (14) paired pores s1, s3 and s6. Supraorbital pore s1 located at posterior portion of anterior nostrils, pore s3 at same longitudinal line of pore s1 posteriorly to posterior nostrils and pore s6 aligned with posterior margin of eyes. Antorbital segment of infraorbital canal present (9) with two pores, i1 laterally through posterior region of anterior nostril, and pore i3 laterally through anterior region of posterior nostril. Five specimens with antorbital segment of infraorbital canal absent. Sphenotic canal present with two (14) pores, i10, located behind eyes, and pore i11 located laterally to posterior margin of eye. One specimen with two pores i11 in left side of head. Otic and postotic canals present with two (14) pores associated: po1 located anterolaterally to opercular odontodophore and po2 located laterally to half-length of opercular odontodophore. Lateral line canal short with two* (14) pores located above pectoral-fin insertion and posterior to gill opening.

Coloration in alcohol. Dorsal and lateral surface of body and head composed of dark-brown spots the size of eye diameter, concentrated and forming irregular dark-brown blotches, sometimes ring-like (clear on middle region). Background of body yellowish, visible on ventral region of body and head, and between rows of blotches. Head densely pigmented by rounded blotches, being scattered on lateral region of head. Pectoral, pelvic, dorsal, anal, and caudal fins with few inconspicuous dark-brown spots equivalent or slightly larger in size to eye diameter, over yellowish background. Barbels with dark-brown spots of melanophores on dorsal surface, and yellowish ventrally.

Geographical distribution. *Cambeva wosiackii* is known from the córrego Jumelo (type locality), a tributary of rio Gonçalves Dias, and in the rio Gonçalves Dias, all from the lower section of rio Iguaçu (*sensu* Ingenito *et al*., 2004), Paraná State, Brazil (Fig. 5).

Ecological notes. The type locality of *C. wosiackii* is located at an elevation of 600 m above sea level, near the boundary of Iguaçu National Park, one of the most important environmental preservation areas in Brazil. The substrate is composed of rocks beds and rocks and peebles of 5 to 30 cm (Fig. 6). The species occurs in sympatry in the type locality with *Ancistrus mullerae*, *B. pyahu*, *C. kaingang*, *P. circummontanus*, *Psalidodon bifasciatus*, *P. dissimilis*, and *R. branneri*.

Conservation status. *Cambeva wosiackii* can be found in two localities, in the Rio Gonçalves Dias basin. The new species has an EOO of 177 km² (< 5,000 km² in criteria B1 for EN), although no threat has been found in the localities of occurrence of the new species. Furthermore, the species are found in the edges of the Iguaçu National Park, an well-conserved federal protected area. Therefore, *C. wosiackii* does not meet any condition of this criteria, and according to the International Union for Conservation of Nature (IUCN) categories and criteria (IUCN Standards and Petitions Subcommittee, 2024), thus our recommendations is that this species can be classified as Least Concern (LC).

Etymology. The specific name "*wosiackii*" is given in honor of Dr. Wolmar Benjamin Wosiacki (MPEG), for his contributions to the taxonomy of Trichomycteridae from the rio Iguaçu basin, and contributions to taxonomy, evolution, and phylogeny of Neotropical fishes. A genitive.

Cambeva longistriata, new species

urn:lsid:zoobank.org:act:19BE9864-B30F-4B11-8305-041ED93D004E

(Figs. 2G–4G, 5, 16–17; Tab. 7)

Holotype. NUP 25430, 48.6 mm SL, Brazil, Paraná State, municipality of Coronel Domingos Soares, unknown name stream, tributary of rio Butiá, 26°11'34.10"S 52°02'26.17"W, 22 Apr 2024, W. J. da Graça, A. Frota, W. M. Domingues & V. A. Teixeira.

Paratype. All from Brazil, Paraná State, municipality of Coronel Domingos Soares, rio Butiá, tributary of lower rio Iguaçu basin, rio Paraná system. MZUSP 130928, 10, 33.0–45.2 mm SL, NUP 25292, 3, 37.0–42.9 mm SL, NUP 25428, 19, 30.0–75.0 mm SL, NUP 25599, 2 c&s, 47.9–48.2 mm SL, UFRGS 30096, 10, 36.0–55.3 mm SL, unknown name stream, 26°11'34.10"S 52°02'26.17"W, 22 Apr 2024, W. J. da Graça, A. Frota, W. M. Domingues & V. A. Teixeira. NUP 25234, 2, 44.4–50.6 mm SL, NUP 25429, 2, 52.0–54.1 mm SL, NUP 25603, 1 c&s, 52.8 mm SL, unknown name stream, 26°13'47.45"S 52°02'4.88"W, 23 Apr 2024, W. J. da Graça, A. Frota, W. M. Domingues & V. A. Teixeira.

Diagnosis. *Cambeva longistriata* is distinguished from all congeners except of *C. perkos* and *C. piraquara* by having a conspicuous, wide, with the size of opercular odontodophore, continuous and irregularly bordered dark-brown longitudinal mid-lateral stripe, extending from the opercular odontodophores to the base of caudal-fin rays (*vs.* presence of dark-brown blotches, spots, or bars, but never forming a longitudinal stripe or, when present, formed by a narrow, continuous, and well-defined dark-brown longitudinal mid-lateral stripe in *C. naipi* and *C. pascuali*; narrow longitudinal mid-lateral stripe composed of rounded blotches, two or three times the size of the eyes, in *C. biseriata*; lateral surface of body composed of juxtaposed large darkbrown blotches, forming a stripe along the lateral midline, irregularly bordered until vertical through the end of the dorsal fin base or peduncle caudal in some small

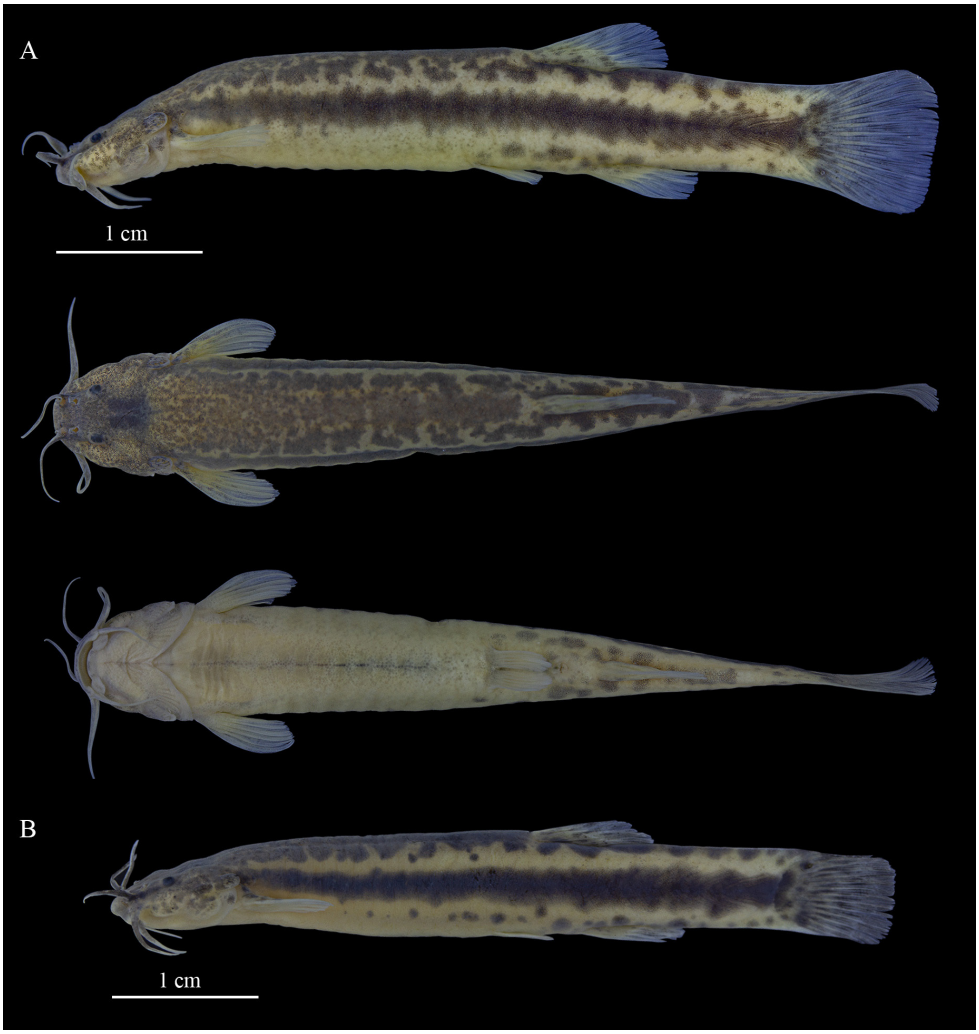

FIGURE 16 | *Cambeva longistriata*. **A.** Holotype, NUP 25430, 48.6 mm SL, **B.** Paratype, NUP 25428, 42.1 mm SL, both from Brazil, Paraná State, unknown name stream, tributary of rio Butiá.

specimens of *C. davisi*, and *C. zonata*; narrow longitudinal mid-lateral stripe, two times the size of eyes diameter, well-defined and never interrupted in small specimens of *C. poikilos*; by the lateral surface of body composed of large, with same size as opercular odontodophore, dark-brown rounded blotches coalescing and forming irregularly bordered and sometimes interrupted longitudinal band, from opercular region to base of caudal-fin ray in *C. balios*, *C. botuvera*, *C. cubataonis*, *C. kaingang*, and C. *urubici*; and narrow longitudinal stripe formed by closely spaced dark-brown spots, with size of eyes diameter, from opercle to vertical through anal-fin origin, and continuing posteriorly to caudal peduncle in *C. tupinamba*). *Cambeva longistriata* can be distinguished by *C. perkos* by the absence of dorso-lateral continuous dark-brown stripe on the surface of body (*vs*. presence of dorso-lateral continuous dark-brown stripe on the surface of body); and by *C. piraquara* by absence of dorso-sagital stripe, composed of coalesced dark-brown blotches (*vs*. presence of dorso-sagital stripe). Additionally, *C. longistriata* can be distinguished by *C. perkos* by the absence of dark-brown spots on the lateral

surface of body (*vs*. presence of dark-brown spots on the lateral surface of body), and by the vertical origin of dorsal-fin being through the tips of pelvic fin (*vs*. vertical origin of dorsal-fin being through anus or papilla urogenital).

Description. Morphometric data in Tab. 7. Body elongate, trunk roughly cylindrical close to head and gradually becoming laterally compressed towards caudal fin. Dorsal profile of trunk straight to convex on anterior half of body. Ventral profile of trunk convex. Dorsal and ventral profile of caudal peduncle concave.

Head depressed, trapezoidal in dorsal view, wider posteriorly. Dorsal profile of head straight, and ventral profile of head convex in lateral view. Snout convex in dorsal view. Eyes located dorsolaterally on anterior half region of head, at same longitudinal line of nasal barbel, rounded to anteroposteriorly elliptical, covered by thin and translucent skin. Orbital rim not free. Each eye located over posterior termination of shallow and small longitudinal crest beginning at posterior nostril and making eyes visible from lateral view.

TABLE 7 | Morphometric data for *Cambeva longistriata*. N = Number of specimens, Min = Minimum, Max = Maximum, SD = Standard deviation.

	Holotype	N	Min	Max	Mean	SD
Standard length (mm)	48.6	18	39.4	55.1	44.8	–
Percents of standard length						
Head length	18.4	18	17.1	18.8	18.3	0.3
Predorsal length	64.2	18	59.6	65.7	64.1	1.1
Prepelvic length	56.3	18	54.7	57.9	56.7	1.2
Preanal length	69.9	18	68.4	72.1	70.3	1.4
Pectoral girdle width	15.9	18	13.5	15.9	14.6	0.7
Trunk length	39.6	18	38.2	41.0	39.8	1.1
Anal-fin Length	15.0	18	12.9	16.2	15.3	0.6
Dorsal-fin length	18.4	18	14.9	19.4	18.5	0.5
Pectoral-fin length	12.9	18	11.9	13.4	12.7	0.6
Pelvic-fin length	8.9	17	8.1	9.4	8.7	0.5
Distance between pelvic-fin base and anus	3.5	18	3.5	10.9	8.6	3.0
Caudal peduncle length	23.0	18	18.0	24.7	23.0	1.0
Caudal peduncle depth	11.5	18	9.5	11.5	10.7	0.6
Body depth	14.5	18	12.3	15.1	14.2	0.9
Length of dorsal-fin base	12.1	18	8.7	12.1	11.3	0.6
Length of anal-fin base	8.3	18	6.5	11.0	8.6	1.5
Pelvic anal distance	14.1	18	11.1	15.0	13.6	1.4
Percents of head length						
Head width	89.2	18	78.9	89.8	86.3	4.7
Rictal barbel length	49.3	18	49.3	60.4	54.0	4.1
Maxillary barbel length	65.4	18	53.1	65.4	60.6	5.0
Nasal barbel length	56.8	18	55.0	61.7	57.7	2.4
Snout lenght	38.1	18	38.1	43.6	41.4	2.3
Interorbital distance	25.3	18	21.6	27.9	24.7	2.2
Mouth width	30.9	18	30.9	40.2	35.7	3.7
Eye diameter	10.0	18	9.0	13.2	10.6	1.5
Supra-orbital pore distance	16.8	18	12.1	17.5	14.7	2.3

Anterior nostril slightly smaller than size of eye, surrounded by flap of integument posterolaterally continuous with base of nasal barbel. Posterior nostril surrounded anterolaterally by thin flap of integument. Gill openings not constricted united with isthmus anteriorly, forming free fold reaching pectoral-fin insertion. Mouth subterminal and slightly curved with corners posteriorly oriented. Upper lip thicker laterally. Lower lip with conspicuous fleshy lobes in lateral limits, continuous with base of rictal barbels. Lips with small and numerous rounded papillae of approximately same size.

Barbels with broad base, tapering gradually towards tips. Nasal barbel emerging from lateral region of anterior nostril with posterior tip surpassing infraorbital pore i11 when adpressed to head. Maxillary barbel emerging from lateral limit of mouth with tip reaching to posterior region of interopercular odontodophore when adpressed to head. Rictal barbel emerging from lateral limit of mouth, shorter than maxillary barbel.

Pectoral fin with distal margin convex, I,5*(1), I,6(19) rays, and first ray unbranched, not prolonged as filament. Pelvic fin with distal margin rounded, reaching anterior margin of anus; I,4*(20) rays. Pelvic-fin insertion anterior to origin of dorsal-fin origin. Inner margins of pelvic fins very close basally. Dorsal fin with distal margin convex, II,7*(12), or II,6(8) rays. Origin of dorsal fin located at vertical line through last third of pelvic fin. Anal fin elongated with distal margin convex and smaller than dorsal fin; II,5*(20) rays. Origin of anal fin located vertical line through last third dorsal-fin base. Caudal fin with distal margin rounded; upper plate with I,5*(20) rays, lower plate with I,6*(20) rays.

Osteology. Mesethmoid with anterior margin straight to slightly concave and cornua short, with tapering distal ends. Anterior cranial fontanel absent. Posterior cranial fontanel long and wide extending from posterior portion of frontals to parieto-supraoccipital. Epiphyseal bar absent, or not ossified. Antorbital slightly elongate, extending over at least one-third of autopalatine. Sesamoid supraorbital elongate, rod-like shape, slightly expanded anteriorly, with small medial process on anterior third. Anterior portion of sphenotic anterolaterally directed in dorsal view. Sphenotic, prootic and pterosphenoid fused. Vomer arrow-shaped with long posterior process extending to parasphenoid. Vomer arrow-shaped with long posterior process extending to parasphenoid. Parasphenoid with long and pointed posterior process extending to basioccipital. Weberian capsule with lateral openings and anterior margin fused to basioccipital (Fig. 2G).

Premaxilla rectangular with 27 or 29(2) spatulate teeth similar in size and roughly distributed in three irregular rows. Dentary with 29(1) spatulate teeth, similar in size, distributed in three irregular transverse rows, and ranging from base of coronoid process to near dentary symphysis (Fig. 3G). Maxilla boomerang-shaped, shorter than premaxilla. Autopalatine with lateral margin concave; anterior margin slightly convex; medial margin slightly concave with conspicuous process posteriorly extending slightly over lateral ethmoid, and long postero-lateral process pointed extending over posterior portion of metapterygoid. Metapterygoid large and laminar, connected to quadrate through cartilage. Quadrate L-shaped with concavity in anterior portion. Hyomandibula well-developed, concave in dorsal margin (Fig. 4G). Opercular odontodophore ovoid to rounded with 6 or 7(3) conical odontodes, gradually curving medially and increasing in size posteriorly, arranged in six irregular rows. Interopercular odontodophore elongate with 21(1) conical odontodes, arranged in two regular transverse rows.

Ventral hypohyal trapezoid-shaped. Anterior ceratohyal elongate and wider at anterior and posterior ends. Posterior ceratohyal round with a pointed posterior process. Eight (1) or nine (2) branchiostegal rays: five in contact with anterior ceratohyal, one or two with interceratohyal cartilage, one with posterior ceratohyal. Four posteriormost branchiostegal rays, wider distally. Parurohyal with expanded anterior head, two elongate lateral processes with wide bases and decreasing in width distally with rounded tips, and sharp and elongate posterior process. Posterior process of parurohyal shorter than lateral processes.

Basibranchials 2 and 3 elongated, connected to each other by cartilage; basibranchial 2 slightly wider than basibranchial 3. Basibranchial 4 hexagonal and entirely cartilaginous. Hypobranchial 1 elongated, with cartilaginous tips, approximately same size than basibranchial 2. Hypobranchials 2 and 3 with narrow anterolateral ossified processes with large area of cartilage distally; Hypobranchial 2 thinner and longer than Hypobranchial 3. Five elongate ceratobranchials with cartilaginous tips. Ceratobranchials 1 and 4 with straight margins. Ceratobranchials 2 and 3 with concavity on posterior margin, very prominent in ceratobranchial 3. Ceratobranchial 5 with 15(2) or 22(1) conical, elongated and pointed teeth arranged in three irregular transverse rows. Four epibranchials; anteriormost three elongated and narrow with cartilage at tips. Epibranchials 1 and 2 with elongated and pointed process along anterior margins; epibranchial 3 with curved process on posterior margin. Epibranchial 4 rectangular, wider posteriorly and with cartilaginous tips. Pharyngobranchial 3 elongated, shorter than hypobranchial 1, with cartilage at tips. Pharyngobranchial 4 ossified and connected to curved plate with 17(2) or 18(1) conical, elongated and pointed teeth, arranged in up to three irregular transverse rows; teeth increasing in size posteriorly.

Dorsal fin with eight pterygiophores, first inserted anterior to neural spine of 18th vertebrae. Anal fin with six pterygiophores, first inserted anterior to haemal spine of 22nd vertebrae. Procurrent caudal-fin rays 16(2) or 17(1) dorsally and 9–11(3) ventrally. Hypural 3 free and hypurals 4 and 5 fused to each other. Parhypural and hypurals 1 and 2 co-ossified and fused to compound caudal centrum. Free vertebrae 37(1) or 38(2), and 13(2) or 14(1) pairs of ribs.

Laterosensory system. Laterosensory canals with simple (non-dendritic) branches ending in single pores. Nasal and frontal canals of supraorbital branch continuous, with three (20) paired pores s1, s3 and s6. Supraorbital pore s1 located at posterior portion of anterior nostrils, pore s3 at same longitudinal line of pore s1 posteriorly to posterior nostrils and pore s6 aligned with posterior margin of eyes. Antorbital segment of infraorbital canal absent. Sphenotic canal present with two (20) pores, i10, located behind eyes, and pore i11 located laterally to posterior margin of eye. Otic and postotic canals present with two (20) pores associated: po1 located anterolaterally to opercular odontodophore and po2 located laterally to half-length of opercular odontodophore. Lateral line canal short with two (20) pores located above pectoral-fin insertion and posterior to gill opening.

Coloration in alcohol. Dorsal region of body and head with irregular dark-brown blotches, with same size as opercular odontodophore, from snout to posterior region of caudal peduncle. Lateral surface of body composed of conspicuous, wide, with size of opercular odontodophore, continuous and irregularly bordered dark-brown longitudinal mid-lateral stripe, extending from the opercular odontodophores to the base of caudal-fin rays. Rounded dark-brown blotches, with size of two eyes diameter, randomly distributed between sagittal line of body and lateral line of body, and ventral portion of lateral surface of body. Background of body yellowish, readily visible in ventral surface of body and head. Head densely pigmented by smallers rounded blotches, being scattered on lateral region of head. Pectoral, dorsal, anal, and caudal fins with few inconspicuous dark-brown blotches equivalent or slightly larger in size to eye diameter, over yellowish background. Pelvic fin yellowish. Barbels with dark-brown blotches on dorsal surface. Smallers specimens (< 40.0 mm SL) with longitudinal stripe on lateral surface of body with few irregular borders (Fig. 16B).

Geographical distribution. *Cambeva longistriata*, is only known from two unknown name streams, tributaries of rio Butiá, tributary of left margin of the lower section of rio Iguaçu (*sensu* Ingenito *et al*., 2004), Paraná State, Brazil (Fig. 5).

Ecological notes. The type locality of *C. longistriata* is located at an elevation of 1,000 m above sea level. The water level reaches 30–60 cm, and the substrate is composed of rocks of 5 to 30 cm (Fig. 17). The species occurs in sympatry in the type locality with *Neoplecostomus* sp., *Pareiorhaphis parmula* Pereira, 2005, *Phalloceros circummontanus*, and *Rhamdia voulezi* Haseman, 1911.

Conservation status. *Cambeva longistriata* can be found in two localities, in the Rio Butiá basin. The new species has an EOO of 164.3 km² (< 5,000 km² in criteria B1 for EN), although no threat has been found in the localities of occurrence of the new species. Therefore, *C. longistriata* does not meet any condition of this criteria, and according to the International Union for Conservation of Nature (IUCN) categories and criteria (IUCN Standards and Petitions Subcommittee, 2024), thus our recommendations is that this species can be classified as Least Concern (LC).

Etymology. The specific name "*longistriata*" is derived from the Latin words *longus* (long) and *striatus* (striped), in reference to the continuous longitudinal stripe along the lateral surface of the body of the species. An adjective in feminine form.

FIGURE 17 | Type locality of *Cambeva longistriata*, unknown name stream, tributary of rio Butiá, lower rio Iguaçu basin, Paraná State, Brazil. Left downstream, right upstream.

Cambeva ytepopo, new species

urn:lsid:zoobank.org:act:3EC4A216-B1EB-4EA5-8CE6-438D24AF3E0D

(Figs. 2H–4H, 5; Tab. 8)

Holotype. NUP 25875, 61.6 mm SL, Brazil, Paraná State, municipality of Coronel Domingos Soares, unknown name stream, tributary of rio Butiá, lower rio Iguaçu basin, rio Paraná system, 26°08'45.10"S 52°05'01"W, 22 Apr 2024, W. J. da Graça, A. Frota, W. M. Domingues & V. A. Teixeira.

Paratype. MZUSP 130929, 2, 36.7–42.5 mm SL, NUP 25314, 2, 43.3–49.3 mm SL, NUP 25427, 2, 34.3–47.7 mm SL, NUP 25876, 3 c&s, 35.8–43.1 mm SL, UFRGS 30097, 2, 35.5–44.2 mm SL, same data as holotype.

Diagnosis. *Cambeva ytepopo*, can be distinguished by the congeners except *C. atrobrunnea*, *C. balios*, *C. davisi*, *C. diffusa* Costa, Feltrin & Katz, 2021, *C. horacioi* dos Reis, Frota, Fabrin & da Graça, 2019, *C. longipalata*, *C. mboycy*, *C. orbitofrontalis* Costa, Feltrin & Katz, 2021, *C. taroba*, and *C. tropeiro* by the color pattern of lateral surface of body composed of rounded blotches, twice the size of eyes on the inner skin layer (*vs*. color pattern of body composed of three paired stripes in *C. naipi* and *C. pascuali*; narrow longitudinal stripe formed by closely spaced dark-brown spots, with size of eye diameter, from opercle to vertical through anal-fin origin, and continuing posteriorly

to caudal peduncle in *C. tupinamba*; conspicuous, wide, continuous and irregularly bordered dark-brown longitudinal mid-lateral stripe in *C. longistriata*, *C. perkos*, and *C. piraquara*; dark-grey or brown homogeneous color pattern in *C. plumbea*, *C. papillifera*, *C. ventropapillata*, and some specimens of *C. perobana*; rounded light-brown blotches, sometimes coalescing, and with dark-brown to black marks delimiting blotches on margins in *C. gamabelardense*, *C. meandrica*, *C. panthera*; or larger blotches coalescing and forming vermiculations or bars on remaining congeners). *Cambeva ytepopo* can be distinguished from *C. taroba* by the absence of filament on first unbranched pectoral-fin ray (*vs*. presence of long filament), and by the number of pectoral-fin rays (I,6 *vs*. I,5); from *C. tropeiro* by the presence of pelvic fin and girdle (*vs*. absence of pelvic fin and girdle); from *C. mboycy* by the number of pectoral fin ray (I,6 *vs*. I,5); from *C. atrobrunnea*, *C. balios*, *C. davisi*, *C. horacioi* by the tip of pelvic fin not reaching the vertical through line of origin of dorsal fin, or not reaching anterior margin of anus (*vs*. tip of pelvic fin reaching the vertical through line of origin of dorsal fin, or reaching anterior margin of anus); from *C. diffusa*, *C. longipalata*, and *C. orbitofrontalis* by the number of vertebrae (37–38 *vs*. 40–42; 41–42; and 39–40, respectively). Additionally, *C. ytepopo* can be distinguished from *C. diffusa* by the absence of interopercular anterior concavity (*vs*. presence of interopercular anterior concavity; see Fig. 12A in Costa *et al*., 2021); from *C. longipalata* by the absence of infraorbitals pores i1, and i3 (*vs*. presence of infraorbitals pores i1, i3); and from *C. orbitofrontalis* by the number of branchiostegal rays (8 *vs*. 7).

Description. Morphometric data in Tab. 8. Body elongate, trunk roughly cylindrical close to head and gradually becoming laterally compressed towards caudal fin. Dorsal profile of trunk straight to convex on anterior half of body. Ventral profile of trunk convex. Dorsal and ventral profile of caudal peduncle slightly concave.

Head depressed, trapezoidal in dorsal view, wider posteriorly. Dorsal profile of head straight, and ventral profile of head convex in lateral view. Snout convex in dorsal view. Eyes located dorsolaterally on anterior half region of head, at same longitudinal line of nasal barbel, rounded to anteroposteriorly elliptical, covered by thin and translucent skin. Orbital rim not free. Each eye located over posterior termination of shallow and small longitudinal crest beginning at posterior nostril and making eyes visible from lateral view.

Anterior nostril slightly smaller than size of eye, surrounded by flap of integument posterolaterally continuous with base of nasal barbel. Posterior nostril surrounded anterolaterally by thin flap of integument. Gill openings not constricted united with isthmus anteriorly, forming free fold reaching pectoral-fin insertion. Mouth subterminal and slightly curved with corners posteriorly oriented. Upper lip thicker laterally. Lower lip with conspicuous fleshy lobes in lateral limits, continuous with base of rictal barbels. Lips with small and numerous rounded papillae of approximately same size.

Barbels with broad base, tapering gradually towards tips. Nasal barbel emerging from lateral region of anterior nostril with posterior tip surpassing infraorbital pore i11 when adpressed to head. Maxillary barbel emerging from lateral limit of mouth with tip reaching to posterior region of interopercular odontodophore when adpressed to head. Rictal barbel emerging from lateral limit of mouth, shorter than maxillary barbel.

TABLE 8 | Morphometric data for *Cambeva ytepopo*. N = Number of specimens, Min = Minimum, Max = Maximum, SD = Standard deviation.

	Holotype	N	Min	Max	Mean	SD
Standard length (mm)	42.5	9	34.2	61.5	44.0	–
Percents of standard length						
Head length	17.9	9	17.7	19.6	18.6	0.8
Predorsal length	63.8	9	61.1	64.7	64.0	0.8
Prepelvic length	56.1	9	54.4	58.2	55.9	1.6
Preanal length	71.1	9	68.7	73.3	71.6	1.8
Pectoral girdle width	13.5	9	13.5	14.8	13.9	0.5
Trunk length	40.9	9	35.6	40.9	38.1	2.1
Anal-fin Length	15.5	9	15.0	18.0	16.3	1.3
Dorsal-fin length	18.0	9	16.5	18.4	18.1	0.2
Pectoral-fin length	13.9	9	10.7	14.8	13.4	1.6
Pelvic-fin length	8.8	9	8.0	9.7	9.0	0.6
Distance between pelvic-fin base and anus	11.6	9	10.0	12.6	11.1	1.0
Caudal peduncule length	22.1	9	20.4	24.4	22.3	1.5
Caudal peduncule depth	9.6	9	9.2	11.2	10.1	0.7
Body depth	13.9	9	10.5	13.9	13.0	0.6
Length of dorsal-fin base	10.0	9	10.0	12.0	11.2	0.9
Length of anal-fin base	10.8	9	6.6	10.8	9.4	0.9
Pelvic anal distance	15.8	9	11.5	19.2	15.6	2.2
Percents of head length						
Head width	91.9	9	82.1	94.6	90.5	4.2
Rictal barbel length	52.6	7	44.9	61.0	51.5	6.0
Maxillary barbel length	66.3	7	55.8	74.4	64.3	8.1
Nasal barbel length	71.4	7	53.6	73.6	65.1	8.4
Snout lenght	39.1	9	38.5	53.0	44.1	5.8
Interorbital distance	25.7	9	24.1	26.0	25.1	0.8
Mouth width	40.6	9	39.0	42.5	40.4	1.3
Eye diameter	11.2	9	9.0	11.2	10.0	0.9
Supra-orbital pore distance	18.9	9	10.7	18.9	14.8	2.9

Pectoral fin with distal margin straight to slightly convex, I,6*(12) rays, and first ray unbranched, not prolonged as filament* (9), or with rudimentary filament (3) about one twentieth pectoral-fin length. Pelvic fin with distal margin rounded, distant from anterior margin of anus; I,4*(12) rays. Pelvic-fin insertion anterior to origin of dorsal-fin origin. Inner margins of pelvic fins very close basally. Dorsal fin with distal margin convex, II,7*(12) rays. Origin of dorsal fin located at vertical line through anal fin aperture. Anal fin elongated with distal margin convex and smaller than dorsal fin; II,5*(12) rays. Origin of anal fin located vertical line through last third dorsal-fin base. Caudal fin with distal margin truncate; upper plate with I,5*(12) rays, lower plate with I,6*(12) rays.

Osteology. Mesethmoid with anterior margin straight to slightly concave and cornua short, with tapering distal ends. Anterior cranial fontanel restricted to small, rounded opening situated between frontals and epiphyseal bar. Posterior cranial fontanel

long and wide extending from posterior portion of frontals to parieto-supraoccipital. Epiphyseal bar, wider than long. Antorbital slightly elongate, extending over at least one-third of autopalatine. Sesamoid supraorbital elongate, with medial process in anterior third. Anterior portion of sphenotic anterolaterally directed in dorsal view. Sphenotic, prootic and pterosphenoid fused. Vomer arrow-shaped with long posterior process extending to parasphenoid. Vomer arrow-shaped with long posterior process extending to parasphenoid. Parasphenoid with long and pointed posterior process extending to basioccipital. Weberian capsule with lateral openings and anterior margin fused to basioccipital (Fig. 2H).

Premaxilla rectangular with 28–31(3) conical to spatulate teeth similar in size and roughly distributed in three irregular transverse rows. Dentary with 30–39(3) spatulate to conical teeth, similar in size, distributed in three irregular transverse rows, and ranging from base of coronoid process to near dentary symphysis (Fig. 3H). Maxilla boomerang-shaped, shorter than premaxilla. Autopalatine with lateral margin concave; anterior margin slightly convex; medial margin slightly concave and long posterior process extending over one-third of metapterygoid. Metapterygoid large and laminar, connected to quadrate through cartilage. Quadrate L-shaped with concavity in anterior portion. Hyomandibula well-developed, dorsal margin with concavity (Fig. 4H). Opercle longer than interopercle. Opercular odontodophores ovoid to rounded with 11(1) or 13(2) conical odontodes, gradually curving medially and increasing in size posteriorly, arranged in five irregular transverse rows. Interopercular odontodophores elongate with 22 (2) or 24 (1) conical odontodes, arranged in two transverse rows.

Ventral hypohyal trapezoid-shaped. Anterior ceratohyal elongate and wider at anterior and posterior ends. Posterior ceratohyal short, rounded with pointed posterior process. Eight (2) or nine (1) branchiostegal rays: five in contact with anterior ceratohyal, one with interceratohyal cartilage, two or three with posterior ceratohyal. Four posteriormost branchiostegal rays, wider distally. Parurohyal with expanded anterior head, two elongate lateral processes with wide bases and decreasing in width distally with rounded tips, and sharp and elongate posterior process. Posterior process of parurohyal shorter than lateral processes.

Basibranchials 2 and 3 elongated, connected to each other by cartilage; basibranchial 2 slightly wider than basibranchial 3. Basibranchial 4 hexagonal and entirely cartilaginous. Hypobranchial 1 elongated, with cartilaginous tips, approximately same size than basibranchial 2. Hypobranchials 2 and 3 with narrow anterolateral ossified processes with large area of cartilage distally; Hypobranchial 2 thinner and longer than Hypobranchial 3. Five elongate ceratobranchials with cartilaginous tips. Ceratobranchials 1 and 4 with straight margins. Ceratobranchials 2 and 3 with concavity on posterior margin, very prominent in ceratobranchial 3. Ceratobranchial 5 with 15(1), 16(1), and 17(1) conical, elongated and pointed teeth arranged in three irregular rows. Four epibranchials; anteriormost three elongated and narrow with cartilage at tips. Epibranchials 1 and 2 with elongated and pointed process along anterior margins; epibranchial 3 with curved process on posterior margin. Epibranchial 4 rectangular, wider posteriorly and with cartilaginous tips. Pharyngobranchial 3 elongated, shorter than hypobranchial 1, with cartilage at tips. Pharyngobranchial 4 ossified and connected to curved plate with 20(1), 23(1), and 24(1) conical, elongated and pointed teeth, arranged in up to three irregular rows; teeth increasing in size posteriorly.

Dorsal fin with eight pterygiophores, first inserted anterior to neural spine of 19th vertebrae. Anal fin with six pterygiophores, first inserted anterior to haemal spine of 22nd or 23rd vertebrae. Procurrent caudal-fin rays 17(1) or 18(2) dorsally, and 10(2) or 12(1) ventrally. Hypural 3 free and hypurals 4 and 5 fused to each other. Parhypural and hypurals 1 and 2 co-ossified and fused to compound caudal centrum. Free vertebrae 37(1) or 38(2), and 13(3) pairs of ribs.

Laterosensory system. Laterosensory canals with simple (non-dendritic) branches ending in single pores. Nasal and frontal canals of supraorbital branch continuous, with three (9) paired pores s1, s3 and s6. Supraorbital pore s1 located at posterior portion of anterior nostrils, pore s3 at same longitudinal line of pore s1 posteriorly to posterior nostrils and pore s6 aligned with posterior margin of eyes. Antorbital segment of infraorbital canal absent. Sphenotic canal present with two (9) pores, i10, located behind eyes, and pore i11 located laterally to posterior margin of eye. Otic and postotic canals present with two pores associated: po1 located anterolaterally to opercular odontodophore and po2 located laterally to half-length of opercular odontodophore. Lateral line canal short with two (9) pores located above pectoral-fin insertion and posterior to gill opening.

Coloration in alcohol. Dorsal and lateral surface of body and head composed of rounded blotches, twice the size of eyes on the inner skin layer, randomly distributed. Background of body yellowish, readily visible in ventral surface of body and head. Head densely pigmented by smallers rounded blotches, being scattered on lateral region of head. Pectoral, dorsal, anal, and caudal fins with few inconspicuous dark-brown blotches equivalent or slightly larger in size to eye diameter, over yellowish background. Pelvic fin yellowish. Barbels with dark-brown blotches on dorsal surface. Smallers specimens (< 40.0 mm SL) with rounded blotches sometimes coalescing and forming interrupted longitudinal stripe on lateral surface of body (Fig. 18B).

Geographical distribution. *Cambeva ytepopo*, is only known from unknown name stream, tributary of rio Butiá, tributary of left margin of the lower section of rio Iguaçu (*sensu* Ingenito *et al*., 2004), Paraná State, Brazil (Fig. 5).

Ecological notes. The type locality of *C. ytepopo* is located at an elevation of 1,000 m above sea level. The water level reaches 30 cm, and the substrate is composed of rocks of 5 to 30 cm (Fig. 19). The species occurs in sympatry in the type locality with *Neoplecostomus* sp., *Pareiorhaphis parmula*, *Phalloceros circummontanus*, and *Rhamdia voulezi*.

Conservation status. *Cambeva ytepopo* can be found in only one locality, in the rio Butiá basin. The new species has an EOO of 164.3 km² (< 5,000 km² in criteria B1 for EN), although no threat has been found in the locality of occurrence of the new species. Therefore, *C. ytepopo* does not meet any condition of this criteria, and according to the International Union for Conservation of Nature (IUCN) categories and criteria (IUCN Standards and Petitions Subcommittee, 2024), thus our recommendations is that this species can be classified as Least Concern (LC).

FIGURE 18 | *Cambeva ytepopo*. **A.** Holotype, NUP 25875, 61.6 mm SL, **B.** Paratype, NUP 25427, 42.1 mm SL, both from Brazil, Paraná State, unknown name stream, tributary of rio Butiá.

Etymology. The specific name "*ytepopo*" originates from the Tupi-Guarani people, where "*Y*" means "river" or "water", "*te*" is a linking particle, and "*po*" is the Guarani verb "to jump", referring to the waterfalls. When duplicated (*popo*), it takes on a superlative meaning, which can be interpreted as "river that jumps a lot", "river of many jumps" or simply "jumping river", referring to the many waterfalls in the rio Chopim basin. It can also be understood as "boiling river", referring to the water vapor rising from the waterfalls.

Molecular data. A total of 226 sequences of ingroup and outgroup species were utilized for COX1 gene, of which 27 are newly generated or have not yet been tested in a gene tree (see Tab. **S1**). The final alignment comprised 510 base pairs (bp), and 136 unique haplotypes (Tab. **S2**) were used for analysis (Fig. 20). The best-fitting model for the unique haplotypes alignment was TIM+F+I+G4. The nucleotide composition of

FIGURE 19 | Type locality of *Cambeva ytepopo*, unknown name stream, tributary of rio Butiá, lower rio Iguaçu basin, Paraná State, Brazil. Left upstream, right downstream.

the unique haplotype alignment was 29.1% (T), 27.5% (C), 25.8% (A), and 17.6% (G), with 121 parsimony informative sites, 160 distinct site patterns, and 348 constant sites.

The genetic distance among the newly proposed species ranged from the lowest, 0.9% between *C. longistriata* and *C. kaingang*, to the highest, 4.9% between *C. ytepopo* and *C. naipi*, and 5.3% between *C. eriveltoi* and *C. naipi*. A summary of the genetic distance among species in the rio Iguaçu is provided in Tab. 9, while the full genetic distance matrix for all unique haplotype sequences is available in Tab. **S3**.

The iterative application of methodologies in this study enabled the delimitation of eight new species of *Cambeva* in the rio Iguaçu region. For all species analyzed, at least one molecular species delimitation method supports the morphological hypothesis of the new species (see Fig. 20). *Cambeva eriveltoi*, *C. meandrica*, and *C. tessellata* are consistently delimited by all methods. In contrast, the remaining five species were lumped together with congeneric species based on the sGMYC and mGMYC. However, geographic overlay is not observed in species lumpered, and morphological diagnosis characters can be seen in all species (see diagnosis of species). The sympatric species *C. kaingang* and *C. wosiackii*, recorded in the rio Gonçalves Dias, and *C. tupan* and *C. meandrica*, recorded in the rio Chopim are separated by all species delimitation methods, and belong to different sub-clades.

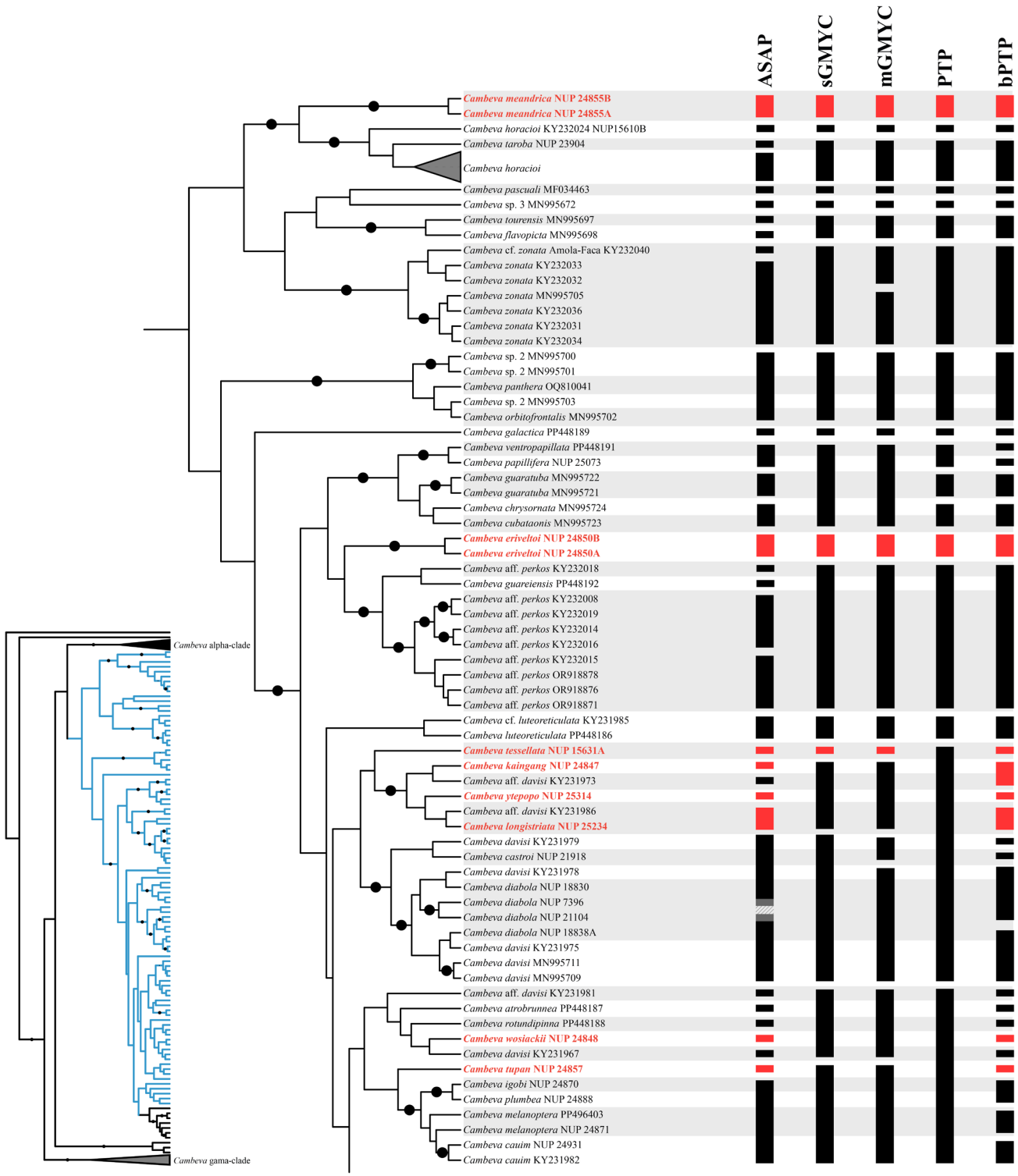

FIGURE 20 | Ultrametric gene tree of *Cambeva* by Bayesian inference constructed from gene COX1. Black circles represent posterior probability ≥ 95. Species highlighted in red represent new species described here. Vertical bars represent species delimitation methods. New species corroborated by the species delimitation methods are represented as red bars. Bars marked with texture indicate species delimitation split, but not in accordance with the tree topology shown.

TABLE 9 | Mean genetic distance k2p between and within species of *Cambeva* from rio Iguaçu basin using COX1 gene using unique haplotypes. DWG = Distance within group.

Species	1	2	3	4	5	6	7	8	9	10	11	12	13	14	15	16	17	18	19	20	21	22	23	DWG
1. *Cambeva kaingang*																								-
2. *Cambeva tessellata*	0.024																							-
3. *Cambeva eriveltoi*	0.039	0.043																						0.004
4, *Cambeva tupan*	0.024	0.024	0.039																					-
5. *Cambeva meandrica*	0.042	0.042	0.044	0.034																				0.002
6. *Cambeva wosiackii*	0.020	0.027	0.039	0.024	0.042																			-
7. *Cambeva longistriata*	0.008	0.016	0.035	0.016	0.034	0.020																		
8. *Cambeva ytepopo*	0.018	0.025	0.045	0.018	0.040	0.029	0.010																	-
9. *Cabeva atrobrunnea*	0.014	0.022	0.031	0.014	0.030	0.018	0.014	0.020																
10. *Cambeva cauim*	0.025	0.025	0.039	0.016	0.042	0.027	0.018	0.027	0.022															0.004
11. *Cambeva castroi*	0.016	0.020	0.035	0.016	0.028	0.020	0.012	0.018	0.014	0.022														-
12. *Cambeva davisi*	0.015	0.019	0.037	0.019	0.032	0.019	0.011	0.021	0.017	0.021	0.007													0.004
13. Cambeva *galactica*	0.029	0.033	0.051	0.033	0.040	0.027	0.029	0.035	0.027	0.039	0.029	0.033												-
14. *Cambeva igobi*	0.020	0.024	0.037	0.014	0.040	0.025	0.016	0.025	0.016	0.010	0.020	0.019	0.037											-
15. *Cambeva luteoreticulata*	0.018	0.018	0.033	0.018	0.032	0.022	0.010	0.020	0.016	0.016	0.014	0.013	0.027	0.018										-
16. *Cambeva mboycy*	0.045	0.041	0.047	0.039	0.042	0.039	0.037	0.043	0.039	0.045	0.037	0.039	0.039	0.043	0.035									-
17. *Cambeva melanoptera*	0.021	0.021	0.038	0.011	0.035	0.023	0.013	0.023	0.017	0.007	0.015	0.014	0.034	0.005	0.015	0.040								0.002
18. *Cambeva naipi*	0.051	0.049	0.053	0.045	0.044	0.043	0.045	0.051	0.043	0.052	0.045	0.047	0.044	0.050	0.043	0.009	0.047							0.010
19. *Cambeva rotundipinna*	0.018	0.022	0.033	0.014	0.036	0.018	0.014	0.024	0.012	0.022	0.018	0.017	0.035	0.012	0.016	0.039	0.017	0.045						-
20. *Cambeva stawiarski*	0.020	0.019	0.036	0.020	0.037	0.021	0.014	0.024	0.017	0.020	0.015	0.016	0.033	0.017	0.016	0.042	0.015	0.048	0.016					0.013
21. *Cambeva taroba*	0.039	0.047	0.051	0.047	0.034	0.043	0.039	0.045	0.037	0.053	0.039	0.041	0.035	0.047	0.041	0.041	0.046	0.043	0.045	0.045				-
22. *Cambeva papillifera*	0.024	0.029	0.041	0.025	0.040	0.029	0.024	0.029	0.016	0.027	0.024	0.027	0.029	0.020	0.022	0.041	0.025	0.046	0.020	0.025	0.043			-
23. *Cambeva plumbea*	0.022	0.025	0.039	0.016	0.042	0.027	0.018	0.027	0.018	0.012	0.022	0.021	0.039	0.002	0.020	0.045	0.007	0.050	0.014	0.018	0.049	0.022		-
24. *Cambeva* cf. *zonata*	0.049	0.051	0.067	0.051	0.042	0.047	0.049	0.047	0.045	0.053	0.049	0.051	0.043	0.051	0.047	0.049	0.048	0.050	0.049	0.052	0.041	0.047	0.053	-

A total of 44 sequences of ingroup and outgroup species were utilized for CYTB gene, of which 16 are newly generated or have not yet been tested in a gene tree (see Tab. **S1**). The final alignment comprised 666 base pairs (bp), representing one outgroup and 42 valid *Cambeva* species, of which seven are described here (*C. tupan* could not be amplified; Fig. 21).

The best-fitting model for the CYTB alignment was TN+F+I+G4. The nucleotide composition of alignment was 28.0% (T), 30.0% (C), 26.9% (A), and 15.1% (G), with 152 parsimony informative sites, 230 distinct site patterns, and 433 constant sites. The genetic distance among the newly proposed species ranged from the lowest, 1.4% between *C. ytepopo* and *C. tessellata*, to the highest, 8.1% between *C. wosiackii* and *C. meandrica*. A summary of the genetic distance among species in the rio Iguaçu is provided in Tab. 10, while the full genetic distance matrix for all sequences is available in Tab. **S4**.

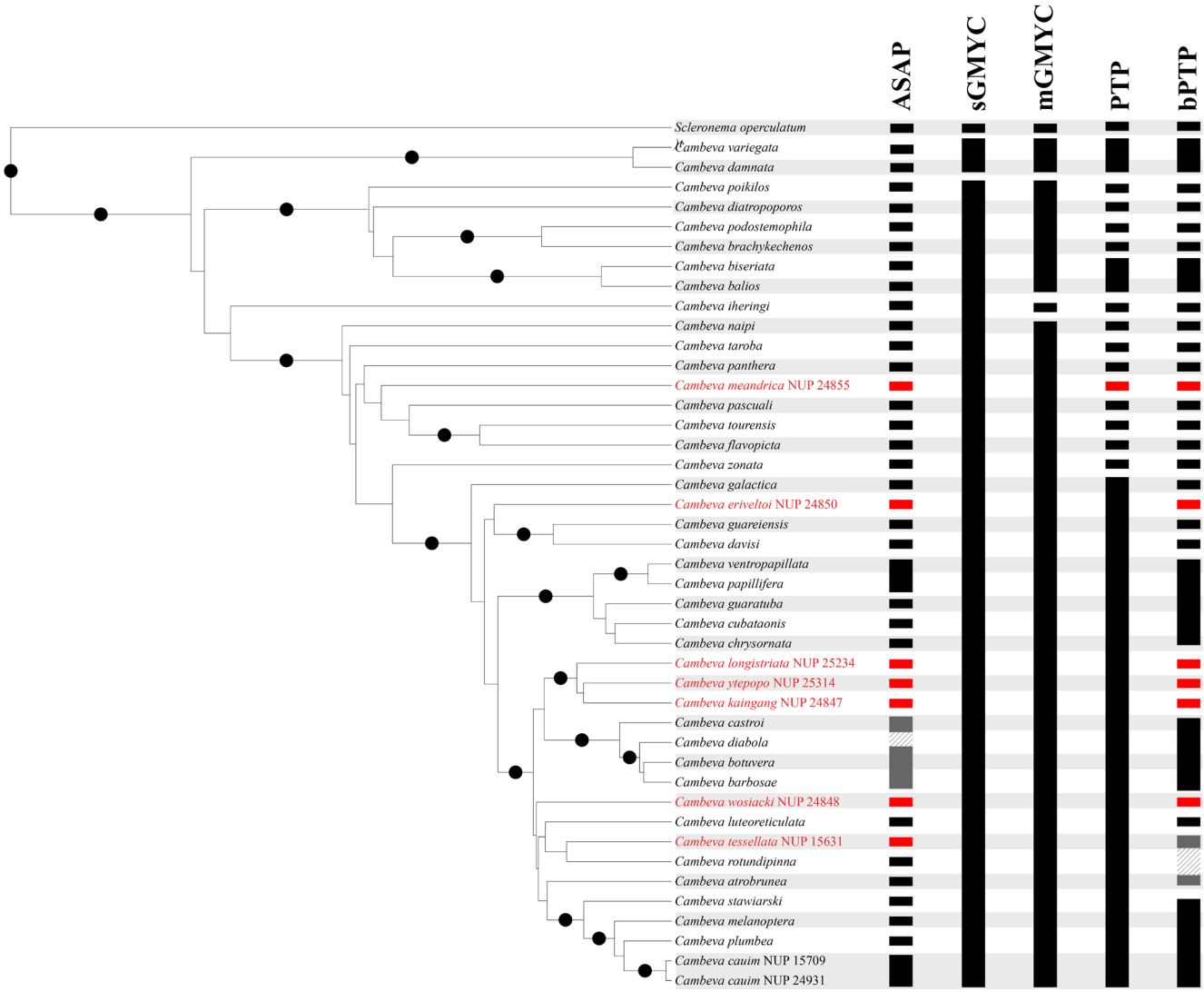

FIGURE 21 | Ultrametric gene tree of *Cambeva* constructed from gene CYTB. Black circles represent posterior probability ≥ 95. Vertical bars represent species delimitation methods. New species corroborated by the species delimitation methods are represented as red bars. Bars marked with texture indicate species delimitation split, but not in accordance with the tree topology shown.

TABLE 10 | Genetic distance k2p between species of *Cambeva* from rio Iguaçu basin using CYTB gene.

Species	1	2	3	4	5	6	7	8	9	10	11	12	13	14	15	16	17	18	19	20
1. *Cambeva kaingang*																				
2. *Cambeva tessellata*	0.034																			
3. *Cambeva longistriata*	0.039	0.024																		
4. *Cambeva meandrica*	0.079	0.063	0.072																	
5. *Cambeva wosiackii*	0.051	0.029	0.037	0.082																
6. *Cambeva ytepopo*	0.029	0.017	0.022	0.064	0.030															
7. *Cambeva eriveltoi*	0.055	0.029	0.041	0.066	0.042	0.037														
8. *Cambeva castroi*	0.037	0.022	0.027	0.070	0.036	0.024	0.036													
9. *Cambeva cauim* NUP 24931	0.032	0.020	0.032	0.068	0.034	0.022	0.034	0.027												
10. *Cambeva cauim* NUP 15709	0.032	0.020	0.032	0.068	0.034	0.022	0.034	0.027	0.000											
11. *Cambeva melanoptera*	0.040	0.019	0.033	0.074	0.036	0.027	0.039	0.025	0.014	0.014										
12. *Cambeva naipi*	0.092	0.071	0.068	0.082	0.077	0.072	0.072	0.071	0.080	0.080	0.079									
13. *Cambeva papillifera*	0.042	0.027	0.039	0.068	0.037	0.028	0.037	0.034	0.022	0.022	0.027	0.076								
14. *Cambeva plumbea*	0.035	0.020	0.025	0.064	0.034	0.025	0.037	0.024	0.009	0.009	0.014	0.077	0.025							
15. *Cambeva stawiarski*	0.041	0.025	0.037	0.074	0.039	0.030	0.043	0.029	0.020	0.020	0.025	0.087	0.030	0.020						
16. *Cambeva taroba*	0.069	0.046	0.049	0.060	0.055	0.044	0.051	0.049	0.054	0.054	0.056	0.053	0.052	0.054	0.060					
17. *Cambeva luteoreticulata*	0.040	0.019	0.027	0.062	0.029	0.020	0.032	0.022	0.024	0.024	0.025	0.074	0.030	0.020	0.029	0.049				
18. *Cambeva atrobrunea*	0.037	0.016	0.027	0.066	0.029	0.020	0.032	0.022	0.020	0.020	0.022	0.076	0.027	0.021	0.025	0.049	0.019			
19. *Cambeva rotundipinna*	0.039	0.017	0.025	0.064	0.034	0.022	0.037	0.027	0.022	0.022	0.023	0.065	0.025	0.022	0.030	0.044	0.024	0.020		
20. *Cambeva galactica*	0.059	0.039	0.055	0.059	0.054	0.048	0.046	0.046	0.045	0.045	0.046	0.076	0.045	0.045	0.046	0.062	0.043	0.043	0.041	
21. *Cambeva davisi*	0.060	0.037	0.040	0.073	0.053	0.042	0.040	0.047	0.045	0.045	0.047	0.075	0.044	0.042	0.047	0.056	0.040	0.040	0.038	0.055

Key of the *Cambeva* species from the rio Iguaçu basin

1a. Presence of papillae on ventral region of head ..... *C. papillifera*
1b. Absence of papillae on ventral region of head 2
2a. Presence of continuous longitudinal mid-lateral dark-brown stripe 3
2b. Absence of continuous longitudinal mid-lateral stripe, or when present, formed by large dark-brown blotches, with the size of opercular odontodophore, but never continuous 5
3a. Presence of three paired dark-brown stripes on body: dorso-sagital, dorso-lateral, and mid-lateral; and I,5 pectoral-fin rays ..... *C. naipi*
3b. Presence of one paired dark-brown stripes on body; and I,6 pectoral-fin rays 4
4a. Presence of dorso-sagital dark-brown stripe ..... *C. piraquara*

4b. Absence of dorso-sagital dark-brown stripe ..... *C. longistriata* (Fig. 16)
5a. Presence of I,5 pectoral-fin rays 6
5b. Presence of I,6 or I,7 pectoral-fin rays 9
6a. The color pattern of dorsal and lateral surface of body composed of rounded light-brown blotches, sometimes coalescing, and with dark-brown to black marks delimiting blotches on margins ..... *C. meandrica* (Fig. 13)
6b. The color pattern of dorsal and lateral surface of body composed of scattered small dark-brown spots, or mottled pale-brown blotches coalescing along the body and head 7
7a. Presence of long filament on first pectoral-fin ray (Fig. 22C)..... *C. taroba*
7b. Absence of filament on first pectoral-fin ray 8
8a. Caudal fin strongly rounded..... *C. mboycy*
8b. Caudal fin subtruncated, slightly rounded at corners..... *C. galactica*
9a. Presence of I,7 pectoral-fin rays 10
9b. Presence of I,6 pectoral-fin rays (except for *C. cauim* I,6, I,7, and I,8; and *C. stawiarski* I,6 and I,7) 14
10a. Absence on the caudal fin of a pale-yellow to unpigmented stripe in the proximal region 11
10b. Presence of a pale-yellow to unpigmented stripe in the proximal region of caudal fin..... 12
11a. Caudal fin strongly forked; more than 22.8% of caudal peduncle depth in SL ..... *C. crassicaudata*
11b. Caudal fin truncate; less than 19% of caudal peduncle depth in SL ..... *C. igobi*
12a. Presence of rounded, well-defined and variated in size of dark-brown blotches on the lateral surface of body; and inferior mouth ..... *C. castroi*
12b. Presence of dark-brown blotches with irregulars shape on the lateral surface of body; and subterminal mouth..... 13
13a. Presence of blotches with two or three times the diameter of the eyes in distal margin of all fins..... *C. tupan* (Fig. 11)
13b. Presence of a broad black bar in distal margin of all fins ..... *C. melanoptera*
14a. Presence of pores i1 and i,3 (Fig. 22) ..... *C. wosiackii* (Fig. 15)
14b. Absence of pores i1 and i3 15
15a. Color pattern of body composed of uniform dark-gray..... *C. plumbea*
15b. Color pattern of body composed of blotches, spots, or blotches forming vermiculation..... 16
16a. Presence of filament on first unbranched pectoral-fin ray..... 17
16b. Absence of filament on first unbranched pectoral-fin ray 18
17a. Color pattern of body composed of blotches coalescing and forming vermiculations ..... *C. eriveltoi* (Fig. 9)
17b. Color pattern of body composed of rounded dark-brown spots or blotches, variable in size, sometimes coalescing and being densely mottled on the lateral surface of the body, forming a mosaic pattern ..... *C. tessellata* (Fig. 7)
18a. Maxillar and rictal barbels not reaching interopercular odontodophores ..... *C. luteoreticulata*
18b. Maxilar and rictal barbels reaching or surpassing interopercular odontodophores 19

19a. Presence of relative shorter and rounded caudal fin ..... *C. rotundipinna*
19b. Presence of relative bigger and truncate or emarginate caudal fin..... 20
20a. Emarginate caudal fin 21
20b. Truncated caudal fin 22
21a. Caudal fin with deep concavity in distal margin..... *C. cauim*
21b. Caudal fin slightly concave in distal margin..... *C. stawiarski*
22a. Color pattern of body composed of large dark-brown rounded blotches coalescing and forming irregularly bordered and interrupted longitudinal band ..... *C. kaingang* (Fig. 1)
22b. Color pattern of body composed of small dark-brown spots or small rounded blotches 23
23a. Tip of pelvic fin not reaching the vertical through line of origin of dorsal fin, or not reaching anterior margin of anus..... *C. ytepopo* (Fig. 18)
23b. Tip of pelvic fin reaching the vertical through line of origin of dorsal fin, or reaching anterior margin of anus 24
24a. Anterior margin of snout relatively convex in dorsal view ..... *C. davisi*
24b. Anterior margin of snout relatively straight in dorsal view..... *C. atrobrunnea*

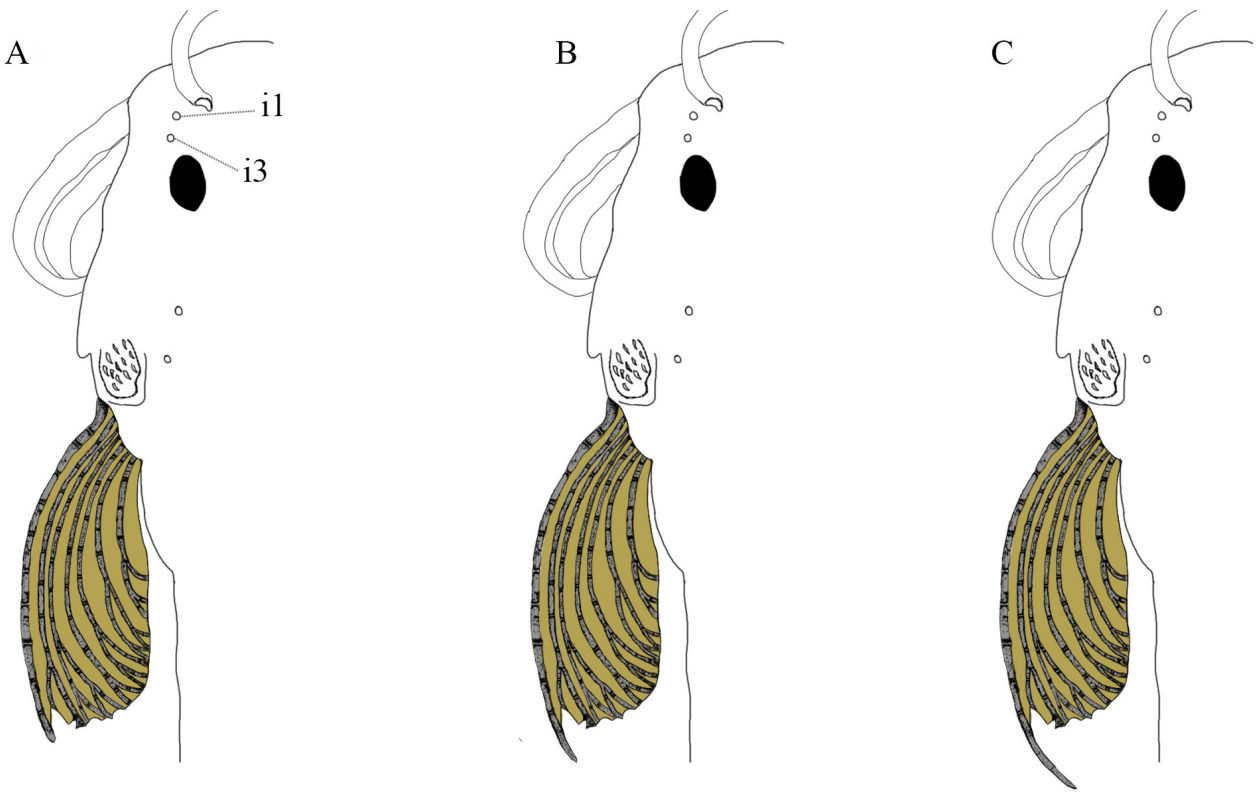

FIGURE 22 | Variations of the first pectoral-fin ray in the form of the filament and the presence of the antorbital segment of the infraorbital canal with two pores, i1, and i3. **A.** Rudimentary filament; **B.** Short filament; and **C.** Long filament.

DISCUSSION

Our study, incorporating external morphology, osteological features, and molecular data, identified the presence of eight new species in the basin. The rio Iguaçu harbor a high level of endemism for *Cambeva* species (Costa *et al*., 2021; dos Reis *et al*., 2023, 2022; Wosiacki, Garavello, 2004; Wosiacki, de Pinna, 2008a,b), and considering the significant anthropogenic impacts on the rio Iguaçu basin, the restricted distribution ranges of *Cambeva* species, morphological variation, and the relative low genetic divergence observed between some species, we emphasize the necessity to describe and understand these species before they potentially face extinction in the wild (dos Reis *et al*., 2023).

Iterative methodologies to delimit *Cambeva* species. Relying solely on genetic distance variation of COX1 to delimit small-sized fish species and groups with recent speciation may obscure local diversity (Ward *et al*., 2005; Hubert *et al*., 2008; Pereira *et al*., 2011, 2013, 2021; Costa-Silva *et al*., 2015; Reis *et al*., 2020; Reis, de Pinna, 2023). The genetic distances between congeneric species in the rio Iguaçu basin ranged from 0.9%, with most species exhibiting values higher than 2% (see Tabs. 9, **S3**). The intraspecific genetic distance ranged from 0.2%, in *C. longistriata* and *C. meandrica*, to 0.4% in *C. eriveltoi*. Thus, applying the 2% threshold for new species, as explored by Pereira *et al.* (2013) for Neotropical fishes, and the barcode gap of ten times the distance of intraspecific genetic distance, some species described here would not be validated based only on DNA barcode data. However, Pereira *et al.* (2013) highlighted that this barcode gap cutoff should be used with caution and that the implementation of species delimitation methods is advised (*e.g.*, as used in *Mesonauta* species delimitation by de Oliveira *et al.* (2025)). These methods were utilized here to delimit species and iterating with morphological diagnosis.

Although, using more than one mitochondrial gene (*e.g.*, as CYTB used here) can accurately help with species description (de Santana *et al*., 2019). Species like *C. longistriata* and *C. kaingang* have a low genetic distance (0.9%) using only COX1. Although, when compared each other by using CYTB the distance was 3.7%, greater than the threshold of approximately 3% widely used as indicative interspecific differences in fishes (Wang *et al*., 2019) and other groups of organism (Johnston *et al*., 2011; Chappell *et al*., 2012; Koroiva, Santana, 2022). The ASAP species delimitation method applied to the CYTB marker successfully distinguished all species described herein and included in the analyses. The bPTP recovered six of the seven species, whereas sGMYC and PTP grouped several taxa together, including lineages that are morphologically and genetically distinct (see Fig. 21). The divergences in results of CYTB and COX1 exemplify the use of iterative methodologies and the cumulative information to accurate delimited species (Yeates *et al*., 2011). Therefore, comparing multiple lines of evidence, such as the use of both mtDNA and the morphology diagnosis, our species boundaries can be considered rigorous, even in a group with recent speciation and few individuals to be used for molecular data.

The considerable variation in color patterns and even in the counts of pectoral fin rays difficulties the diagnosis of some species (Silva *et al*., 2010; Nascimento *et al*., 2017; dos Reis *et al*., 2022; Martins *et al*., 2024). However, with the aid of osteological data,

increasingly detailed species descriptions within the group, and molecular methods being implemented (*e.g.*, Bockmann *et al*., 2004; Ferrer, Malabarba, 2013; Costa *et al*., 2024b), allowed species comparisons not only for diagnosis purposes but also for the establishment of intrageneric groups (Costa *et al*., 2021). In the present study, we applied an iterative taxonomic approach combining two mitochondrial markers (COX1 and CYTB) with analyses of external morphology and osteological characters. This framework allowed us to evaluate congruence among independent lines of evidence, and reduce uncertainties associated with highly variable diagnostic traits. Using molecular and morphological datasets a more comprehensive understanding of diversification patterns within *Cambeva* can be achieved.

Insights about *Cambeva* species delimitation and future perspective. Instances of low genetic distance between morphologically distinct and already described species are well documented in *Cambeva* (Donin *et al*., 2022; Martins *et al*., 2024; dos Reis *et al*., 2025b), such as *C. davisi* and *C. diabola* (see fig. 2 from dos Reis *et al*., 2025b), as well as *C. castroi* (see Tab. **S1**). In this case, the genetic divergence between *C. davisi* and *C. castroi* was only 0.7%, highlighting the importance of iterative species delimitation frameworks using more than one molecular marker, species delimitation methods, and morphological data to achieve accurate species delimitation, specially in Trichomycteridae (Reis, de Pinna, 2023). Another group that our results indicated to be genetically closely related comprises *C. tupan*, *C. igobi*, *C. plumbea*, *C. melanoptera*, and *C. cauim*, which cluster together in a genetic group. Notably, *C. melanoptera* and *C. cauim* exhibit a low genetic distance of 0.7%, and *C. igobi* and *C. plumbea* 0.2% (Tab. 9). In addition to these species, *C. naipi* and *C. mboycy* also exhibit low genetic divergence, 0.4%, and are consistently clustered together by molecular delimitation methods. However, they display several distinct morphological characters that clearly differentiate them (Wosiacki, Garavello, 2004).

Several factors may influence genetic distances measured from a single mtDNA gene, including past introgression events resulting from historical contact between species (Funk, Omland, 2003), as well as lineages undergoing recent speciation that have not yet surpassed the "gray zone" from De Queiroz (2007). These patterns could be driven by the low genetic distance (*i.e.*, 0.9%) between *C. longistriata*, from rio Butiá, tributary of the left margin of Rio Iguaçu, and *C. kaingang*, from rio Gonçalves Dias, tributary of the right margin of rio Iguaçu. Despite the low genetic distance, the species could be diagnosed for several morphological characters (see Diagnosis) including osteological features, such as the absence of epiphyseal bar in *C. longistriata* (*vs*. the presence of epiphyseal bar in *C. kaingang*, see Figs. 2A, H), and high genetic distance using CYTB gene (3.7%, see Tab. 10).

On the other hand, the high genetic distances observed here correspond to groups that likely colonized the basin during an older geological period and independently, and then co-occurring in a secondary contact (*e.g.*, *C. kaingang* and *C. wosiackii*, recorded in the rio Gonçalves Dias, *C. tupan* and *C. meandrica*, recorded in the rio Chopim, and *C. longistriata* and *C. ytepopo*, recorded in the rio Butiá). Consequently, probably with the arrival of species in more recent periods, these newly dispersal taxa established themselves in sympatry with the preexisting species in the region, a pattern also found for other Neotropical river basins (Albert *et al*., 2020). Given that these groups are genetically

highly distinct and likely more ancient, such as the group formed by *C. taroba* and *C. meandrica*, as well as *C. mboycy* and *C. naipi*, they may have undergone speciation due to prezygotic factors concerning to other species-rich groups of potentially more recent origin in the basin. This process could have prevented recent introgression events and the mixing of mtDNA.

Species of *Cambeva* have shown significant morphological variation (see Silva *et al*., 2010; Nascimento *et al*., 2017; Martins *et al*., 2024). When analyzing only a single source of data (*e.g*., exclusively molecular or morphological data), there is a risk of misinterpreting species delimitation. This is exemplified by species delimiters in the present study, particularly in the case of *C. horacioi* and *C. taroba*, where a population of *C. horacioi* appears to be separated by *C. taroba*. However, the population of *C. horacioi* occurs in the same localities, and the morphological differences between these species are substantial (see Wosiacki, Garavello, 2004; dos Reis *et al*., 2020b). Another example involves *C. orbitofrontalis* and *C. panthera*, which are grouped as a single potential species based on molecular data. Nevertheless, these taxa exhibit pronounced morphological differences, such as distinct coloration patterns and the presence of a long filament on the first pectoral-fin ray in *C. panthera* (see Costa *et al*., 2021). This pattern has also been reported in other trichomycterids, such as *Trichomycterus alternatus* (Eigenmann, 1917), *T. astromycterus* Reis, de Pinna & Pessali, 2019, and *T. vinnulus* Reis & de Pinna, 2022, which are morphologically distinct yet exhibit low genetic divergence. Conversely, morphologically similar species (*e.g*., *T. immaculatus* (Eigenmann & Eigenmann, 1889) and *T. melanopygius* Reis, Santos, Britto, Volpi & de Pinna, 2020) may show high genetic distances in the COX1 gene (Reis *et al*., 2020; Reis, de Pinna, 2023).

However, a particularly noteworthy case is the lumping of *C. papillifera* and *C. ventropapillata*, with the former being at risk of extinction (MMA, 2022). The species shares a haplotype (see Tab. **S2**), and shows low genetic variation between these two haplotypes (0.4%, see Tab. **S3**). Furthermore, all species delimiters indicated the existence of a single taxon. Despite the morphological differences proposed by Costa *et al.* (2023b), these differences appear to represent intraspecific variation within *C. papillifera*. In this case, a recent headwater capture event likely separated the lineages, leading to population structuring with morphological differences in different river basins (Iguassu, and Southeastern Mata Atlantica *sensu* Abell *et al.* (2008), for *C. papillifera*, and *C. ventropapillata*, respectively). Here, we do not propose any synonymization, however, further studies involving both species are necessary to better understand the distribution pattern of *C. papillifera*, its conservation status, and the potential senior synonymy of this species in relation to *C. ventropapillata*.

Another noteworthy case is the potential merging of *C. zonata* from the rio Ribeira de Iguape (type locality) with specimens from the upper rio Iguaçu basin identified as *C. davisi* in Morais-Silva *et al.* (2018). The specimens were collected in the Amola Faca stream, near the type locality of *C. davisi*, Serrinha (see Haseman, 1911). The morphological variation between these two species, particularly in small individuals of *C. davisi*, difficulties their identification. A possible explanation for this pattern is the occurrence of *C. zonata* in the upper rio Iguaçu basin, with the distribution range confirmation based on the specimens identified here as *C.* cf. *zonata* (see Fig. 20). Thus, the type-series individuals of *C. davisi* that exhibit a wide and broad longitudinal stripe (FMNH 54242, see Haseman, 1911; Nascimento *et al*., 2017) may correspond to *C.*

zonata, and one specimen with thin and paired stripe (also FMNH 54242) present the diagnosis character of *C. naipi* (see Wosiacki, Garavello, 2004). Therefore, testing the hypothesis and confirming the presence of *C. zonata* in the rio Iguaçu could provide valuable insights into the morphological variation of *C. davisi*, allowing for a more precise delimitation of this species and its distribution range.

Biogeographic patterns and conservation of rio Iguaçu basin. Significant biogeographic and intrageneric patterns were identified by Costa *et al.* (2024b), revealing that species from the rio Iguaçu in the Serra do Espigão (RISE *sensu* Costa *et al*., 2024b) exhibit two distinct distributional patterns: western and eastern. Eastern species are phylogenetically closer to species from coastal basins, whereas western species share a closer relationship with species from the rio Iguaçu. Additionally, species from the lower rio Iguaçu region, along with the phylogenetic topology generated here, suggest multiple colonization events of the rio Iguaçu by *Cambeva* species. This aligns with Costa *et al*. (2024b), who found that species from RISE are not monophyletic. Despite the description and delimitation of these eight species in this study, their precise phylogenetic placement within the group is still under investigation to improve our understanding of both phylogenetic relationships and the biogeographic patterns that shaped the distribution and speciation in this basin (RBR, work in progress).

The rio Iguaçu has proven to be an important area of endemism and harboring, currently, 24 endemic species of *Cambeva*, and approximately one-third of all diversity of the group, reinforcing the hypothesis of a hotspot for the genus (dos Reis *et al*., 2022; Frota, da Graça, 2025). Despite extensive sampling throughout its course, the rio Iguaçu basin still presents sample gaps, particularly in left-bank tributaries, such as the rio Chopim (where two new species have been recorded here), as well as the rio Jangada, Iratim, and some tributaries from Santa Catarina and in the Misiones region in Argentina. Therefore, it is likely that additional endemic species remain undiscovered and formally undescribed by science.

Throughout its course, the rio Iguaçu is subject to numerous anthropogenic impacts, including pollution, urbanization, extensive agriculture, flow modification caused by dams, and the introduction of non-native species (Garavello *et al*., 1998; Baumgartner *et al*., 2012; Daga *et al*., 2016; Mezzaroba *et al*., 2021). Among these, the construction of hydroelectric dams is the most detrimental to fish species with restricted distributions. As a result, four species of *Cambeva* are threatened in the basin: *C. crassicaudata* (EN; Endangered), *C. igobi* (VU; Vulnerable), *C. mboycy* (EN), and *C. papillifera* (EN); and *C. piraquara* is considered a potential species to be included in this list as CR; Critically Endangered (MMA, 2022; dos Reis *et al*., 2023).

Despite these impacts on their habitats, the region still contains areas of high biodiversity, a characteristic shaped by the geomorphological evolution of the landscape, being a result of long-term isolation of the rio Iguaçu drainage from the remaining parts of rio Paraná basin by the Cataratas do Iguaçu, and compartmentalization of sub-basins due to biogeographic barriers (Haseman, 1911; Garavello, Sampaio, 2010; Baumgartner *et al*., 2012; Mello *et al*., 2015; dos Reis *et al*., 2020a; Costa *et al*., 2024a). Thus, mitigating anthropogenic impacts in the region and knowing the basin's biodiversity and the range distribution of species are crucial for the conservation of freshwater fish species, avoiding the known Linnean and Wallacean Shortfalls (Bini *et al*., 2006; Hortal *et al*., 2015; Haelewaters *et al*., 2024).

Comparative material examined. Argentina. *Trichomycterus pseudosilvinichthys* Fernández & Vari, 2004: FMNH 112974, 1 paratype, 52.1 mm SL, Province de La Rioja, Departamento Chilecito, Valle Gauchin. **Brazil. Paraná State:** *Cambeva cauim*: rio Iguaçu basin: all paratypes, MPEG 39109, 4, 29.2–82.3 mm SL, municipality of Mangueirinha, córrego Verde. NUP 2416, 19, 20.0–97.4 mm SL, municipality of Mangueirinha, córrego Verde. NUP 22756, holotype, 89.6 mm SL, municipality of Cruz Machado, unnamed stream. *Cambeva castroi*: rio Iguaçu basin: NUP 3127, 3, 110.0–140.0 mm SL, municipality of Reserva do Iguaçu, Jordão reservoir, rio Jordão basin. *Cambeva crassicaudata*: rio Iguaçu basin: MHNCI 12297, 4, 47.0–164.3 mm SL, municipality of Candói/Pinhão, rio Jordão, UHE Santa Clara. MZUSP 88519, 1, paratype, 105.6 mm SL, municipality of Foz do Jordão, rio Jordão. MZUSP 88517, 2, 110.9–121.3 mm SL, municipality of Candói, rio Jordão. NUP 3123, 1, 52.3 mm SL, municipality of Foz do Jordão, Córrego Passo do Aterrado. NUP 3783, 3, 78.6–134.5 mm SL, municipality of Candói, rio Jordão. NUP 4006, 3, 107.5–114.3 mm SL, municipality of Candói, rio Jordão. NUP 4826, 1, 109.7 mm SL, municipality of Candói, rio Jordão. NUP 9998, 1, 95.1 mm SL, municipality of Guarapuava, rio Pinhãozinho. NUP 10827, 4, 50.7–102.4 mm SL, municipality of Foz do Jordão, Jordão reservoir. *Cambeva davisi*: rio Iguaçu basin: NUP 4008, 11, 22.1–82.1 mm SL, municipality of Santa Clara, rio da Lage, tributary to the rio Jordão. NUP 15914, 67, 21.3–78.2 mm SL, municipality of Cruz Machado, rio Jacutinga, tributary to the rio Santana. NUP 17364, 34, 38.7–74.3 mm SL, municipality of Pinhão, unnamed river, tributary to the rio Lajeado Feio. *Cambeva diabola*: rio Tibagi basin: NUP 17403, 4, 31.9–67.2 mm SL, municipality of Teixeira Soares, arroio Lajeado, tributary to the arroio Chapada. NUP 17447, 2, 109.3–114.8 mm SL, municipality of Palmeira, rio São Benedito, tributary to the rio Caniú. NUP 17457, 2, 53.8–92.9 mm SL, municipality of Carambeí, rio Jotuba, tributary to the rio Pitangui. NUP 17471, 2, 57.8–83.2 mm SL, municipality of Carambeí, unnamed river, tributary to the rio Maracanã. NUP 18830, 2, 46.1–59.6 mm SL, municipality of Palmeira, rio São Benedito, tributary to the rio Caniú. NUP 18832, 1, 62.5 mm SL, municipality of Carambeí, rio Jotuba, tributary to the rio Pitangui. NUP 14772, 3, 34.9–78.2 mm SL, municipality of Jacarezinho, ribeirão Ubá, tributary to the rio das Cinzas. NUP 20510, 10, 39.9–54.8 mm SL, municipality of Ibaiti, unnamed river, tributary to the rio das Pedras. Rio Itararé basin: NUP 20439, 9, 40.5–62.9 mm SL, municipality of Sengés, rio Pelame, tributary to the rio Itararé. Rio Pirapó basin: NUP 4802, 2, 55.0–60.0 mm SL, municipality of Pulinópolis, rio Atlântico, tributary to the rio Pirapó. NUP 5579, 2, 46.0–72.7 mm SL, municipality, corrégo Remo. Rio Ivaí basin: NUP 5482, 3, 19.4–35.3 mm SL, municipality of Prudentópolis, rio Barra Grande, tributary to the rio Ivaí. *Cambeva horacioi*: rio Ivaí basin. MCP 54181, holotype, 88.1 mm SL, municipality of Prudentópolis. NUP 15669, 2 paratypes, 51.8–57.4 mm SL, municipality of Iretama. NUP 16016, 3 paratypes, 39.8–91.7 mm SL, municipality of Peabiru. NUP 16059, 10 paratypes, 64.4–72.2 mm SL, municipality of Iretama. NUP 16091, 6, 35.8–61.7 mm SL, municipality of Prudentópolis. *Cambeva igobi*: rio Iguaçu basin: MHNCI 12298, 1, 170.0 mm SL, municipality of Candói/Pinhão, rio Jordão, UHE Santa Clara. MZUSP 94843, 3 paratypes, 63.0–89.8 mm SL, municipality of Candói, rio Jordão. NUP 611, 4, 107.6–150.2 mm SL, municipality of Foz do Jordão, córrego Passo do Aterrado. NUP 3704, 4, 59.4–129.9 mm SL, municipality of Candói, rio Capivara. NUP 3824, 2, 21.2–68.0 mm SL, municipality of Candói, rio Jordão. NUP 4007, 2 paratypes, 62.0–66.3 mm SL, municipality of Candói, rio do Sobradinho, tributary to the rio Jordão. NUP 4009, 4, 20.8–32.3 mm SL, municipality of Pinhão, rio Capivara. NUP 4743, 3, 119.4–144.1 mm SL, municipality of Reserva do Iguaçu, rio das Torres. NUP 4827, 1, 66.2 mm SL, municipality of Candói, rio Sobradinho. NUP 9866, 1, 125.9 mm SL, municipality of Guarapuava, rio Pinhãozinho. NUP 16101, 74.4 mm SL, municipality of Pinhão, unknown name stream. NUP 18280, 6, 69.0–99.6 mm SL, municipality of Guarapuava, unnamed river stream. NUP 18873, 2, 71.2–82.9 mm SL, municipality of Guarapuava, unnamed river stream. *Cambeva iheringi*: rio Itararé basin: NUP 20440, 1, 57.9 mm SL, municipality of Sengés, rio Pelame. NUP 20463, 2, 61.6–77.8 mm SL, municipality of Jaguariaíva, unnamed river, tributary to the rio Espigão Alto. NUP 20480, 1, 74.1 mm SL, rio das Lanças, tributary to the rio Jaguariaíva. NUP 21042, 1, 51.0 mm SL, municipality of Sengés, rio Pelame. NUP 21059,

1, 69.2 mm SL, municipality of Jaguariaíva, unnamed river, tributary to the rio Espigão Alto. *Cambeva mboycy*: rio Iguaçu basin: NUP 612, 7, 39.3–88.0 mm SL, municipality of Foz do Jordão, rio Jordão. NUP 632, 2, 57.9–59.9 mm SL, municipality of Foz do Jordão, rio Jordão. *Cambeva melanoptera*: rio Iguaçu basin: NUP 24871, 2, 35.2–91.0 mm SL, municipality of Coronel Domingos Soares, rio Iratim. *Cambeva naipi*: rio Iguaçu basin, municipality of Rebouças: NUP 15548, 4, 57.5–59.6 mm SL. NUP 16013, 7, 15.9–64.8 mm SL. *Cambeva perobana*: NUP 23907, holotype, 75.9 mm SL, rio Mouro, basin of rio Piquiri. *Cambeva taroba*: rio Iguaçu: NUP 23891, 34, 16.6–41.1 mm SL, municipality of Reserva do Iguaçu, tributary of rio Capão Grande, rio Jordão basin. NUP 1616, 3 paratypes, 47.4–53.8 mm SL, municipality of Foz do Jordão, córrego Passo do Aterrado, tributary of rio Jordão basin. *Cambeva papillifera*: NUP 1615, 1 paratype, 94.4 mm SL, municipality of Foz do Jordão. NUP 2415, 3, 35.6–62.3 mm SL, municipality of Mangueirinha. NUP 2418, 4, 100.0–126.2 mm SL, municipality of Mangueirinha. NUP 10828, 3, 100.6–114.4 mm SL, municipality of Foz do Jordão. NUP 15883, 1, 96.5 mm SL, municipality of Cruz Machado. NUP 17363, 1, 83.2 mm SL, municipality of Pinhão. NUP 20131, 1, 66.6 mm SL, municipality of Pinhão. NUP 25073, 2, 59.6–89.5 mm SL, municipality of Pinhão. NUP 25470, 7, 58.0–98.0 mm SL, municipality of Foz do Jordão. NUP 25535, 2, 71.0–82.3 mm SL, municipality of Coronel Domingos Soares. NUP 25558, 1, 69.6 mm SL, municipality of Pinhão. *Cambeva pascuali*: rio Paranapanema: NUP 23341, 1, 45.0 mm SL, municipality of Jaguariaíva. NUP 23342, 2, 43.0–48.0 mm SL, municipality of Jaguariaíva, Paraná State. NUP 23343, 3, 40.5–48.0 mm SL, municipality of Jaguariaíva. *Cambeva piraquara*: upper rio Iguaçu, municipality of Piraquara: MCP 39091, 2 paratypes, 23.5–25.3 mm SL. MHNCI 9135, 1 paratype, 30.4 mm SL. MPEG 39144, holotype, 41.6 mm SL. MPEG 39115, 1 paratype, 60.9 mm SL. MZUSP 126889, 1 paratype (c&s), 61.3 mm SL. NUP 23642, 1 paratype, 26.5 mm SL. *Cambeva plumbea*: rio Iguaçu basin: NUP 1614, 3 paratypes, 72.5–78.5 mm SL, municipality of Foz do Jordão. *Cambeva stawiarski*: rio Iguaçu basin: MNRJ 9739, holotype, 67.1 mm SL, municipality of Bituruna. NUP 1378, 239, 24.3–89.5 mm SL. NUP 3240, 59, 24.8–66.7 mm SL, municipality of Foz do Jordão. **Minas Gerais State.** *Ituglanis parahybae* (Eigenmann, 1918): FMNH 58576 [formerly CM 7598], holotype, 28.1 mm SL, municipality of São José da Barra, rio Parahyba (rio Paraíba do Sul). **Santa Catarina State:** *Cambeva balios*: NUP 18123, 38, 33.3–80.7 mm SL, municipality of São Joaquim, rio Pelotas. **São Paulo State:** *Cambeva pascuali*: rio Paranapanema: MZUSP 121681, holotype, 48.8 mm SL, municipality of Itatinga. *Cambeva zonata*: FMNH 58573, holotype, 52.5 mm SL, FMNH 58574, 2 paratypes, 42.3–47.4 mm SL, rio Ribeira de Iguape, Água quente, Cubatão, 7 miles west from Santos. *Microcambeva triguttata* (Eigenmann, 1918): FMNH 58670 [formerly CM7600a], holotype, 30.0 mm SL, Jacarahy (Jacareí), rio Paraíba do Sul. *Trichomycterus paolence*: FMNH 58085, holotype, 59.4 mm SL, district of Paranapiacaba, municipality of Santo André, near to Alto da Serra, rio Jurubatuba/Grande, basin of rio Tietê, upper rio Paraná system. FMNH 58119, 11, 18.9–25.0 mm SL, municipality of Mogi das Cruzes, rio Tietê, upper rio Tietê basin. LBP 7684, 1 (tissue 36308), municipality of São Paulo, stream tributary of Guarapiranga reservoir, upper rio Tietê basin. *Trichomycterus* cf. *mimonha* Costa, 1992: paratype of *Pygidium paolence*: FMNH 58575, 1, 56.5 mm SL, rio Paranahyba bridge, 15 Aug 1908, J. D. Haseman. **Colombia.** *Trichomycterus bogotense* (Eigenmann, 1912): FMNH 56030, holotype, 65.3 mm SL, Puente de Supa, beyond Chapinero, near Bogotá. **Guyana.** *Trichomycterus guianensis* (Eigenmann, 1909): FMNH 52676 [formerly CM 1003], holotype, 64.4 mm SL, Aruataima Falls, upper Potaro River. **Peru.** *Ituglanis gracilior* (Eigenmann, 1912): FMNH 142659, 2, 71.6–83.4 mm SL, municipality of La Convencion, rio Ticumpinã, sub-basin of rio Ucoyali, tributary of rio Amazonas.

ACKNOWLEDGMENTS

We are deeply grateful to Matheus Z. Roloff, Carlos E. V. Grou, Lucas D. Lima, Sérgio K. Utiyama, and Natália Paula for helping in field collection in Iguaçu National Park; to Wladimir M. Domingues, Francisco A. Teixeira, Valmir A. Teixeira, and Augusto Frota for helping with field collection in the Iguaçu basin. To Marli C. Campos and Sandra R. de Souza for cataloging the vouchers; to PEA and Nupélia for logistical support. To Caleb D. McMahan, Susan Mochel, and Kevin Swagel for help in the FMNH.

REFERENCES

- **Abell R, Thieme ML, Revenga C, Bryer M, Kottelat M, Bogutskaya N *et al.*** Freshwater ecoregions of the world: a new map of biogeographic units for freshwater biodiversity conservation. BioScience. 2008; 58(5):403–14. https://doi.org/10.1641/B580507
- **Adriaens D**, **Baskin JN**, **Coppens H.** Evolutionary morphology of trichomycterid catfishes: about hanging on and digging in. Origin and Phylogenetic Interrelationships of Teleosts. München, Germany: Verlag Dr. Friedrich Pfeil; 2010. p.337–62.
- **Albert JS**, **Tagliacollo VA**, **Dagosta F.** Diversification of Neotropical freshwater fishes. Annu Rev Eco Evo Syst. 2020; 51:27–53. https://doi.org/10.1146/annurev-ecolsys-011620-031032
- **Arratia G**, **Schultze H-P.** The urohyal: development and homology within osteichthyans. J Morphol. 1990; 203(3):247–82. https://doi.org/10.1002/jmor.1052030302
- **Baumgartner G**, **Pavanelli CS**, **Baumgartner D**, **Bifi AG**, **Debona T**, **Frana VA.** Peixes do Baixo rio Iguaçu. Maringá: Eduem; 2012.
- **Bini LM**, **Diniz-Filho JAF**, **Rangel TFLVB**, **Bastos RP**, **Pinto MP**. Challenging Wallacean and Linnean shortfalls: knowledge gradients and conservation planning in a biodiversity hotspot. Divers Distrib. 2006; 12(5):475–82. https://doi.org/10.1111/j.1366-9516.2006.00286.x
- **Bockmann FA**, **Casatti L**, **Pinna MCC.** A new species of trichomycterid catfish from the Rio Paranapanema basin, southeastern Brazil (Teleostei: Siluriformes), with comments on the phylogeny of the family. Ichthyol Explor Freshw. 2004; 15(3):225–42.
- **Britz R**, **Bartsch P.** The myth of dorsal ribs in gnathostome vertebrates. Proc Biol Sci. 2003; 270(Suppl. 1):1–04. https://doi.org/10.1098/rsbl.2003.0035
- **Casciotta J**, **Almirón A**, **Piálek L**, **Rícan O.** *Gymnogeophagus taroba* (Teleostei: Cichlidae), a new species from the río Iguazú basin, Misiones, Argentina. Hist Nat. 2018; 7(2):5–22.
- **Chappell EM**, **Trewick SA**, **Morgan-Richards M**. Shape and sound reveal genetic cohesion not speciation in the New Zealand orthopteran, *Hemiandrus pallitarsis*, despite high mitochondrial DNA divergence: intraspecific variation in a ground weta. Biol J Linn Soc. 2012; 105(1):169–86. https://doi.org/10.1111/j.1095-8312.2011.01777.x
- **Costa-Silva GJ, Rodriguez MS, Roxo FF, Foresti F, Oliveira C.** Using different methods to access the difficult task of delimiting species in a complex neotropical hyperdiverse group. PLoS ONE. 2015; 10(9):e0135075. https://doi.org/10.1371/journal. pone.0135075
- **Costa WJEM.** Description de huit nouvelles espèces du genre *Trichomycterus* (Siluriformes: Trichomycteridae), du Brésil oriental. RFAH. 1992; 18(4):101–10.
- **Costa WJEM**, **Abilhoa V**, **Dalcin RH**, **Katz AM.** A new catfish species of the genus *Cambeva* (Siluriformes: Trichomycteridae) from the rio Iguaçu drainage, southern Brazil, with a remarkable unique colour pattern. J Fish Biol. 2022; 101(1):69–76. https://doi.org/10.1111/jfb.15071

- **Costa WJEM**, **Feltrin CRM**, **Katz AM.** Field inventory reveals high diversity of new species of mountain catfishes, genus *Cambeva* Katz, Barbosa, Mattos & Costa, 2018 (Siluriformes: Trichomycteridae), in south-eastern Serra Geral, southern Brazil. Zoosystema. 2021; 43(28):659–90. https://doi.org/10.5252/zoosystema2021v43a28
- **Costa WJEM**, **Feltrin CRM**, **Mattos JLO**, **Dalcin RH**, **Abilhoa V**, **Katz AM.** Morpho-molecular discordance? Re-approaching systematics of *Cambeva* (Siluriformes: Trichomycteridae) from the Guaratuba-Babitonga-Itapocu area, Southern Brazil. Fishes. 2023b; 8(2):63. https://doi.org/10.3390/fishes8020063
- **Costa WJEM**, **Feltrin CRM**, **Mattos JLO**, **Katz AM.** Top mountain areas of subtropical southern Brazil sheltering four new small-ranged catfishes (Siluriformes, Trichomycteridae): relationships and taxonomy. Evol. Syst. 2024a; 8:199–218. https://doi.org/10.3897/evolsyst.8.126393
- **Costa WJEM**, **Feltrin CRM**, **Mattos JLO**, **Katz AM.** Monophyly or Homoplasy? The relationships of a rare new species of *Cambeva* (Siluriformes: Trichomycteridae) from the Brazilian Atlantic Forest with a bicolored caudal pattern. Taxonomy. 2024b; 4(2):341–53. https://doi.org/10.3390/taxonomy4020017
- **Costa WJEM**, **Mattos JLO**, **Amorim PF**, **Mesquita BO**, **Katz AM.** Chromatic polymorphism in *Trichomycterus albinotatus* (Siluriformes, Trichomycteridae), a mountain catfish from south-eastern Brazil and the role of colouration characters in trichomycterine taxonomy. Zoosyst Evol. 2023a; 99(1):161–71. https://doi.org/10.3897/zse.99.98341
- **Daga V**, **Debona T**, **Abilhoa V**, **Gubiani ÉA**, **Vitule J.** Non-native fish invasions of a Neotropical ecoregion with high endemism: a review of the Iguaçu River. Aquat Invas. 2016; 11(2):209–23. https://doi.org/10.3391/ai.2016.11.2.10
- **Donin LM**, **Ferrer J**, **Carvalho TP.** Uncertainties and risks in delimiting species of *Cambeva* (Siluriformes: Trichomycteridae) with single-locus methods and geographically restricted data. Neotrop Ichthyol. 2022; 20(3):e220019. https://doi.org/10.1590/1982-0224-2022-0019
- **Drummond AJ**, **Suchard MA**, **Xie D**, **Rambaut A.** Bayesian phylogenetics with BEAUti and the BEAST 1.7. Mol Biol Evol. 2012; 29(8):1969–73. https://doi.org/10.1093/molbev/mss075
- **Ferrer J**, **Malabarba LR.** Taxonomic review of the genus *Trichomycterus* Valenciennes (Siluriformes: Trichomycteridae) from the laguna dos Patos system, Southern Brazil. Neotrop Ichthyol. 2013; 11(2):217–46. https://doi.org/10.1590/S1679-62252013000200001
- **Fricke R**, **Eschmeyer WN**, **Van der Laan R.** Eschmeyer's catalog of fishes: genera, species, references [Internet]. San Francisco: California Academy of Science; 2026. Available from: http://researcharchive.calacademy.org/research/ichthyology/catalog/fishcatmain.asp
- **Frota A**, **Graça WJ.** Establishing new grid-size–dependent attributes to rank areas of endemism for conservation priorities. Cladistics. 2025; 41(5):493–512. https://doi.org/10.1111/cla.70002
- **Fujisawa T**, **Barraclough TG.** Delimiting species using single-locus data and the Generalized Mixed Yule Coalescent approach: a revised method and evaluation on simulated data sets. Syst Biol. 2013; 62(5):707–24. https://doi.org/10.1093/sysbio/syt033
- **Funk DJ**, **Omland KE.** Species-level paraphyly and polyphyly: frequency, causes, and consequences, with insights from animal mitochondrial DNA. Annu Rev Ecol Evol Syst. 2003; 34:397–423. https://doi.org/10.1146/annurev.ecolsys.34.011802.132421
- **Garavello JC**, **Pavanelli CS**, **Suzuki HI.** Caracterização da ictiofauna do rio Iguaçu. In: Agostinho AA, Gomes LC, editors. Reservatório de Segredo: bases ecológicas para o manejo. 1st ed. Maringá: EDUEM; 1998. p.61–84.
- **Garavello JC**, **Sampaio FAA.** Five new species of genus *Astyanax* Baird & Girard, 1854 from rio Iguaçu, Paraná, Brasil (Ostariophysi, Characiformes, Characidae). Braz J Biol. 2010; 70(3):847–65. https://doi.org/10.1590/S1519-69842010000400016
- **Guindon S**, **Dufayard J-F**, **Lefort V**, **Anisimova M**, **Hordijk W**, **Gascuel O.** New algorithms and methods to estimate maximum-likelihood phylogenies: assessing the performance of PhyML 3.0. Syst Biol. 2010; 59(3):307–21. https://doi.org/10.1093/sysbio/syq010

- **Haelewaters D, Matthews TJ, Wayman JP, Cazabonne J, Heyman F, Quandt CA *et al.*** Biological knowledge shortfalls impede conservation efforts in poorly studied taxa - A case study of Laboulbeniomycetes. J Biogeogr. 2024; 51(1):29–39. https://doi.org/10.1111/jbi.14725
- **Hall TA.** BioEdit: a user-friendly biological sequence alignment editor and analysis program for Windows 95/98/NT. Nucleic Acids Symp Ser. 1999; 41:95–98. Available from: https://www.scirp.org/reference/ReferencesPapers?ReferenceID=1383440
- **Haseman JD.** Some new species of fishes from the rio Iguassu. Z Arztl Fortbild (Jena). 1911; 7:374.
- **Hortal J**, **De Bello F**, **Diniz-Filho JAF**, **Lewinsohn TM**, **Lobo JM**, **Ladle RJ.** Seven shortfalls that beset large-scale knowledge of biodiversity. Annu Rev Ecol Evol Syst. 2015; 46:523–49. https://doi.org/10.1146/annurev-ecolsys-112414-054400
- **Hubert N, Hanner R, Holm E, Mandrak NE, Taylor E, Burridge M *et al.*** Identifying Canadian freshwater fishes through DNA barcodes. PLoS ONE. 2008; 3(6):e2490. https://doi.org/10.1371/journal.pone.0002490
- **Ingenito LFdS**, **Duboc LF**, **Abilhoa V.** Contribuição ao conhecimento da ictiofauna da bacia do alto rio Iguaçu, Paraná, Brasil. Arq Ciênc Vet Zool UNIPAR. 2004; 7(1):23–36. Available from: https://www.revistas.unipar.br/index.php/veterinaria/article/view/540/479
- **International Union for Conservation of Nature (IUCN).** IUCN Freshwater Biodiversity Unit. Freshwater species mapping standards for IUCN red list assessments. 2019. Available from: https://www.iucnredlist.org/resources/mappingstandards
- **International Union for Conservation of Nature (IUCN). Standards and petitions committee.** Guidelines for using the IUCN Red List categories and criteria. Version 16 [Internet]. Gland; 2024. Available from: http://www.iucnredlist.org/documents/RedListGuidelines.pdf
- **Ivanova NV**, **Zemlak TS**, **Hanner RH**, **Hebert PDN.** Universal primer cocktails for fish DNA barcoding. Mol Ecol Notes. 2007; 7(4):544–48. https://doi.org/10.1111/j.1471-8286.2007.01748.x
- **Johnston AR**, **Morikawa MK**, **Ntie S**, **Anthony NM.** Evaluating DNA barcoding criteria using African duiker antelope (Cephalophinae) as a test case. Conserv Genet. 2011; 12(5):1173–82. https://doi.org/10.1007/s10592-011-0220-2
- **Kalyaanamoorthy S**, **Minh BQ**, **Wong TKF**, **von Haeseler A**, **Jermiin LS.** ModelFinder: fast model selection for accurate phylogenetic estimates. Nat Methods. 2017; 14(6):587–89. https://doi.org/10.1038/nmeth.4285
- **Katz AM**, **Barbosa MA**, **Mattos JLO**, **Costa WJEM.** Multigene analysis of the catfish genus *Trichomycterus* and description of a new South American trichomycterine genus (Siluriformes, Trichomycteridae). Zoosyst Evol. 2018; 94(2):557–66. https://doi.org/10.3897/zse.94.29872
- **Koroiva R**, **Santana DJ.** Evaluation of partial 12S rRNA, 16S rRNA, COI and Cytb gene sequence datasets for potential single DNA barcode for hylids (Anura: Hylidae). An Acad Bras Ciênc. 2022; 94(4):e20200825. https://doi.org/10.1590/0001-3765202220200825
- **Kumar S**, **Stecher G**, **Tamura K.** MEGA7: Molecular Evolutionary Genetics Analysis Version 7.0 for Bigger Datasets. Mol Biol Evol. 2016; 33(7):1870–74. https://doi.org/10.1093/molbev/msw054
- **Letunic I**, **Bork P.** Interactive Tree Of Life (iTOL) v5: an online tool for phylogenetic tree display and annotation. Nucleic Acids Resear. 2021; 49(W1):W293–96. https://doi.org/10.1093/nar/gkab301
- **Maack R.** Geografia física do estado do Paraná. 4th ed. Ponta Grossa: UEPG; 2012.
- **Martins IC**, **Reis RB**, **Stabile BHM**, **Graça WJ.** Iterative taxonomy reveals a new species of *Cambeva* (Siluriformes: Trichomycteridae) with intraspecific variation from the rio Piquiri and Ivaí basin, upper rio Paraná basin, Brazil. Neotrop Ichthyol. 2024; 22:e230140. https://doi.org/10.1590/1982-0224-2023-0140
- **Mello R**, **Maniglia TC**, **Prioli SMAP**, **Prioli AJ.** Genetic and biogeographical relationships among species of *Astyanax* (Teleostei, Characidae) in Brazilian river basins. Genetics Mol. Res. 2015; 14(4):15356–64. https://doi.org/10.4238/2015.November.30.13

- **Mezzaroba L**, **Debona T**, **Frota A**, **Graça WJ**, **Gubiani ÉA.** From the headwaters to the Iguassu Falls: Inventory of the ichthyofauna in the Iguassu River basin shows increasing percentages of nonnative species. Biota Neotrop. 2021; 21(2):e20201083. https://doi.org/10.1590/1676-0611-BN-2020-1083
- **Miranda-Ribeiro P.** Notas para o estudo dos Pygidiidae brasileiros. Bol Mus Nac. 1968; VIII(265):1–03.
- **Ministério do Meio Ambiente (MMA).** Portaria MMA Nº 148, de 7 junho de 2022. Lista Nacional de Espécies Ameaçadas de Extinção. Brasília: MMA; 2022. Available from: https://www.gov.br/icmbio/pt-br/assuntos/centros-de-pesquisa/aves-silvestres/arquivos/portaria-148-2022.pdf
- **Monaghan MT, Wild R, Elliot M, Fujisawa T, Balke M, Inward DJG *et al.*** Accelerated species inventory on Madagascar using coalescent-based models of species delineation. Syst Biol. 2009; 58(3):298–311. https://doi.org/10.1093/sysbio/syp027
- **Morais-Silva JP, Oliveira AV, Fabrin TM, Diamante NA, Prioli SMAP, Frota A *et al.*** Geomorphology influencing the diversification of fish in small-order rivers of neighboring basins. Zebrafish. 2018; 15(4):zeb.2017.1551. https://doi.org/10.1089/zeb.2017.1551
- **Nascimento RHC**, **Frantine-Silva W**, **Souza-Shibatta L**, **Sofia SH**, **Ferrer J**, **Shibatta OA.** Intrapopulational variation in color pattern of *Trichomycterus davisi* (Haseman, 1911) (Siluriformes: Trichomycteridae) corroborated by morphometrics and molecular analysis. Zootaxa. 2017; 4290(3):503–18. https://doi.org/10.11646/zootaxa.4290.3.5
- **de Oliveira RC**, **Britzke R**, **Oliveira C**, **Graça WJ.** Species delimitation in Neotropical fishes of *Mesonauta* Günther 1862 (Cichliformes: Cichlidae). Org Divers Evol. 2025; 25:343–55. https://doi.org/10.1007/s13127-025-00675-0
- **Pereira LHG**, **Castro JRC**, **Vargas PMH**, **Gomez JAM**, **Oliveira C.** The use of an integrative approach to improve accuracy of species identification and detection of new species in studies of stream fish diversity. Genetica. 2021; 149(2):103–16. https://doi.org/10.1007/s10709-021-00118-6
- **Pereira LHG**, **Hanner R**, **Foresti F**, **Oliveira C.** Can DNA barcoding accurately discriminate megadiverse Neotropical freshwater fish fauna? BMC Genet. 2013; 14:1–14. https://doi.org/10.1186/1471-2156-14-20
- **Pereira LHG**, **Maia GMG**, **Hanner R**, **Foresti F**, **Oliveira C.** DNA barcodes discriminate freshwater fishes from the Paraíba do Sul River basin, São Paulo, Brazil. Mitochondrial DNA. 2011; 22 (Suppl. 1):71–79. https://doi.org/10.3109/19401736.2010.532213
- **Piálek L**, **Burress E**, **Dragová K**, **Almirón A**, **Casciotta J**, **Říčan O.** Phylogenomics of pike cichlids (Cichlidae: *Crenicichla*) of the *C. mandelburgeri* species complex: rapid ecological speciation in the Iguazú River and high endemism in the Middle Paraná basin. Hydrobiologia. 2019; 832(1):355–75. https://doi.org/10.1007/s10750-018-3733-6
- **de Pinna MCC.** *Trichomycterus castroi*, a new species of trichomycterid catfish from the Rio Iguaçu of Southeastern Brazil (Teleostei: Siluriformes). Ichthyol Explor Freshw. 1992; 3(1):89–95.
- **de Pinna MCC**, **Dagosta FCP.** A taxonomic review of the vampire catfish genus *Paracanthopoma* Giltay, 1935 (Siluriformes, Trichomycteridae), with descriptions of nine new species and a revised diagnosis of the genus. Pap Avulsos Zool. 2022; 62:e202262072. https://doi.org/10.11606/1807-0205/2022.62.072
- **Puillandre N**, **Brouillet S**, **Achaz G.** ASAP: assemble species by automatic partitioning. Mol Ecol Resour. 2021; 21(2):609–20. https://doi.org/10.1111/1755-0998.13281
- **de Queiroz K.** Species concepts and species delimitation. Syst Biol. 2007; 56(6):879–86. https://doi.org/10.1080/10635150701701083
- **Rambaut A**, **Drummond AJ**, **Xie D**, **Baele G**, **Suchard MA.** Posterior summarization in Bayesian phylogenetics using tracer 1.7. Syst Biol. 2018; 67(5):901–04. https://doi.org/10.1093/sysbio/syy032
- **dos Reis RB**, **Ferrer J**, **Graça WJ.** A new species of *Cambeva* (Siluriformes, Trichomycteridae) from the rio Iguaçu basin, Paraná State, Brazil and redescription of *Cambeva stawiarski* (Miranda Ribeiro 1968). J Fish Biol. 2022; 100(1):279–99. https://doi.org/10.1111/jfb.14947

- **dos Reis RB**, **Frota A**, **Deprá GC**, **Ota RR**, **Graça WJ.** Freshwater fishes from Paraná State, Brazil: an annotated list, with comments on biogeographic patterns, threats, and future perspectives. Zootaxa. 2020a; 4868(4):451–94. https://doi.org/10.11646/zootaxa.4868.4.1
- **dos Reis RB**, **Frota A**, **Fabrin TMC**, **Graça WJ.** A new species of *Cambeva* (Siluriformes, Trichomycteridae) from the rio Ivaí basin, upper rio Paraná basin, Paraná State, Brazil. J Fish Biol. 2020b; 96(2):350–63. https://doi.org/10.1111/jfb.14204
- **dos Reis RB, Martins IC, Stabile BHM, Ferrer J, Oliveira AV, McMahan CD *et al*.** Taxonomy, phylogeny, and conservation of an endangered freshwater fish species from Southeastern Brazil: revisiting historical descriptions using integrative approaches. Ichthyol Herpetol. 2025a; 113(4):647–66. https://doi.org/10.1643/i2025022
- **dos Reis RB**, **Stabile BH**, **Frota A**, **Ferrer J**, **Oliveira A**, **Graça WJ.** Recent dispersion routes between freshwater ecoregions evidence headwater captures in southern Brazil: a case study using cryptic species of the neotropical freshwater fish genus *Cambeva* (Siluriformes: Trichomycteridae). Hydrobiologia. 2025b; 852:873–90. https://doi.org/10.1007/s10750-024-05731-y
- **dos Reis RB**, **Wosiacki WB**, **Ferrer J**, **Donin LM**, **Graça WJ.** A new species of *Cambeva* (Siluriformes: Trichomycteridae) from an area of high anthropogenic impacts in the headwaters of rio Iguaçu, Southern Brazil. Can J Zool. 2023; 101(6):1–11. https://doi.org/10.1139/cjz-2022-0150
- **Reis V, de Pinna M.** Diversity and systematics of *Trichomycterus* Valenciennes 1832 (Siluriformes: Trichomycteridae) in the rio Doce basin: iterating DNA, phylogeny and classical taxonomy. Zool J Linn Soc. 2023; 197(2):344–441. https://doi.org/10.1093/zoolinnean/zlac018
- **Reis VJC, Santos SA, Britto MR, Volpi TA, de Pinna MCC.** Iterative taxonomy reveals a new species of *Trichomycterus* Valenciennes 1832 (Siluriformes, Trichomycteridae) widespread in rio Doce basin: a pseudocryptic of *T. immaculatus*. J Fish Biol. 2020; 97(6):1607–23. https://doi.org/10.1111/jfb.14490
- **Ribeiro FHNP, Bonan MEP, Silva JLD, Azevedo-Santos VM, Manoel PS, Brambilla EM *et al.*** Length-weight relationship and diet of the catfish *Cambeva guareiensis* (Siluriformes; Trichomycteridae). Biota Neotrop. 2021; 21(4):e20211236. https://doi.org/10.1590/1676-0611-BN-2021-1236
- **Rizzato PP**, **Bichuette ME.** The laterosensory canal system in epigean and subterranean *Ituglanis* (Siluriformes: Trichomycteridae), with comments about troglomorphism and the phylogeny of the genus. J Morphol. 2017; 278(1):4–28. https://doi.org/10.1002/jmor.20616
- **Rosenthal A**, **Coutelle O**, **Craxton M.** Large-scale production of DNA sequencing templates by microtitre format PCR. Nuc Acids Res. 1993; 21(1):173–74. https://doi.org/10.1093/nar/21.1.173
- **Rozas J, Ferrer-Mata A, Sánchez-DelBarrio JC, Guirao-Rico S, Librado P, Ramos-Onsins SE *et al.*** DnaSP 6: DNA sequence polymorphism analysis of large data sets. Mol Biol Evol. 2017; 34(12):3299–302. https://doi.org/10.1093/molbev/msx248
- **Sabaj MH.** Codes for Natural History Collections in Ichthyology and Herpetology (online supplement). Version 9.0. Washington, DC. American Society of Ichthyologists and Herpetologists; 2022. Available from: https://asih.org
- **de Santana CD, Crampton WGR, Dillman CB, Frederico RG, Sabaj MH, Covain R *et al.*** Unexpected species diversity in electric eels with a description of the strongest living bioelectricity generator. Nat Commun. 2019; 10(1):1–10. https://doi.org/10.1038/s41467-019-11690-z
- **Silva CCF**, **Matta SLSF**, **Hilsdorf AWS**, **Langeani F**, **Marceniuk AP.** Color pattern variation in *Trichomycterus iheringi* (Eigenmann, 1917) (Siluriformes: Trichomycteridae) from rio Itatinga and rio Claro, São Paulo, Brazil. Neotrop Ichthyol. 2010; 8(1):49–56. https://doi.org/10.1590/S1679-62252010000100007
- **Taylor WR**, **Van Dyke G.** Revised procedures for staining and clearing small fishes and other vertebrates for bone and cartilage study. Cybium. 1985; 9(2):107–19.
- **Tchernavin VV.** A revision of some Trichomycterinæ based on material preserved in the British Museum (Natural History). Proc Zool Soc London. 1944; 114(1–2):234–75. https://doi.org/10.1111/j.1096-3642.1944.tb00219.x

- **Thompson JD**, **Higgins DG**, **Gibson TJ.** CLUSTAL W: improving the sensitivity of progressive multiple sequence alignment through sequence weighting, position-specific gap penalties and weight matrix choice. Nuc Acids Res. 1994; 22(22):4673–80. https://doi.org/10.1093/nar/22.22.4673
- **Trifinopoulos J**, **Nguyen L-T**, **von Haeseler A**, **Minh BQ.** W-IQ-TREE: a fast online phylogenetic tool for maximum likelihood analysis. Nuc Acids Res. 2016; 44(W1):W232–35. https://doi.org/10.1093/nar/gkw256
- **Villa-Verde L**, **Lazzarotto H**, **Lima SMQ.** A new glanapterygine catfish of the genus *Listrura* (Siluriformes: Trichomycteridae) from southeastern Brazil, corroborated by morphological and molecular data. Neotrop Ichthyol. 2012; 10(3):527–38. https://doi.org/10.1590/S1679-62252012000300005
- **Wang X**, **Liu F**, **Yu D**, **Liu H.** Mitochondrial divergence suggests unexpected high species diversity in the opsariichthine fishes (Teleostei: Cyprinidae) and the revalidation of *Opsariichthys macrolepis*. Ecol Evol. 2019; 9(5):2664–77. https://doi.org/10.1002/ece3.4933
- **Ward RD**, **Zemlak TS**, **Innes BH**, **Last PR**, **Hebert PDN.** DNA barcoding Australia's fish species. Philos Trans R Soc B Biol Sci. 2005; 360(1462):1847–57. https://doi.org/10.1098/rstb.2005.1716
- **Wosiacki WB**, **Garavello JC.** Five new species of *Trichomycterus* from the rio Iguaçu (rio Paraná basin), southern Brazil (Siluriformes: Trichomycteridae). Ichthyol Explor Freshw. 2004; 15(1):1–16.
- **Wosiacki WB**, **de Pinna M.** A new species of the Neotropical catfish genus *Trichomycterus* (Siluriformes: Trichomycteridae) representing a new body shape for the family. Copeia. 2008b; 2008(2):273–78. https://doi.org/10.1643/CI-06-237
- **Wosiacki WB**, **de Pinna MCC**. *Trichomycterus igobi*, a new catfish species from the rio Iguaçu drainage: the largest head in Trichomycteridae (Siluriformes: Trichomycteridae). Neotrop Ichthyol. 2008a; 6(1):17–23. https://doi.org/10.1590/S1679-62252008000100003
- **Yeates DK**, **Seago A**, **Nelson L**, **Cameron SL**, **Joseph L**, **Trueman JWH.** Integrative taxonomy, or iterative taxonomy? Syst Entomol. 2011; 36(2):209–17. https://doi.org/10.1111/j.1365-3113.2010.00558.x
- **Zhang J**, **Kapli P**, **Pavlidis P**, **Stamatakis A.** A general species delimitation method with applications to phylogenetic placements. Bioinformatics. 2013; 29(22):2869–76. https://doi.org/10.1093/bioinformatics/btt499

AUTHORS' CONTRIBUTION

Renan B. dos Reis: Conceptualization, Formal analysis, Investigation, Methodology, Project administration, Visualization, Writing-original draft, Writing-review and editing.

Bruno H. M. Stabile: Formal analysis, Investigation, Methodology, Writing-original draft, Writing-review and editing.

Alessandra V. Oliveira: Formal analysis, Investigation, Supervision, Validation, Writing-original draft, Writing-review and editing.

Juliano Ferrer: Conceptualization, Formal analysis, Investigation, Supervision, Validation, Writing original draft, Writing-review and editing.

Weferson J. da Graça: Conceptualization, Formal analysis, Funding acquisition, Investigation, Methodology, Project administration, Resources, Supervision, Validation, Visualization, Writing-original draft, Writing-review and editing.

FUNDING INFORMATION

The research was financed in part by the Fundação Araucária process numbers: 10558/2016 JDT2022271000007, and PBA2025401000119 to WJG, and personal grants from Conselho Nacional de Desenvolvimento Científico e Tecnológico (CNPq), process numbers: 305200/2018–6, 307089/2021–5, and 303571/2024–1. RBR has been supported by a scholarship from Coordenação de Aperfeiçoamento de Pessoal de Nível Superior (CAPES) process number: 88887.629034/2021–00. BHMS has been supported by a scholarship from CAPES, process number: 88887.629037/2021–00. JF has been supported by a PNPD scholarship from CAPES, process number: 88887.463771/2019–00.

ETHICAL STATEMENT

Samplings were approved by the Committee of Ethics for the Use of Animals in Experimentation, Universidade Estadual de Maringá (UEM) (CEUA #002/2012, #5680160117, and #9681150222), with permissions for the collection and transport of zoological material provided by SISBIO (ICMBio), process number 14028–1 to WJG. The specimens were euthanized with benzocaine following Resolution 1,000/2012 of the Conselho Federal de Medicina Veterinária, Brazil, and later fixed and preserved in 4% formalin for morphological analysis, or 99% ethanol for molecular studies.

DATA AVAILABILITY STATEMENT

The authors confirm that the data supporting the findings of this study are available within the article.

AI STATEMENT

The authors did not use any AI-assisted technologies in the creation of this manuscript or its figures

COMPETING INTEREST

The authors declare there are no competing interests.

SUPPLEMENTARY MATERIAL

Supplementary Material File

PEER REVIEW REPORT

Reviewers:

Anonymous reviewer #1

Anonymous reviewer #2

Anonymous reviewer #3

The peer review report is available at: Neotropical Ichthyology

HOW TO CITE THIS ARTICLE

- **dos Reis RB, Stabile BHM, Oliveira AV, Ferrer J, Graça WJ.** Revealing hidden diversity through iterative approaches: eight new species of *Cambeva* (Siluriformes: Trichomycteridae) from the highly endemic rio Iguaçu basin. Neotrop Ichthyol. 2026; 24(3):e250183. https://doi.org/10.1590/1982-0224-2025-0183

Neotropical Ichthyology

OPEN ACCESS

Official Journal of the
Sociedade Brasileira de Ictiologia